
# Posters

# From the Grid Science Winter School

# January 11-14, 2015

LA-UR-15-20830

# Decentralized Primary Frequency Control in Power Networks

Changhong Zhao and Steven Low
Electrical Engineering, Caltech

## Motivation

- Normal operation of power networks: all buses synchronized to nominal frequency (60 Hz)
- **Supply-demand imbalance → frequency deviation**
  degrade load performance; overload transmission lines; trigger protection devices; damage equipment

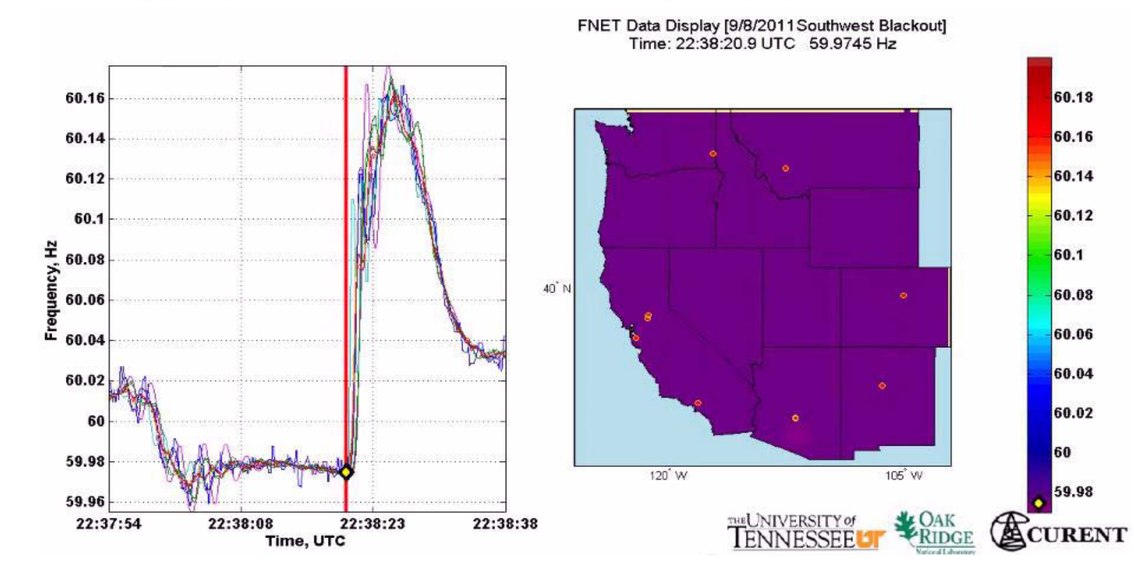


WECC frequency profile, 9/8/2011 Southwest Blackout

**Primary frequency control**: balance power and stabilize frequency

- Traditionally done on generator side
- Increased power intermittency (33% renewable in CA by 2020) requires faster and more spinning reserves, which have higher cost and emission

**Load-side participation** in primary frequency control

- A faster and cleaner supplement to generator-side
- Decentralized control for scalable and flexible plug-n-play
- Challenge: Joint design and stability analysis with generator-side (purpose of this work)

## Main Results

- Design decentralized primary frequency control which operates jointly on generators and loads
- Stabilize bus frequencies and achieve economic efficiency at closed-loop equilibrium
- Prove asymptotic stability with a relatively realistic generator model and nonlinear AC power flows
- Show performance improvement with simulation

## Power Network Model

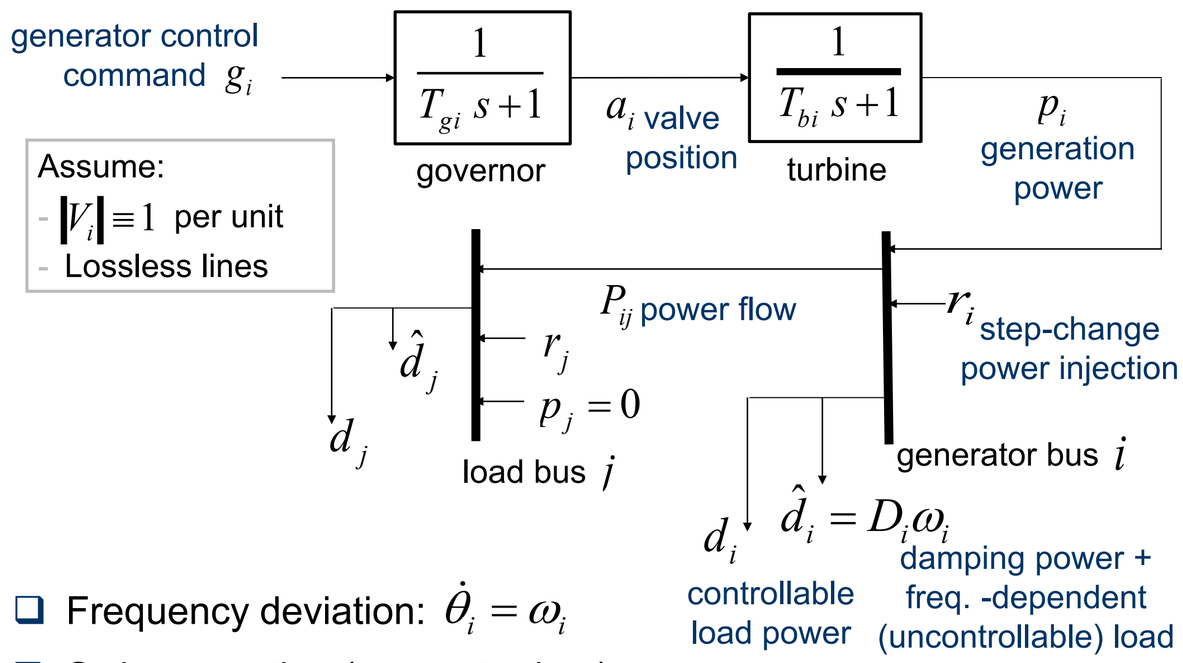


- Frequency deviation: $\dot{\theta}_i = \omega_i$
- Swing equation (generator-bus):

$$M_i\dot{\omega}_i = r_i + p_i - d_i - \hat{d}_i - \sum_{j\in N(i)} P_{ij}$$

- Power balance (load-bus):

$$0 = r_i + p_i - d_i - \hat{d}_i - \sum_{j\in N(i)} P_{ij}$$

- AC power flow: $P_{ij} = B_{ij}\sin(\theta_i - \theta_j)$

## Technical Approach

### Problem Formulation

Design **decentralized** controllers for $(g, d)$, such that the closed-loop system has an **asymptotically stable** equilibrium, where $(p^*, d^*, \hat{d}^*, P^*)$ solves the **economic efficiency** problem:

user utility (concave); generation cost (convex); penalty for freq. deviation

$$\max_{p,d,\hat{d},P} \sum_i U_i(d_i) - C_i(p_i) - \frac{\hat{d}_i^2}{2D_i}$$

$$\text{s.t.} \quad r_i + p_i - d_i - \hat{d}_i - \sum_{j\in N(i)} P_{ij} = 0 \qquad \forall i$$

$$\underline{p}_i \le p_i \le \overline{p}_i, \quad \underline{d}_i \le d_i \le \overline{d}_i \qquad \forall i$$

### Controller Design

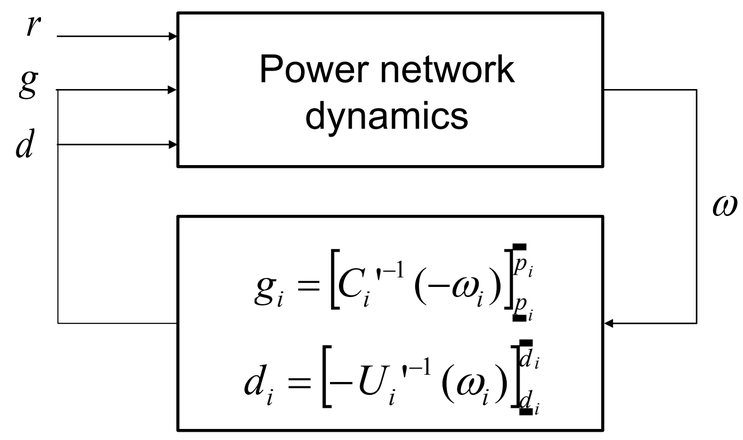


### Equilibrium Analysis

- All closed-loop equilibria are economically efficient
- Dual optimal $\omega_i^* = \omega_j^*$ : Bus frequencies stabilized to the same
  - Proof approach: Equilibrium condition ⇒ KKT condition
  - Need secondary frequency control to restore bus frequencies to the nominal value

### Stability analysis

Lyapunov function candidate: $V = E + \sum_{i\in\text{gen}} V_i$

where $E = \frac{1}{2}\sum_{i\in\text{gen}} M_i\Delta\omega_i^2 + \sum_{(i,j)\in\text{line}} \int_{\theta_{ij}^*}^{\theta_{ij}} B_{ij}(\sin u - \sin\theta_{ij}^*)du$

kinetic energy; potential energy

and $V_i = [\Delta a_i, \Delta p_i]\, P_i\, [\Delta a_i, \Delta p_i]^T$ with $P_i \succ 0$

Construct $P_i$ such that $V$ is a Lyapunov function, proving asymptotic stability of any equilibrium satisfying mild conditions

## Simulation Result

IEEE 39-bus test case, in Power System Toolbox (Chow et al.)

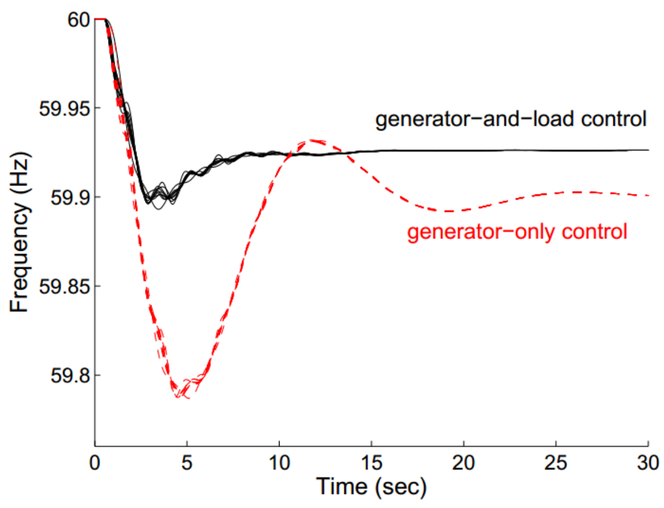


Show generator frequencies when:

- **Red**: only generators are controlled
- **Black**: 50% control capacity on generators and 50% on loads

Both cases: same total control capacity

Load-side participation improves both steady-state and transient

Supported by Los Alamos National Laboratory, Southern California Edison, National Science Foundation, National Science Council, Resnick Institute, arpa·e

# Grid Integration of Distributed Wind Generation: A Markovian and Interval Approach

Yaowen Yu*, *Student Member*, *IEEE*, Peter B. Luh*, *Fellow*, *IEEE*, Eugene Litvinov+, *Fellow*, *IEEE*, Tongxin Zheng+, *Senior Member*, *IEEE*, Feng Zhao+, *Member*, *IEEE*, and Jinye Zhao+, *Member*, *IEEE*

*: University of Connecticut, +: Independent System Operator New England

This work was supported in part by ISO New England, and in part by National Science Foundation under grants ECCS-1028870

## Introduction

- This work develops a synergistic combination of Markovian and interval optimization for unit commitment problems with wind generation and transmission
- Motivation: Important to accommodate high penetration of wind
  - DOE's goal: 20% wind by 2030
  - Obama's goal: 80% clean energy by 2035
  - In Spain, an unprecedented decrease in wind generation in Feb. 2012 is equivalent to the sudden down of 6 nuclear plants (4 is not unusual)
  - Texas Emergency Electric Curtailment Plan is called on in Feb. 2008
- Difficulties:
  - Intermittent/uncertain nature of wind generation
    - Cannot be dispatched as conventional units
    - Large uncertainty: Mean Absolute Error (normalized over capacity) of day-ahead wind power forecast: 15%~20%
  - Complicated structures of transmission networks
  - Computational complexity: NP hard problems

## Literature Review

- Stochastic programming
  - Modeling wind generation – Representative scenarios
  - To minimize the expected cost over scenarios
  - Difficult to choose an appropriate number of scenarios to balance computational complexity and solution feasibility
- Robust optimization
  - Uncertainties modeled by an uncertainty set w/o probabilities
  - To optimize against the worst-case realization
  - Min Max conservative and computationally challenging
- Pure interval optimization [1]
  - Modeling wind generation – Closed intervals w/o probabilities
  - Capturing the bounds of uncertain inputs in different types of constraints, and making decisions feasible for these bounds
  - System demand constraints: As long as min. and max. wind realizations are feasible, other realizations within them will be feasible
    - E.g., wind farm 1 outputs [10 MW, 40 MW], and wind farm 2 [20 MW, 50 MW]. Total wind generation = [30 MW, 90 MW].
    - System demand = 200 MW. Net system demand = [110 MW, 170 MW]
    - If a set of committed units with $p_i^{min}$ and $p_i^{max}$ can meet the 110 MW and 170 MW, can it satisfy possible demand at 140 MW?
  - Transmission capacity constraints: |Power flow| $\le f_l^{max}$
    - A line flow is a linear combination of nodal injections weighted by generation shift factors (GSFs can be + or -)

$$f_l(t) = \sum_i a_l^i \left( p_i^I(t) + p_i^W(t) - p_i^L(t) \right), \forall l, \forall t \quad (1)$$

    - "Passively" capture bounds of uncertain inputs

$$\sum_i a_l^i p_i(t) \le f_l^{\max} - \max\left[ \sum_i a_l^i \left( p_i^W(t) - p_i^L(t) \right) \right], \forall l, \forall t \quad (2)$$

Pre-computed based on interval arithmetic

  - Objective function: To minimize the cost of the expected realization
  - Linear and efficient via interval arithmetic; conservative

## Previous Work - Markovian Optimization w/o Transmission [2]

- Model aggregated wind generation – A Markov chain
  - Given the present, the future is independent of the past

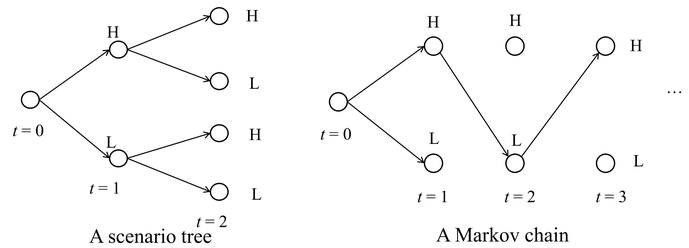


$N^T$ possible scenarios at one node

$T \cdot N$ possible states at one node

  - Advantage: State at a time instant summarizes the information of all previous instants in a probabilistic sense for reduced complexity
- Stochastic UC depends on states instead of scenarios

## Markovian and Interval Unit Commitment

- Wind model considering transmission constraints
  - With congestion, wind generation cannot be aggregated together
  - Wind states for farms at different nodes may not be the same
    - Nearby wind farms: Generation aggregated
    - Wind farms far apart: States assumed independent
  - A Markov chain per node
  - With $I$ wind nodes (Markov chains): $N^I$ possible global states at time $t$
    - *Curse of dimensionality!*

**Key idea: Markov + interval-based optimization**

  - Markovian analysis to depend on local states; interval analysis to manage extreme combinations of non-local states
    - Local state: Wind generation state at the node under consideration (will be extended into zonal state in future work)
  - Physical infrastructure supporting this idea: Wind-diesel system
  - How to combine two distinct approaches? Divide the generation (dispatch decision) of a conventional unit into two components
    - *Markovian component* depends on the local state $n_i$

$$x_i(t) p_i^{\min} \le \boxed{p_{i,n_i}^M(t)} + \boxed{p_{i,\bar{n}_i}^I(t)} \le x_i(t) p_i^{\max}, \forall i, \forall t, \forall n_i, \forall \bar{n}_i \quad (3)$$

    - *Interval component* manages extreme combinations of non-local states
  - Constraints innovatively formulated to guarantee solution feasibility for all realizations without much complexity
  - The effective use of local wind states alleviates the over-conservativeness of interval optimization

- System demand constraints
  - Based on interval optimization [1]: As long as min. and max. global states are feasible, all other realizations within them will be feasible

$$\sum_i \left( p_{i,\min n_i}^M(t) + p_{i,m_i}^I(t) \right) = \sum_j \left( p_i^L(t) - p_{i,\min n_i}^W(t) \right), \forall t \quad (4)$$

The minimum local state at node $i$

The minimum combination of non-local states (where other nodes are at their minimum possible states)

$$\sum_i \left( p_{i,\max n_i}^M(t) + p_{i,M_i}^I(t) \right) = \sum_j \left( p_i^L(t) - p_{i,\max n_i}^W(t) \right), \forall t \quad (5)$$

- Transmission capacity constraints: |Power flow| $\le f_l^{max}$
  - Flexibility of local conventional generation used to shrink ranges of RHS

$$\sum_i a_l^i p_i^I(t) \le f_l^{\max} - \max\left[ \sum_i a_l^i \left( p_{i,n_i}^W(t) + p_{i,n_i}^M - p_i^L(t) \right) \right], \forall l, \forall t \quad (6)$$

Markovian nodal injection $\equiv P_{i,n_i}^M(t)$ (containing decision variables)

- Ramp rate constraints
  - Required for possible local states, local state transitions, $p_{i,m_i}^I(t)$, and $p_{i,M_i}^I(t)$
- The objective function: To approximate the expected cost w/o much complexity
  - A weighted sum of extreme realizations and the expected realization

$$\min \sum_{t=1}^{T} \sum_{i=1}^{I} \left\{ \sum_{n_i=1}^{Ni} \left[ w_{n_i,m_i}(t) C_i \left( p_{i,n_i}^M(t) + p_{i,m_i}^I(t) \right) + w_{n_i,M_i}(t) C_i \left( p_{i,n_i}^M(t) + p_{i,M_i}^I(t) \right) \right] \right.$$
$$\left. w_E(t) C_i \left( p_{i,E}(t) \right) + u_i(t) S_i + x_i(t) S_i^{NL} \right\} \quad (7)$$

Weights adding up to 1

- A non-linear MIP formulation
  - Non-linearity lies in max/min (negative flow direction) operations in (6)

## Solution Methodology – Branch-and-cut

- Max/Min operations transformed into a linear form
  - Idea: Analyze the monotonicity of Markovian nodal injections w.r.t. local states, then select indices of local states w/o optimization
  - *The Monotonicity Conjecture*: The local state with lower wind generation provides less or equal Markovian nodal injection at the optimum, i.e.,

$$P_{i,n_i-1}^M(t) \le P_{i,n_i}^M(t), \forall i, \forall t, \forall n_i, \forall (n_i - 1) \in \{ n_i - 1 \mid \varphi_{n_i-1}(t) > 0 \}. \quad (8)$$

    - *Generalized monotonicity analysis* used to support this conjecture

$$\max_{n_i} P_{i,n_i}^M(t) = P_{i,\max n_i}^M(t), \quad \min_{n_i} P_{i,n_i}^M(t) = P_{i,\min n_i}^M(t), \forall i, \forall t. \quad (9)$$

  - Overall problem converted linearly after
    - Including (8) as constraints
    - Substituting the min/max operations with corresponding states
- State transition matrices given and state probabilities pre-computed

## Numerical Testing Results

- CPLEX 12.5.1.0 on a PC laptop with an Intel Core(TM) i7-2820QM 2.30GHz CPU and 8GB memory
- Illustrative examples
  - Conservativeness – Consider 3 nodes, 2 wind farms, 2 units, and 1 hour

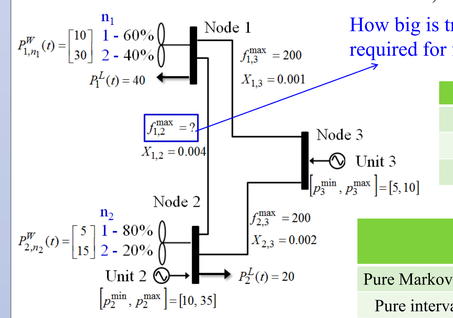


How big is transmission capacity required for feasible solutions?

| | $f_{1,2}^{max}$ |
|---|---|
| Pure Markovian | 10 |
| Pure interval | 12.86 Conservative! |
| Our approach | 10 |

| | No. of dispatch decisions per unit | No. of flow levels per line |
|---|---|---|
| Pure Markovian | $10^6$ | $10^6$ |
| Pure interval | 2+1 | 2+1 |
| Our approach | 10 + 2 + 1 | 2 + 2 + 1 |

  - Complexity – Consider 6 wind farms at different buses, 10 states for each
- Solution feasibility and modeling accuracy
  - IEEE 30-bus system with 2 wind farms at 40% wind penetration
    - Free wind curtailment and load shedding at $5,000/MWh penalty
    - Stopping MIP gap 0.1% and then 10,000 Monte Carlo runs
    - Our approach provides 5.23% lower simulation cost than pure interval
    - Our approach is the most accurate, as it has the smallest APE#

| Approach | | Deter. | Interval | Ours |
|---|---|---|---|---|
| Optimization | CPU time | 2s | 53s | 1min53s |
| | Cost (k$) | 248.66 | 280.67 | 253.40 |
| | Penalty (k$) | 0 | 0.47 | 0.01 |
| UC cost (k$) | | 89.46 | 67.72 | 65.22 |
| Simulation | E(Cost) (k$) | 314.89 | 263.26 | 250.17 |
| | APE# | 21.03% | 6.61% | 1.29% |
| | STD(cost) (k$) | 74.46 | 33.77 | 35.13 |
| | Penalty (k$) | 40.82 | 0 | 0 |

# Absolute percentage error (APE) = |optimization cost – simulation cost| / simulation cost × 100%)

- Computational efficiency
  - IEEE 118-bus system with 3 wind farms

| | | Ours |
|---|---|---|
| Optimization | CPU time | 41s |
| | MIP GAP | 0.01% |
| | Cost (k$) | 911.48 |
| UC Cost (k$) | | 12.83 |
| Simulation | E(cost) (k$) | 920.97 |
| | APE | 1.03% |
| | STD(cost) (k$) | 24.64 |

## Conclusion

- An important but difficult issue
- Hybrid Markovian and interval optimization to overcome the complexity caused by transmission constraints
  - Markovian analysis to depend on local state/reduce conservativeness
  - Interval analysis to ensure feasibility against realizations
- Problem transformed into a linear form based on monotonicity, and then solved efficiently by using branch-and-cut
- Opens a new and effective way to address stochastic problems w/o scenario analysis and avoid over-conservativeness

## References

1. Y. Wang, Q. Xia, and C. Kang, "Unit commitment with volatile node injections by using interval optimization," *IEEE Transactions on Power Systems*, vol. 26, no. 3, pp. 1705-1713, 2011.
2. P. B. Luh, Y. Yu, B. Zhang, E. Litvinov, T. Zheng, F. Zhao, J. Zhao, and C. Wang, "Grid integration of intermittent wind generation: A Markovian approach," *IEEE Trans. Smart Grid*, vol.5, no.2, pp.732-741, March 2014.
3. Y. Yu, P. B. Luh, E. Litvinov, T. Zheng, F. Zhao, and J. Zhao, "Grid integration of distributed wind generation: A Markovian and interval approach," submitted.

**Thank you!**

# Designing Resilient Electrical Distribution Grids

Emre Yamangil, Russell Bent and Scott Backhaus

Rutgers University & Los Alamos National Laboratory

Grid Science Winter School & Conference, Jan. 12th

## Presidential Policy Directive - Critical Infrastructure Security and Resilience

"The ability to prepare for and adapt to changing conditions and **withstand** and **recover** rapidly from disruptions. Resilience includes the ability to withstand and recover from deliberate attacks, accidents, or naturally occurring threats or incidents."

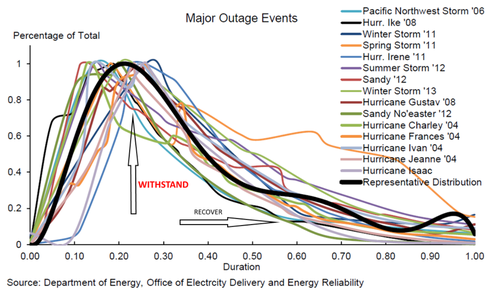


Source: Department of Energy, Office of Electrcity Delivery and Energy Reliability

## A Simplified Model

Given a graph $G = (V, E)$ where $V$ corresponds to node based upgrades (i.e. building facilities and microgrid generation capacity) and $E$ corresponds to line based upgrades (i.e. building new lines, hardening lines and building switches) we want to find:

$$\begin{aligned}
\textbf{min}\quad & \mathit{Budget}(G') \\
\text{s.t.}\quad & G' \subseteq G \\
& T_s \subseteq G' && \forall s \in S \\
& T_s \in \mathit{Trees}(G) && \forall s \in S \\
& \mathit{CriticalDemand}(T_s) \geq \mathit{MinCriticalDemand} && \forall s \in S \\
& \mathit{TotalDemand}(T_s) \geq \mathit{MinTotalDemand} && \forall s \in S
\end{aligned}$$

## Algorithm 1: Greedy[1]

**input**: A set of disasters $S$;
**for** $s \in S$ **do**
  $\sigma^s \leftarrow \mathit{Solve}(P'(s))$;
$\sigma^*(x) = \max\{\sigma^s(x) | \forall s \in S\}, \ \forall x \in \mathcal{X}$;
Update $\sigma^*(x_i)$ with switches to preserve feasibility;
**return** $\sigma^*$

## Algorithm 2: Scenario Based Decomposition[1]

**input**: A set of disasters $S$ and let $S' = S_0$;
**while** $S \setminus S' \neq \emptyset$ **do**
  $\sigma^* \leftarrow$ Solve $P(S')$ exactly (SBD) or with VNS (SBVNDS);
  $I \leftarrow \langle s_1, s_2 \ldots s_{|S \setminus S'|} \rangle s \in S \setminus S' : l(P'(s_i, \sigma^*)) \geq l(P'(s_{i+1}, \sigma^*))$;
  **if** $l(P'(I(0), \sigma^*)) \leq 0$ **then**
    **return** $\sigma^*$;
  **else**
    $S' \leftarrow S' \cup I(0)$;
  **return** $\sigma^*$

## Algorithm 3: Variable Neighborhood Search[1]

**input**: $\sigma'$, MAXTIME, MAXRESTARTS and MAXITERATIONS;
Let $\sigma^{LP} \leftarrow \mathit{Solve}(P^{LP})$, $\sigma^* \leftarrow \sigma'$, $\mathit{restart} \leftarrow \mathit{false}$;
**while** $t <$ MAXTIME *and* $i <$ MAXRESTARTS **do**
  $j \leftarrow 0$;
  $n \leftarrow |x \in \mathcal{X} : |\sigma^*(x) - \sigma^{LP}(x)| \neq 0|$;
  $J \leftarrow \langle \pi_1, \pi_2 \ldots \pi_{|J|} \rangle \in \mathcal{X} :$
  $|\sigma^*(\pi_i) - \sigma^{LP}(\pi_i)| \leq |\sigma^*(\pi_{i+1}) - \sigma^{LP}(\pi_{i+1})|$;
  **if** *restart* **then**
    $i \leftarrow i + 1$;
    $\mathit{step} \leftarrow \frac{4n}{d}$, $k = |\mathcal{X}| - \mathit{step}$;
    shuffle($J$)
  **else**
    $\mathit{step} \leftarrow \frac{n}{d}$, $k = |\mathcal{X}| - \mathit{step}$;
  **while** $t <$ MAXTIME *and* $j \leq$ MAXITERATIONS **do**
    $\sigma' \leftarrow \mathit{Solve}(P(\sigma^*, J(1, \ldots, k))$;
    **if** $f(\sigma') < f(\sigma^*)$ **then**
      $\sigma^* \leftarrow \sigma'$;
      $i \leftarrow 0$;
      $\mathit{restart} \leftarrow \mathit{false}$;
      $j \leftarrow$ MAXITERATIONS;
    **else**
      $j \leftarrow j + 1$;
      $k = k - \frac{\mathit{step}}{2}$;
      **if** $j >$ MAXITERATIONS **then**
        $\mathit{restart} \leftarrow \mathit{true}$;
  **return** $\sigma^*$

[1] Yamangil, Bent, Backhaus (2015), Resilient Upgrade of Electrical Distribution Grids, *in proceedings of AAAI-15*, AAAI press.

## Withstand

Develop new tools, methodologies, and algorithms to enable the design of resilient power distribution systems, using:

- asset hardening
- system design
  - building new lines
  - building switches
  - building microgrid facilities
  - building microgrid generation capacity

$\Rightarrow$ binary decisions, mixed-integer programming.

## Nomenclature

**Parameters**

| | |
|---|---|
| $\mathcal{N}$ | set of nodes (buses). |
| $\mathcal{E}$ | set of edges (lines and transformers). |
| $\mathcal{S}$ | set of disaster scenarios. |
| $\mathcal{D}_s$ | set of edges that are inoperable during $s \in S$. |
| $\mathcal{D}'_s$ | set of hardened edges that are inoperable during disaster $s \in S$. |
| $c_{ij}$ | cost to build a line between bus $i$ and $j$. 0 if line already exists. |
| $\kappa_{ij}$ | cost to build a switch on a line between bus $i$ and $j$. |
| $\psi_{ij}$ | cost to harden a line between bus $i$ and $j$. |
| $\zeta_{i,k}$ | cost of generation capacity on phase $k$ at bus $i$. |
| $\alpha_i$ | cost to build a generation facility at node $i$. |
| $Q_{ijk}$ | line capacity between bus $i$ and bus $j$ on phase $k$. |
| $\mathcal{P}_{ij}$ | set of phases for the line between bus $i$ and bus $j$. |
| $\mathcal{P}_i$ | set of phases allowed to consume or inject at bus $i$. |
| $\beta_{ij}$ | parameter for controlling maximum flow variation between the phases. |
| $d_{i,k}$ | demand for power at bus $i$ for phase $k$. |
| $G_{i,k}$ | existing generation capacity on phase $k$ at node $i$. |
| $Z_{i,k}$ | maximum amount of generation capacity on phase $k$ that can be built at node $i$. |
| $\mathcal{C}$ | the set of sets of nodes that includes a cycle. |
| $\lambda$ | fraction of critical load that must be served. |
| $\gamma$ | fraction of all load that must be served. |
| $\mathcal{L}$ | set of buses whose load is critical. |

**Variables**

| | |
|---|---|
| $x_{ij}$ | determines if line $i,j$ is built. |
| $\tau_{ij}$ | determines if line $i,j$ has a switch. |
| $t_{ij}$ | determines if line $i,j$ is hardened. |
| $z_{i,k}$ | determines the capacity for generation on phase $k$ at node $i$. |
| $u_i$ | determines the generation capacity built at node $i$. |
| $x^s_{ij}$ | determines if line $i,j$ is used during disaster $s$. |
| $\tau^s_{ij}$ | determines if switch $i,j$ is used during disaster $s$. |
| $t^s_{ij}$ | determines if line $i,j$ is hardened during disaster $s$. |
| $z^s_{i,k}$ | determines the capacity for generation on phase $k$ at bus $i$ during disaster $s$. |
| $u^s_i$ | indicates if the generation capacity is used at node $i$ during disaster $s$. |
| $g^s_{i,k}$ | generation produced for bus $i$ on phase $k$ during disaster $s$. |
| $l^s_{i,k}$ | load delivered at bus $i$ on phase $k$ during disaster $s$. |
| $y^s_{ij}$ | determines if the $j$th load at bus $i$ is served or not during disaster $s$. |
| $f^s_{ij,k}$ | flow between bus $i$ and bus $j$ on phase $k$ during disaster $s$. |
| $x^s_{ij}$ | determines if at least one edge between $i$ and $j$ is used during disaster $s$. |
| $\tau^s_{ij}$ | determines if at least one switch between $i$ and $j$ is used during disaster $s$. |
| $x^s_{ij,0}$ | determines if there exists flow on line $i,j$ from $j$ to $i$, during disaster $s$. |
| $x^s_{ij,1}$ | determines if there exists flow on line $i,j$ from $i$ to $j$, during disaster $s$. |

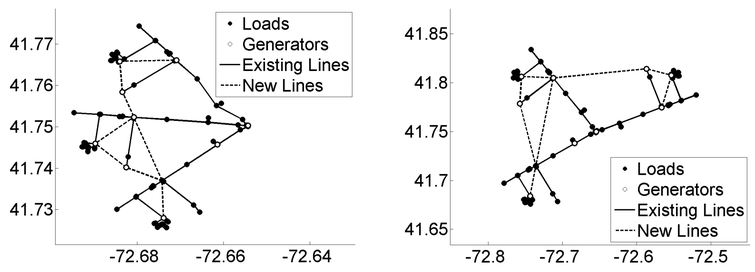


(a) Urban (b) Rural

Figure : Each problem contains three copies of the IEEE 34 system to mimic situations where there are three normally independent distribution circuits that could support each other during extreme events. These problems include 100 scenarios, 109 nodes, 118 possible generators, 204 loads, and 148 edges, resulting in problems with $> 90k$ binary variables. The cost of single and three phase underground lines is between $\$40k$ and $\$1500k$ per mile and we adopt the cost of $\$100k$ per mile and $\$500k$ per mile, respectively. The cost of single and three phase switches is estimated to be $\$10k$ and $\$15k$, respectively. Finally, the installed cost of natural gas-fired CHP in a microgrid is estimated to be $\$1500k$ per MW.

## Scenario Definition

We assume each scenario can be associated to a subset of the lines of the power distribution system that are inoperable:

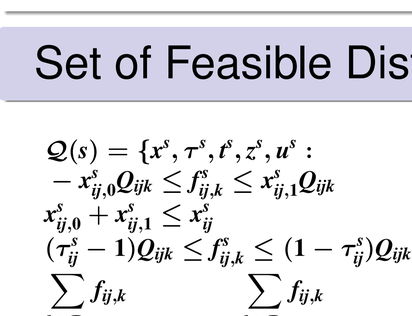

(c) Damaged line

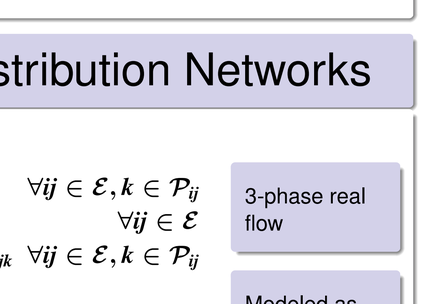


(d) Fragility

## Resilient Distribution Grid Design

$$\begin{aligned}
\textbf{min}\quad & \sum_{ij \in \mathcal{E}} c_{ij} x_{ij} + \sum_{ij \in \mathcal{E}} \kappa_{ij} \tau_{ij} + \sum_{ij \in \mathcal{E}} \psi_{ij} t_{ij} \\
& + \sum_{i \in \mathcal{N}} \alpha_i u_i + \sum_{i \in \mathcal{N}, k \in \mathcal{P}_i} \zeta_{i,k} z_{i,k}
\end{aligned}$$

Minimize budget

s.t.

$$\begin{aligned}
& x^s_{ij} \leq x_{ij} && \forall ij \in \mathcal{E}, s \in \mathcal{S} \\
& \tau^s_{ij} \leq \tau_{ij} && \forall ij \in \mathcal{E}, s \in \mathcal{S} \\
& t^s_{ij} \leq t_{ij} && \forall ij \in \mathcal{E}, s \in \mathcal{S} \\
& z^s_{i,k} \leq z_{i,k} && \forall i \in \mathcal{N}, k \in \mathcal{P}_i, s \in \mathcal{S} \\
& u^s_i \leq u_i && \forall i \in \mathcal{N}, s \in \mathcal{S} \\
& z_{i,k} \leq M_{i,k} u_i && \forall i \in \mathcal{N}, k \in \mathcal{P}_i \\
& (x^s, \tau^s, t^s, z^s, u^s) \in \mathcal{Q}(s) && \forall s \in \mathcal{S} \\
& x, \tau, t, u \in \{0, 1\}
\end{aligned}$$

1st stage: construction

2nd stage: assets in use flow delivery

## Set of Feasible Distribution Networks

$$\begin{aligned}
& \mathcal{Q}(s) = \{x^s, \tau^s, t^s, z^s, u^s : \\
& -x^s_{ij,0} Q_{ijk} \leq f^s_{ij,k} \leq x^s_{ij,1} Q_{ijk} && \forall ij \in \mathcal{E}, k \in \mathcal{P}_{ij} \\
& x^s_{ij,0} + x^s_{ij,1} \leq x^s_{ij} && \forall ij \in \mathcal{E} \\
& (\tau^s_{ij} - 1) Q_{ijk} \leq f^s_{ij,k} \leq (1 - \tau^s_{ij}) Q_{ijk} && \forall ij \in \mathcal{E}, k \in \mathcal{P}_{ij} \\
& \frac{\sum_{k \in \mathcal{P}_{ij}} f_{ij,k}}{\frac{|\mathcal{P}_{ij}|}{(1-\beta_{ij})}} \leq f^s_{ij,k'} \leq \frac{\sum_{k \in \mathcal{P}_{ij}} f_{ij,k}}{\frac{|\mathcal{P}_{ij}|}{(1+\beta_{ij})}} && \forall ij \in \mathcal{E}, k' \in \mathcal{P}_{ij} \\
& x^s_{ij} = t^s_{ij} \leq \begin{cases} 0 & \text{if } ij \in \mathcal{D}'_s \\ 1 & \text{else} \end{cases} && \forall ij \in \mathcal{D}_s \\
& l^s_{i,k} = \sum_{j=0}^{n_i} y^s_{ij} d_{ij,k} && \forall i \in \mathcal{N}, k \in \mathcal{P}_i \\
& 0 \leq g^s_{i,k} \leq z^s_{i,k} + G_{i,k} && \forall i \in \mathcal{N}, k \in \mathcal{P}_i \\
& g^s_{i,k} - l^s_{i,k} - \sum_{j \in \mathcal{N}} f^s_{ij,k} = 0 && \forall i \in \mathcal{N}, k \in \mathcal{P}_i \\
& 0 \leq z^s_{i,k} \leq Z_{i,k} u_i && \forall i \in \mathcal{N}, k \in \mathcal{P}_i \\
& \sum_{ij \in \mathcal{E}(C)} (x^s_{ij} - \tau^s_{ij}) \leq |V| - 1 && \forall C \in \mathcal{C} \\
& \tau^s_{ij} \leq x^s_{ij} && \forall ij \in \mathcal{E} \\
& \sum_{i \in \mathcal{L}, k \in \mathcal{P}_i} l^s_{i,k} \geq \lambda \sum_{i \in \mathcal{L}, k \in \mathcal{P}_i} d_{i,k} \\
& \sum_{i \in \mathcal{N} \setminus \mathcal{L}, k \in \mathcal{P}_i} l^s_{i,k} \geq \gamma \sum_{i \in \mathcal{N} \setminus \mathcal{L}, k \in \mathcal{P}_i} d_{i,k} \\
& x^s, y^s, \tau^s, u^s, t^s \in \{0, 1\}\}
\end{aligned}$$

3-phase real flow

Modeled as multicommodity flow with phase variation

Hardened lines can still be damaged

Distribution network $\Rightarrow$ tree

Minimum service requirement as resilience criteria

Urban, Hardened lines are not damageable (a)

| | CPLEX | | Greedy | SBD | | SBVNDS | |
|---|---|---|---|---|---|---|---|
| | CPU | OBJ | OBJ | CPU | OBJ | CPU | OBJ |
| 10% | 19984.7 | 322.9 | 1044.5 | 465.8 | 322.9 | 289.9 | 353.7 |
| 25% | 166352 | 635.4 | 1643.5 | 8028.3 | 635.4 | 811.4 | 635.4 |
| 50% | TO | X | 2021.2 | 2840.7 | 647.7 | 791.3 | 647.7 |
| 75% | TO | X | 1874.2 | 991.1 | 652.1 | 692.5 | 652.1 |
| 100% | TO | X | 1934.4 | 712.7 | 654.1 | 662.5 | 654.1 |

Rural, Hardened lines are not damageable (b)

| | CPLEX | | Greedy | SBD | | SBVNDS | |
|---|---|---|---|---|---|---|---|
| | CPU | OBJ | OBJ | CPU | OBJ | CPU | OBJ |
| 10% | 33083.5 | 2337.0 | 3274.8 | 1837.9 | 2337.0 | 503.3 | 2337.0 |
| 25% | 32170.8 | 2390.3 | 3427.6 | 571.0 | 2390.3 | 457.8 | 2390.3 |
| 50% | 20840.3 | 2397.6 | 3449.9 | 471.2 | 2397.6 | 421.2 | 2397.6 |
| 75% | 15556.1 | 2400.4 | 3452.7 | 337.5 | 2400.4 | 299.8 | 2400.4 |
| 100% | 17225.9 | 2400.6 | 2780.6 | 385.8 | 2400.6 | 346.9 | 2400.6 |

Urban, Hardened lines are damaged at a $\frac{1}{100}$ rate (c)

| | CPLEX | | Greedy | SBD | | SBVNDS | |
|---|---|---|---|---|---|---|---|
| | CPU | OBJ | OBJ | CPU | OBJ | CPU | OBJ |
| 10% | 159166 | 445.8 | 1061.7 | 2232.9 | 445.8 | 2721.3 | 476.5 |
| 25% | TO | X | 1441.9 | 14299.2 | 662.9 | 2994.7 | 701.5 |
| 50% | TO | X | 1571.2 | 2848.7 | 646.0 | 1917.7 | 760.2 |
| 75% | TO | X | 1787.3 | 16040.6 | 687.6 | 1481.4 | 687.6 |
| 100% | TO | X | 2744.8 | 24270.3 | 1320.5 | 2157.5 | 1330.5 |

Rural, Hardened lines are damaged at a $\frac{1}{100}$ rate (d)

| | CPLEX | | Greedy | SBD | | SBVNDS | |
|---|---|---|---|---|---|---|---|
| | CPU | OBJ | OBJ | CPU | OBJ | CPU | OBJ |
| 10% | 77947.9 | 2363.0 | 3375.4 | 759.0 | 2363.0 | 576.9 | 2363.0 |
| 25% | TO | X | 8238.6 | TO | X | 919.4 | 6744.3 |
| 50% | TO | X | 12336.0 | TO | 9288.9 | 4361.8 | 7121.0 |
| 75% | TO | X | 23099.5 | TO | X | 23142.6 | 11500.0 |
| 100% | TO | X | 16600.7 | TO | X | 5879.5 | 9797.3 |

Urban, Hardened lines are damaged at a $\frac{1}{10}$ rate (e)

| | CPLEX | | Greedy | SBD | | SBVNDS | |
|---|---|---|---|---|---|---|---|
| | CPU | OBJ | OBJ | CPU | OBJ | CPU | OBJ |
| 10% | TO | X | 859.1 | 5265.1 | 460.8 | 2505.7 | 594.1 |
| 25% | TO | X | 1742.2 | 12530.3 | 961.2 | 2843.2 | 961.2 |
| 50% | TO | X | 3133.8 | 34822.7 | 1417.2 | 3363.5 | 1555.2 |
| 75% | TO | X | 3472.0 | TO | X | 7486.5 | 1894.2 |
| 100% | TO | X | 10479.1 | TO | X | 32289.8 | 7959.4 |

Rural, Hardened lines are damaged at a $\frac{1}{10}$ rate (f)

| | CPLEX | | Greedy | SBD | | SBVNDS | |
|---|---|---|---|---|---|---|---|
| | CPU | OBJ | OBJ | CPU | OBJ | CPU | OBJ |
| 10% | TO | X | 7503.3 | 141718.0 | 4325.9 | 7756.8 | 4424.8 |
| 25% | TO | X | 18021.3 | TO | X | 21993.5 | 7371.9 |
| 50% | TO | X | 28865.0 | TO | 12017.7 | 74729.0 | 12031.2 |
| 75% | TO | X | 31887.0 | TO | 13522.2 | 107165.0 | 13500.8 |
| 100% | TO | X | 32901.9 | TO | 16794.4 | 114354.0 | 16778.2 |

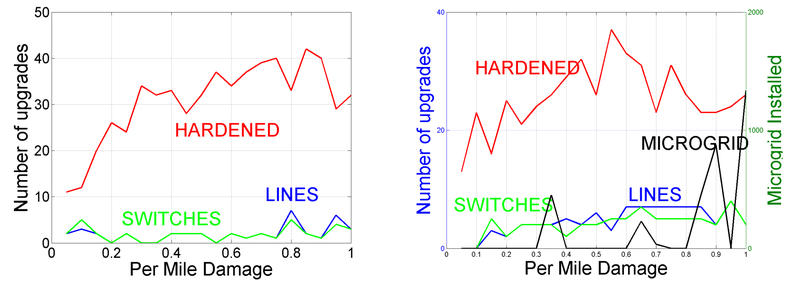


(a) Urban - 1/100 Rate (b) Urban - 1/10 Rate

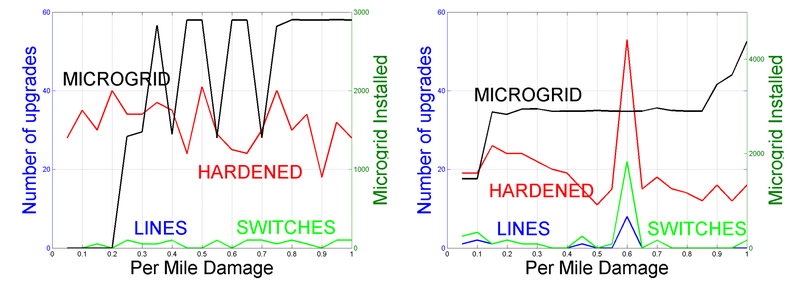


(e) Rural - 1/100 Rate (f) Rural - 1/10 Rate

http://public.lanl.gov/rbent/ yamangil@rutgers.edu

# Lyapunov Functions Family Approach to Transient Stability Assessment

Thanh Long Vu and Konstantin Turitsyn
Massachusetts Institute of Technology

## Motivations

1. Emerging technologies are changing the way power grids operate
2. The existing planning and operation computational techniques have to be reassessed
3. Variations in the grids (e.g. mechanical torques, topology) result in different operating conditions

## Problems

We consider two stability assessment problems of power grids:

**Transient stability:** *Estimate the region of attraction of the stable equilibrium point* $\delta^* = [\delta_1^*, ..., \delta_n^*, 0, ..., 0]^T$*, i.e. the set of initial conditions* $\{\delta_k(0), \dot{\delta}_k(0)\}_{k=1}^n$ *starting from which the system* (1)-(2) *converges to* $\delta^*$*.*

**Robust transient stability:** *Certify the stability of the system* (1)-(2)*, where the mechanical torques* $P_k$ *are varying such that the stable equilibrium point* $\delta^*$ *is in the polytope* $\Theta$ *defined by the inequalities* $|\delta_{kj}^*| \leq \Delta_{kj}$*.*

## Contributions

1. Introduced the LFF approach to certify the transient stability of structure-preserving multimachine power grids
2. This approach is applicable to lossy power grids, which is impossible by the standard energy methods
3. Presented optimization and LMI-based techniques to explicitly construct the stability certificates and to adapt the Lyapunov functions to initial states
4. Posed a new control problem of stability assessment for systems with unknown equilibria
5. Applied the LFF approach to uncertain power grids with unknown equilibrium points and provided robust stability certificates

## Future Directions

1. Extend the LFF stability assessment approach to more realistic models of generators, loads, and transmission network:
   - Structure-preserving models with reactive powers: extending the nonlinearity $F$
   - Higher-order models of generators with voltage dynamics, and higher-order loads
2. Design optimization algorithms to improve computational efficiency

## Structure Preserving Dynamical Swing Equations

Consider the structure-preserving model of power grids described by the swing equations:

$$(\mathcal{G}) \quad m_k\ddot{\delta_k} + d_k\dot{\delta_k} = P_{m_k} - V_k^2 G_k - \sum_{j\in\mathcal{N}_k} V_k V_j B_{kj}\sin(\delta_k - \delta_j), \qquad k = 1, ..., m \tag{1}$$

$$(\mathcal{L}) \quad d_k\dot{\delta_k} = -P_{d_k}^0 - \sum_{j\in\mathcal{N}_k} V_k V_j B_{kj}\sin(\delta_k - \delta_j), \qquad k = m+1, ..., n \tag{2}$$

The operating condition is characterized by the angle differences $\delta_{kj}^* = \delta_k^* - \delta_j^*$ satisfying:

$$\sum_{j\in\mathcal{N}_k} V_k V_j B_{kj} \sin\delta_{kj}^* = P_k, k = 1, \ldots, n \tag{3}$$

## LFF Approach

### Nonlinearity separation and bounding

$$\dot{x} = Ax - BF(Cx) \tag{4}$$

$x = [\delta_1, \ldots, \delta_m, \dot{\delta}_1, \ldots, \dot{\delta}_m, \delta_{m+1}, \ldots, \delta_n]^T$
$F(Cx) = [(\sin\delta_{kj} - \sin\delta_{kj}^*)]_{\{k,j\}\in\mathcal{E}}^T$

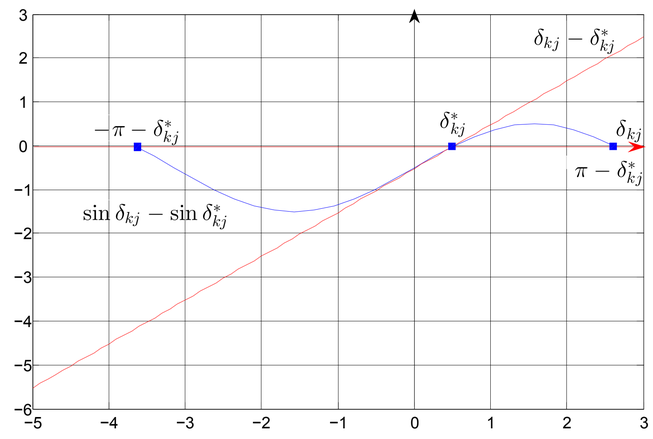


FIG. 1: Linear bounding of the nonlinear couplings

### Lyapunov Functions Family

$$V(x) = \frac{1}{2}x^T Q x - \sum K_{k,j}(\cos\delta_{kj} + \delta_{kj}\sin\delta_{kj}^*)$$

where $Q, K, H$ are solutions of the LMIs:

$$\begin{bmatrix} A^TQ + QA & R \\ R^T & -2H \end{bmatrix} \leq 0, \tag{5}$$

with $R = QB - C^TH - (KCA)^T$.
Then, $\dot{V}(x) \leq 0$ for any state $x$ stays within the polytope $\mathcal{P} := \{x : |\delta_{kj} + \delta_{kj}^*| \leq \pi\}$.

### Adaptation to Initial States

Let $\epsilon$ be a positive constant.
*Step 1:* Find $Q^{(1)}, K^{(1)}, H^{(1)}$ by solving (5).
*Step n:* Find $Q^{(n)}, K^{(n)}, H^{(n)}$ by solving the following LMIs:

$$\begin{bmatrix} A^TQ^{(n)} + Q^{(n)}A & R^{(n)} \\ (R^{(n)})^T & -2H^{(n)} \end{bmatrix} \leq 0,$$
$$V^{(n)}(x_0) \leq V_{min}^{(n-1)} - \epsilon$$

Once infeasible, $\epsilon$ is replaced by $\epsilon/2$.

## Results

*Let* $V_{\min} := \min_{x\in\partial\mathcal{P}^{out}} V(x)$*. Then, the set* $\mathcal{R} := \{x \in \mathcal{P} : V(x) < V_{\min}\}$ *is invariant, and an estimate of stability region of the SEP* $\delta^*$*.*

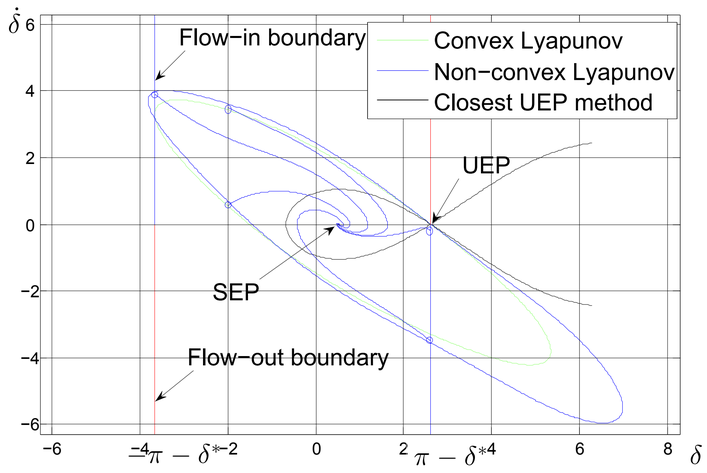


FIG. 2: Stability region estimates are intersections of the Lyapunov function sublevel sets and $\mathcal{P}$

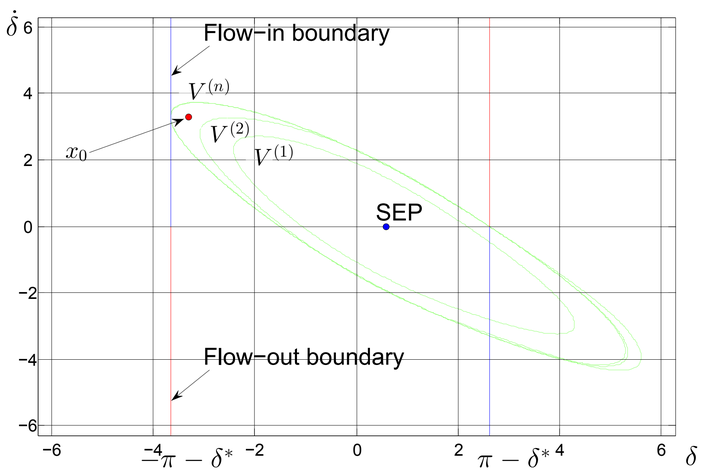


FIG. 3: Adaptation of the Lyapunov functions to $x_0$

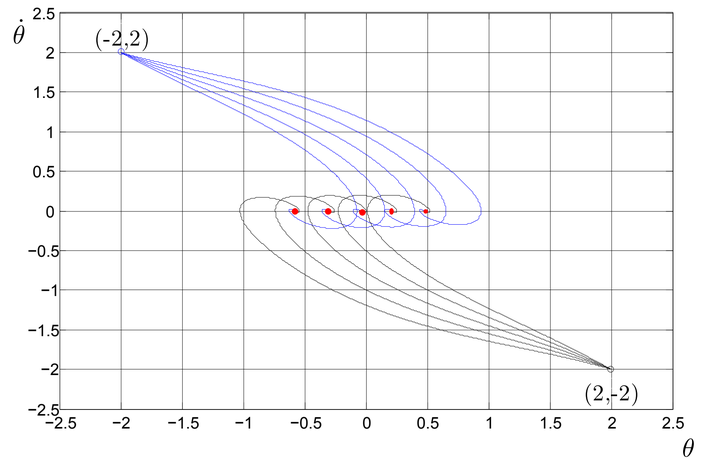


FIG. 4: Robust stability of $\{\delta_0 = -2, \dot{\delta}_0 = 2\}$ when $\delta^*$ is in the set $-\pi/6 - 0.05 \leq \delta^* \leq \pi/6 - 0.05$

## References

[1] T. L. Vu, K. Turitsyn. Lyapunov Functions Family Approach to Transient Stability Assessment. *IEEE Transactions on Power Systems*, in revision.

[2] T. L. Vu, K. Turitsyn. Synchronization Stability of Lossy and Uncertain Power Grids. *2015 American Control Conference*, accepted.

[3] T. L. Vu, K. Turitsyn. Geometry-based Estimation of Stability Region for a Class of Structure Preserving Power Systems. *2015 PES General Meeting*, in review.

## Acknowledgement

This work was partially supported by NSF and MIT/Skoltech and Masdar initiatives.

**Contact:** {longvu, turitsyn}@mit.edu

ETH
Eidgenössische Technische Hochschule Zürich
Swiss Federal Institute of Technology Zurich

eeh power systems laboratory

# Security Constrained Optimal Power Flow with Distributionally Robust Chance Constraints


*Line Roald*, Frauke Oldewurtel*, Bart Van Parys°, Göran Andersson**
** Power Systems Laboratory and °Automatic Control Laboratory, ETH Zurich*


**PROBLEM: Uncertain power injections → uncertain power flows**

Uncertainty from
- Renewables
- Market liberalization (intra-day trading)

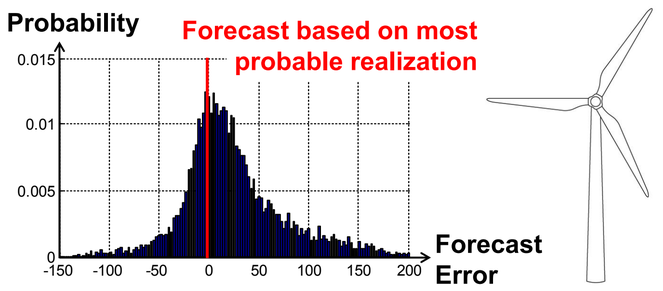


**GOAL: Keep the system operation N-1 secure despite uncertainty**

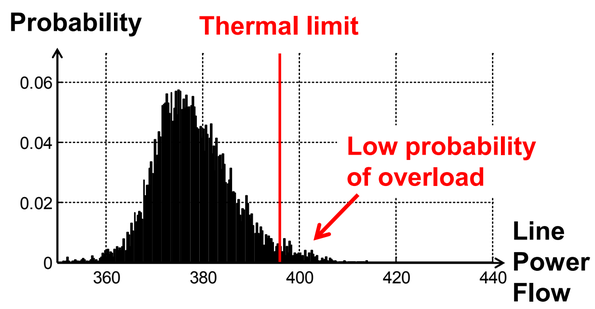


Use *chance constrained optimal power flow* to keep the *probability of line overload* below acceptable values

## 1. CHANCE CONSTRAINED OPTIMAL POWER FLOW

- Chance constraints reflect the probability of constraint violation
- Optimal power flow formulation based on DC power flow
- If a violation occurs, additional remedial actions are required from the system operator in real-time

- **CHANCE CONSTRAINT FOR POST-CONTINGENCY LINE FLOW**

Scheduled power flow + change due to outage — Change due to RES fluctuations — Desired confidence level

$$\mathbb{P}\left(A^i P^i_{inj} + D^i \delta P_{inj} \leq P^{max}_{ij}\right) \geq 1 - \varepsilon$$

| | | | |
|---|---|---|---|
| $P_{inj}$ | Scheduled in-feeds | $\delta P_{inj}$ | Uncertain in-feeds |
| $A^i$ | System topology | $\mu$ | Mean vector |
| $D^i$ | Influence of RES fluctuations | $\Sigma$ | Covariance matrix |
| $P^{max}_{ij}$ | Line flow limit | $\varepsilon$ | Accepted violation prob. |

## 2. ANALYTIC REFORMULATION OF THE CHANCE CONSTRAINTS

+ Influence of each uncertainty source is traceable
+ Deterministic solution (not dependent on the choice of samples)
– Only applicable when $D^i$ is constant (linear program) or linearly in the decision variables (SOCP)

- **REFORMULATED CONSTRAINT**

Deterministic constraint — Stochastic tightening of constraint

$$A^i P^i_{inj} \leq P^{max}_{ij} - f^{-1}(1-\varepsilon)\left\|D^i \Sigma^{1/2}\right\|_2 - D^i \mu$$

## 3. $f^{-1}(1-\varepsilon)$ DEPENDS ON (UNKNOWN) DISTRIBUTION OF $\delta P_{inj}$

**More information about the distribution yields less tightening**

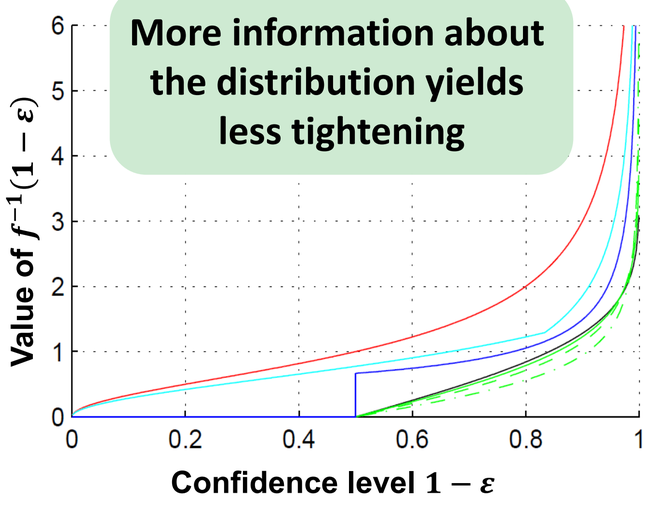


Exact reformulation if distribution is known and elliptical:
- normal distribution
- t distribution

Distributionally robust constraints if distribution is partially known:
- Chebyshev (known $\mu$ & $\Sigma$)
- Unimodal with known $\mu$ & $\Sigma$
- Symmetric, unimodal with known $\mu$ & $\Sigma$

## CASE STUDY: IEEE RTS 96 WITH UNCERTAIN IN-FEEDS

- Two uncertain in-feeds (bus 8, 15)
- $\mu$, $\Sigma$ based on samples of historical data from APG
- **Not normally distributed!**
- Accepted violation probability: $\varepsilon = 0.075$
- Different assumptions on probability distribution of $\delta P_{inj}$

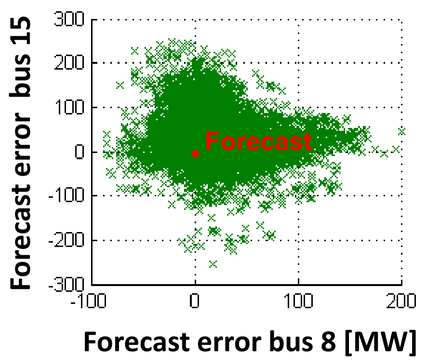


## CASE STUDY RESULTS

### POWER FLOW ON LINE 15 – 16

**Active constraint:** Power flow on line 15-16 after outage of line 15 – 21

**Cumulative distribution function:**

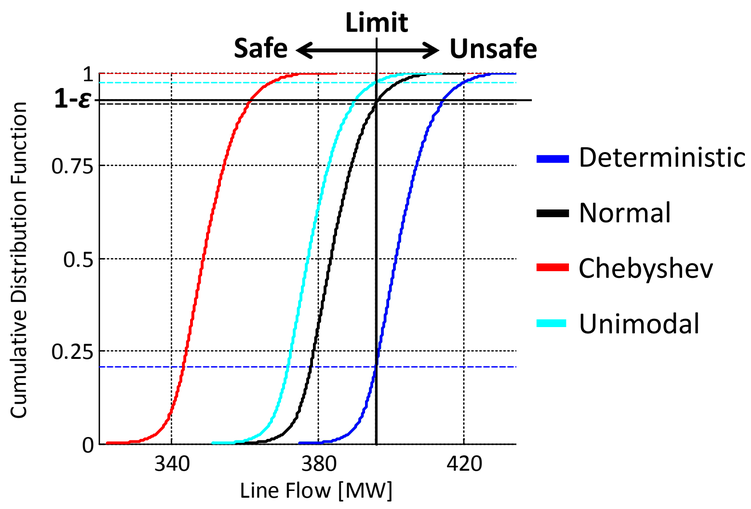


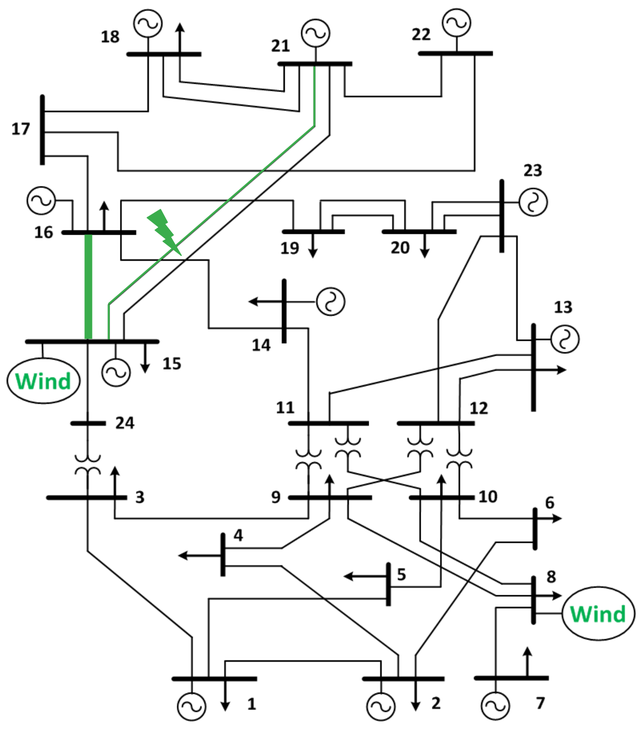


### COST AND VIOLATIONS

**More information = lower cost**

**Objective function cost**

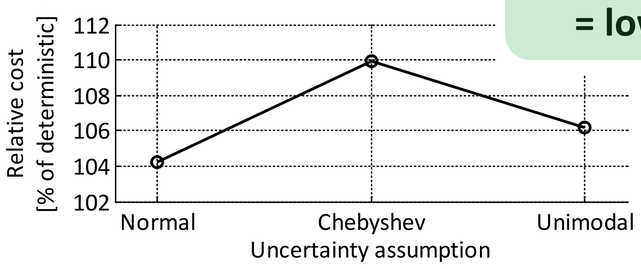


**Empirical vs Guaranteed Violation probabilities**

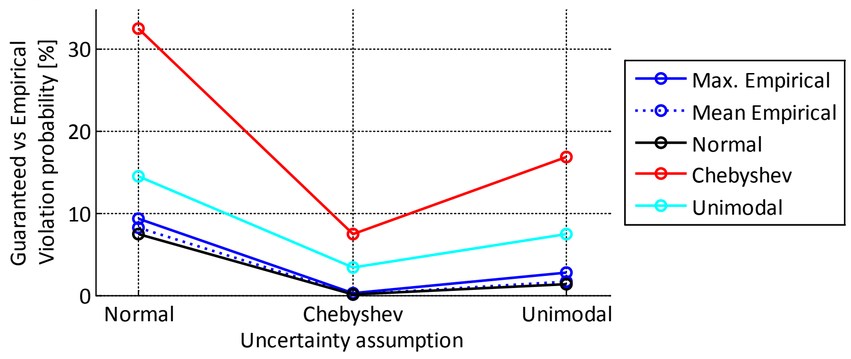


**Normal distribution is a «good guess», but provides no probabilistic guarantees**

**Chebyshev provides probabilistic guarantees, but is very conservative**

**Unimodal provides probabilistic guarantees, and is less conservative**

Poster presenter: Line Roald
Contact: roald@eeh.ee.ethz.ch

# Cascading Failure Risk Estimation and Decentralized Mitigation

Pooya Rezaei, Paul D.H. Hines and Margaret J. Eppstein

*College of Engineering and Mathematical Sciences, University of Vermont, Burlington, VT*

## Abstract

We propose a new method to estimate the risk of large cascading blackouts triggered by multiple contingencies, using a search algorithm called "Random Chemistry". Risk estimates converge at least two orders of magnitude faster than a conventional Monte-Carlo simulation for two test systems (e.g., Fig. 1). Using this method, we can quickly estimate how risk changes with load level (Fig. 2) and find the most critical components in a power grid (Fig. 3). We further propose a decentralized overload mitigation approach to stop a potential cascade (Fig. 4).

## Estimating Cascading Failure Risk

A standard measure of risk due to a random disturbance:

$$R(x) = \sum_{\forall c \in \Omega} \Pr(c) S(c,x)$$

**Monte-Carlo** → $\hat{R}_{MC}(x) = \frac{1}{|\Omega_a|} \sum_{c \in \Omega_a} S(c,x)$

**Random Chemistry** → $\hat{R}_{RC,k}(x) = \frac{m_k}{|\Omega_{RC,k}|} \sum_{d \in \Omega_{RC,k}} S(d,x) \left( \prod_{i \in d} p_i \right)$

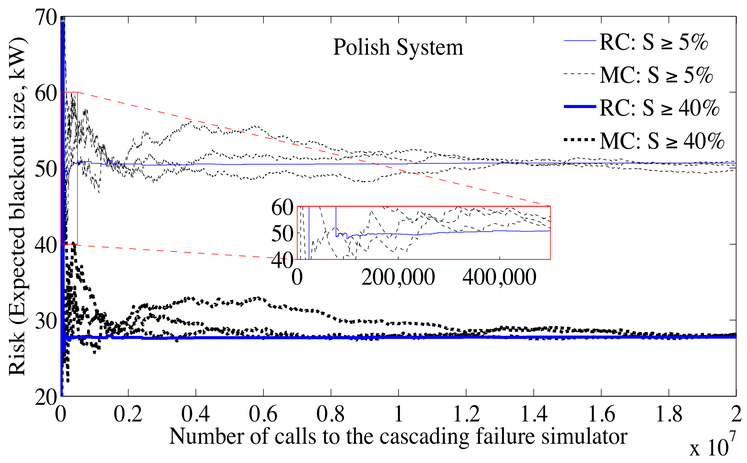


Figure 1. Cascading failure risk estimates using the Random Chemistry and Monte-Carlo methods in the Polish grid with 2896 branches.

## Risk as a function of load

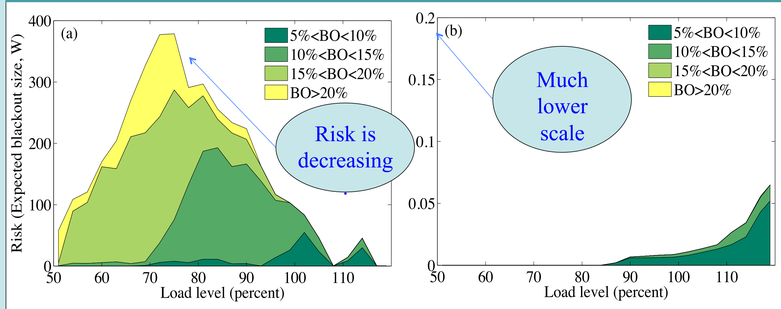


Figure 2. Cascading failure risk vs. load level for RTS-96: (a) SCDCOPF, and (b) Proportional dispatch. The proportional dispatch is more expensive, but has a much lower risk, which shows a trade-off between cost of dispatch and risk.

## Sensitivity of Risk to individual branch outage probabilities

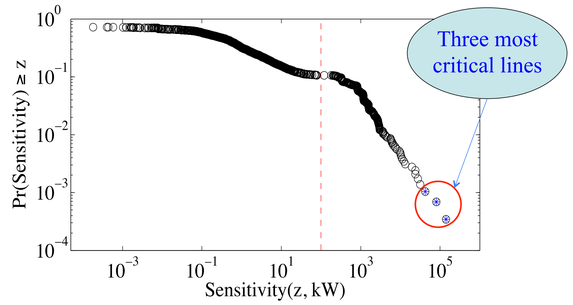


Figure 3. Complementary Cumulative Distribution Function of sensitivities (one circle per branch)

$$\frac{\partial \hat{R}_{RC,k}(x)}{\partial p_i} = \frac{m_k}{|\Omega_{RC,k}|} \sum_{d \in \Omega_{RC,k}} S(d,x) \left( \frac{\partial \Pr(d)}{\partial p_i} \right)$$

## Disadvantages of Centralized Control

A central controller has certain flaws when it comes to implementation, which makes it impractical:

- It needs a huge communication infrastructure to collect and submit information to the whole network
- It is more vulnerable to failures. One failure in a part of the system can collapse the control scheme.
- There are multiple control regions in an actual large-scale power grid, with operators each being in charge of their own area.
- Variation in load/generation on a bus typically has localized effects and does not generally affect the whole system.

## Decentralized Overload Mitigation Problem

$$\begin{aligned}
\underset{\Delta\mathbf{P}_{D,\Omega}, \Delta\mathbf{P}_{G,\Omega}}{\text{Minimize}} \quad & -\mathbf{1}^{\mathbf{T}} \Delta\mathbf{P}_{D,\Omega} + \mathbf{\Lambda}^{\mathbf{T}} \mathbf{f}_{\text{over},\Omega} \\
\text{subject to} \quad & \Delta\mathbf{f} = \mathbf{X}_b^{-1} \mathbf{A}^{\mathbf{T}} \Delta\boldsymbol{\theta} \\
& -\mathbf{f}_{\max,\boldsymbol{\Omega}} - \mathbf{f}_{\text{over},\Omega} \le \mathbf{f}_{0,\Omega} + \Delta\mathbf{f}_{\boldsymbol{\Omega}} \le \mathbf{f}_{\max,\boldsymbol{\Omega}} + \mathbf{f}_{\text{over},\Omega} \\
& \mathbf{B}\,\Delta\boldsymbol{\theta} = \mathbf{A}_G \Delta\mathbf{P}_G - \mathbf{A}_D \Delta\mathbf{P}_D \\
& -(\mathbf{P}_{G0,\Omega} - \mathbf{P}_{G,\min,\Omega}) \le \Delta\mathbf{P}_{G,\Omega} \le 0 \\
& -\mathbf{P}_{D0,\Omega} \le \Delta\mathbf{P}_{D,\Omega} \le 0 \\
& \Delta\mathbf{P}_{G,\Omega^c} = 0 \\
& \Delta\mathbf{P}_{D,\Omega^c} = 0 \\
& \mathbf{f}_{\text{over},\Omega} \ge 0
\end{aligned}$$

$\Omega$: node/line local neighborhood, $\Omega^c$: nodes outside $\Omega$
$\Delta\mathbf{P}_D/\Delta\mathbf{P}_G$: variation in load/generation
$\mathbf{f}_{\text{over}}$: slack variable to define a soft constraint for overload
$\mathbf{B}$: bus susceptance matrix

After each agent solves their own optimization problem with the optimization control variables to exist only in the local neighborhood, it implements the load/generation reduction only on its own when negotiation is off, or the whole local neighborhood when negotiation is on.

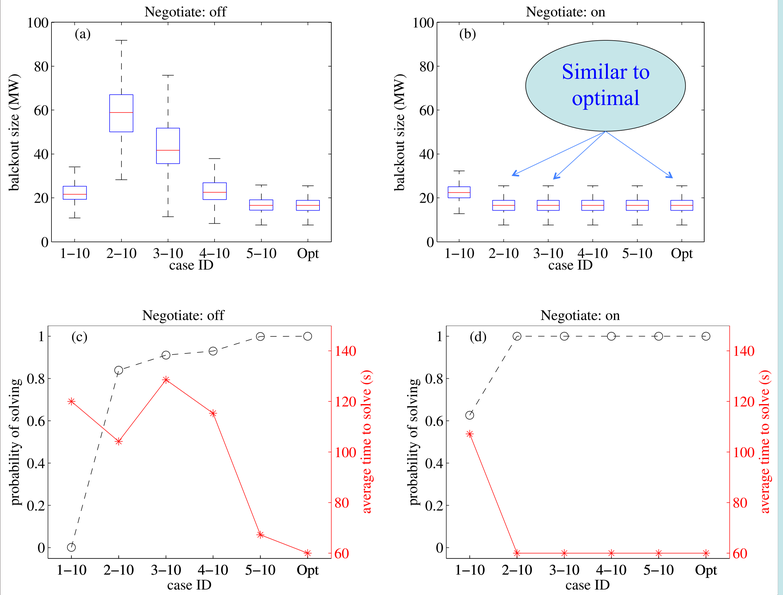


Figure 4. Statistical performance of the decentralized controller after applying all n-2 contingencies to a modified IEEE 30-bus case: The box plot indicates total blackout sizes, where the line shows the median value (a) without, and (b) with negotiation capability; bottom panels show empirical probability of eliminating overloads (dashed line and circle markers) and the average time (solid line and asterisk markers) that it takes to solve the problem (c) without, and (d) with negotiation. The case ID p-q represents the local neighborhood size p and extended neighborhood size q.

# Constrained Mean Field Control for Large Populations of Plug-in Electric Vehicles

Francesca Parise, Sergio Grammatico, Marcello Colombino and John Lygeros
Automatic Control Laboratory ETH Zürich, Switzerland

## Introduction

Vehicles obtaining some or all of their energy from the electricity grid, as Plug-in (hybrid) Electric Vehicles (PEVs), may achieve significant market penetration over the next few years. This raises the question of how to optimally fulfill the corresponding energy requirement, by regulating the collective charging profile of large populations of PEVs, while guaranteeing the interest and the privacy of the users.

Here we address this task using a mean field game theoretical approach [1,2]. We consider PEVs as heterogeneous agents, with different charging constraints (plug-in times and deadlines), that minimize their own charging cost and are weakly coupled via a common electricity price.

## Problem Formulation

Consider a charging horizon of $T$ time steps. Let $\mathbf{u}_n = [u_{n,1}, \dots, u_{n,T}]^\top$ be the vector of the energy required by vehicle $n \in \{1, \dots, N\}$, which must belong to the personalized constraint set

$$\mathcal{U}_n := \left\{ \mathbf{u}_n \in \mathbb{R}^T \mid \sum_t u_{n,t} = \gamma_n, \;\; 0 \le u_{n,t} \le M_{n,t} \right\},$$

and $p\left(u_t^{\text{avg}}\right) := a(u_t^{\text{avg}} + d_t)$, $a > 0$, be an affine price function that depends on the total energy demand at time $t$. Each agent minimizes its charging cost by solving

$$\mathbf{u}_n^\star\left(\{\mathbf{u}_i\}_{i\neq n}^N\right) := \arg\min_{\mathbf{u}_n} \sum_t p\left(u_t^{\text{avg}}\right) u_{n,t} \qquad (1)$$
$$\text{s.t.} \quad \mathbf{u}_n \in \mathcal{U}_n$$

which leads to the aggregate behavior

$$\mathbf{u}^{\text{avg}} = \frac{1}{N}\sum_{n=1}^N \mathbf{u}_n.$$

As shown in Figure 1 (left) if uncontrolled the total energy demand may present undesirable peaks.

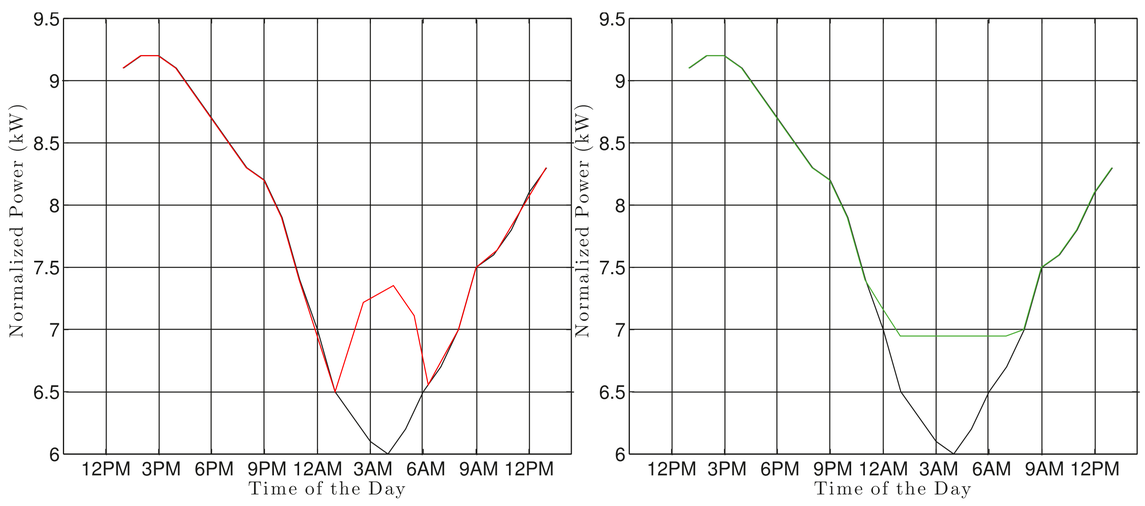


Figure 1 : Total energy demand divided by the number of vehicles $N$, according to different charging policies. The black line is the normalized base load demand $d_t$.

## Nash Equilibrium

A set of strategies $\{\bar{\mathbf{u}}_n\}_{n=1}^N$ is stable if no agent has interest in deviating from its strategy given what the others are doing. Formally it is an $\varepsilon$-Nash equilibrium if

$$J(\bar{\mathbf{u}}_n | \{\bar{\mathbf{u}}_i\}_{i\neq n}^N) \le J(\mathbf{u}_n | \{\bar{\mathbf{u}}_i\}_{i\neq n}^N) + \varepsilon \quad \forall \mathbf{u}_n \in \mathcal{U}_n.$$

It was proven in [3], that the Nash equilibrium of problem (1), *in the absence of upper bounds*, is valley-filling, see Figure 1 (right). Hence the Nash equilibrium is both valley-filling and socially fair.

To steer the population to such desirable equilibrium we consider a quadratic relaxation of the original problem using the modified cost

$$J_\delta(\mathbf{u}^{\text{avg}}) := \sum_t p\left(u_t^{\text{avg}}\right) u_{n,t} + \delta(u_{n,t} - u_t^{\text{avg}})^2$$

where the parameter $\delta > 0$ has to be as small as possible. Note that, in the limit of infinite population size, the average $\mathbf{u}^{\text{avg}}$ can be though of as an exogenous signal $\mathbf{z}$ that must satisfy

$$\mathcal{A}(\mathbf{z}) := \frac{1}{N}\sum_{n=1}^N \mathbf{u}_n^\star(\mathbf{z}) := \frac{1}{N}\sum_{n=1}^N \arg\min_{\mathbf{u}_n \in \mathcal{U}_n} J_\delta(\mathbf{z}) = \mathbf{z}.$$

$\bar{\mathbf{z}}$ fixed point of the aggregation mapping $\mathcal{A}(\cdot)$

$\Downarrow$

$\{\mathbf{u}_n^\star(\bar{\mathbf{z}})\}_{n=1}^N$ is an $\varepsilon$-Nash equilibrium, with $\varepsilon \sim \mathcal{O}(1/N)$

## Acknowledgments

Research partially supported by the European Commission under project DYMASOS (FP7-ICT 611281), by the Swiss grant Nano-Tera.ch under project HeatReserves and by CTI under project SCCER-FEEB&D.

## A Mean Field Control Algorithm

In order to find the fixed point of the aggregation mapping we consider an iterative scheme between

- a *central operator* that broadcasts at each iteration $k$ the price signal $p(\mathbf{z}_k)$,
$$\mathbf{z}_k := \Phi_{k-1}(\mathbf{z}_{k-1}, \mathcal{A}(\mathbf{z}_{k-1}));$$
- the *agents* that respond by computing $\mathbf{u}_n^\star(\mathbf{z}_k)$;
- an *aggregator* that computes $\mathcal{A}(\mathbf{z}_k)$ and send it back to the central operator.

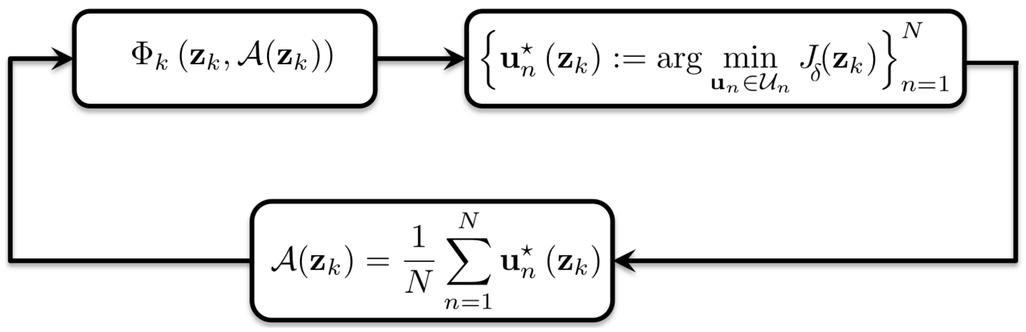


The iteration-dependent feedback mapping $\Phi_k(\cdot,\cdot)$ should be selected such that the algorithm converges to a fixed point of the aggregation mapping. To this end, we consider two fixed point iteration mappings

Picard-Banach [3] : $\Phi^{\text{P–B}}(\mathbf{z}_k, \mathcal{A}(\mathbf{z}_k)) := \mathcal{A}(\mathbf{z}_k)$
Mann [4] : $\Phi_k^{\text{M}}(\mathbf{z}_k, \mathcal{A}(\mathbf{z}_k)) := (1-\alpha_k)\mathbf{z}_k + \alpha_k \mathcal{A}(\mathbf{z}_k), \quad \alpha_k \propto 1/k$

The following convergence guarantees hold

| | $\Phi^{\text{P–B}}$ | $\Phi^{\text{M}}$ |
|---|---|---|
| $\delta > a/2$ | ✓ | ✓ |
| $\delta > 0$ | | ✓ |

## Simulation

The use of the Mann iteration instead of the Picard-Banach allows one to find the fixed point for arbitrarily small values of $\delta$, hence allowing to recover the Nash-equilibrium of the original Problem (1), [4]

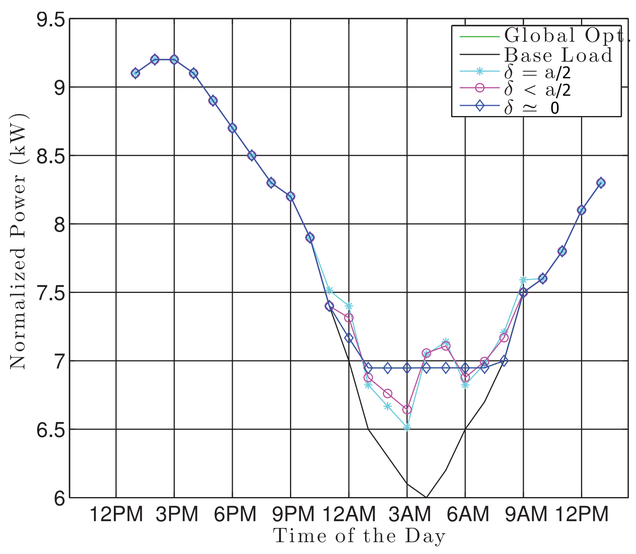


Figure 2 : Normalized total energy consumption relative to the Nash-equilibrium for different values of $\delta$.

## Generalization

The above results can be generalized to the broader class of quadratic, convex constrained, mean field games where each agent computes

$$\mathbf{x}_n^\star(\mathbf{z}) := \arg\min_{\mathbf{x}} \; \mathbf{x}^\top Q\mathbf{x} + (\mathbf{x}-\mathbf{z})^\top \Delta(\mathbf{x}-\mathbf{z}) + 2(C\mathbf{z}+c)^\top \mathbf{x}$$
$$\text{s.t.} \quad \mathbf{x} \in \mathcal{X}_n$$

In [5], it is proven that, under different conditions on the matrices $Q, \Delta, C$, different feedback mappings $\Phi(\mathbf{z}, \mathcal{A}(\mathbf{z}))$ can be used to steer the population to an $\varepsilon$-Nash equilibrium, with $\varepsilon \sim \mathcal{O}(1/N)$.

## References

[1] Lasry and Lions, “Mean field games”, Japanese Journal of Mathematics, 2007.
[2] Huang, Caines and Malhamè, “Large-population cost-coupled LQG problems with nonuniform agents: Individual-mass behavior and decentralized $\varepsilon$-Nash equilibria”, IEEE Trans. on Automatic Control, 2007.
[3] Ma, Callaway, and Hiskens,“Decentralized charging control of large populations of plug-in electric vehicles”, IEEE Trans. on Control Systems Technology, 2013.
[4] Parise, Colombino, Grammatico, and Lygeros, “Mean field constrained charging policy for large populations of plug-in electric vehicles”, IEEE CDC, 2014.
[5] Grammatico, Parise, Colombino, and Lygeros, “Decentralized convergence to Nash equilibria in constrained mean field control”, sub. to IEEE Trans. on Automatic Control, 2014. Available online at http://arxiv.org/pdf/1410.4421.pdf

Mail: parisef@control.ee.ethz.ch
Web: http://control.ee.ethz.ch/~parisef/

# Investigating the Impact of Communication Loss on Power Grid Stability during a Large Disturbance

Massachusetts Institute of Technology

**Marzieh Parandehgheibi, Konstantin Turitsyn and Eytan Modiano**
**(marp,turitsyn,modiano@mit.edu)**

LIDS

## Introduction

- In order to avoid large cascading failures, a communication network is required for online monitoring & control
- Power grid and communication network make a strong interdependency
- Literature suggests that interdependency makes networks more vulnerable
- A proper analysis of interdependent networks should account for the availability of control schemes applied by the communication networks

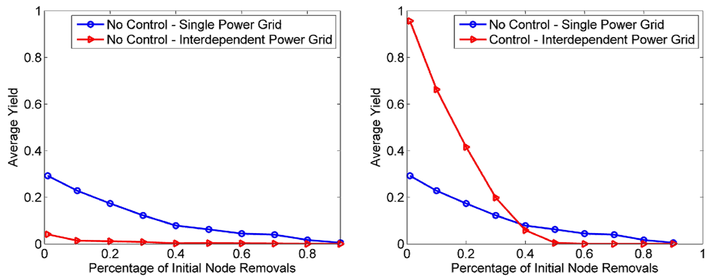


**Interdependency increases the robustness of power grid**

**Question:**
A point-wise failure model seems too simplistic.
How does the loss of communication network impact the power grid?

## Ideal Model of Communication Network Responsible for Wide-Area Control

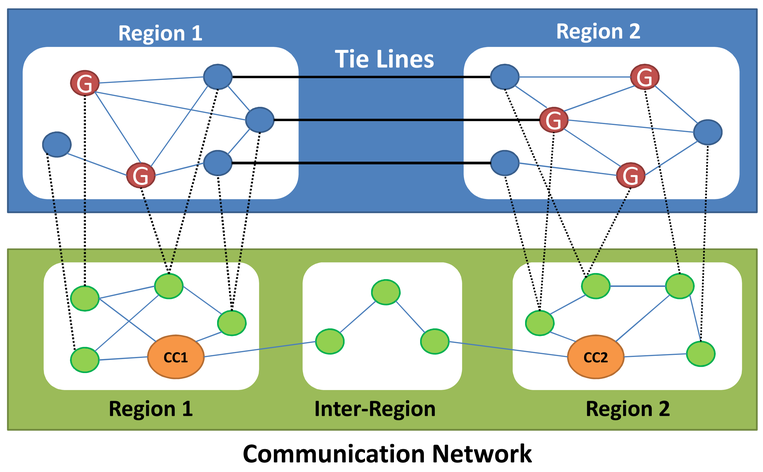


**Types of Communication Failures:**
- **Intra-Region**
- **Inter-Region**

**Intra-Region Failures:**

1) Uncontrollable area and power failures are **disjoint**:
   - Complete Information about the last state of Grid
   - Partial Control

2) Uncontrollable area and power failures **overlap**:
   - Incomplete Information about the state of Grid
   - Partial Control

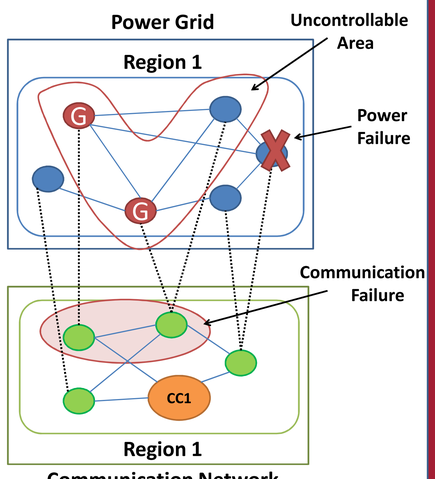


## Role of Communication Network

**Information collected by Communication Network**

| | |
|---|---|
| $V_k(t)$ | Magnitude of voltage at node k |
| $\theta_k(t)$ | Phase of voltage at node k |
| $\omega_k(t)$ | Frequency of Power at node k |
| $f_{kj}(t)$ | Flow in power line (k,j) |

**Control Actions**

| **Centralized** Control Requires Communication | **Decentralized** control-protection Performs locally- No Need to Communication |
|---|---|
| Ramping down generators | 5% droop control at generators |
| Intelligent load shedding | Over-frequency generator tripping (protection) |
| Intelligent line tripping | Under-frequency load shedding (protection) |
| | Overloaded line tripping (protection) |

## Full Control Model

$$\min \sum_{i \in V_L} PL_i$$

$$\sum_{j \in E} f_{ij} - \sum_{j \in E} f_{ji} = PG_i - \alpha_i(\omega_i - \omega_s) \quad \forall i \in V_G$$

$$\sum_{j \in E} f_{ij} - \sum_{j \in E} f_{ji} = PL_i \quad \forall i \in V_L$$

$$\sum_{j \in E} f_{ij} - \sum_{j \in E} f_{ji} = 0 \quad \forall i \in V_B$$

$$-M(1-z_{ij}) \le X_{ij} f_{ij} - \Delta\theta_{ij} \le M(1-z_{ij}) \quad \forall (i,j) \in E$$

$$-z_{ij} f_{ij}^{\max} \le f_{ij} \le z_{ij} f_{ij}^{\max} \quad \forall (i,j) \in E$$

$$-M(1-z_{ij}) \le \omega_i - \omega_j \le M(1-z_{ij}) \quad \forall (i,j) \in E$$

$$\omega_i^{\min} \le \omega_i \le \omega_i^{\max} \quad \forall i \in V_G$$

$$PG_i^{\min} \le PG_i \le PG_i^{\max} \quad \forall i \in V_G$$

$$PL_i^{\min} \le PL_i \le PL_i^{\max} \quad \forall i \in V_L$$

$$z_{ij} \in \{0,1\} \quad \forall (i,j) \in E$$

## Partial Control Model

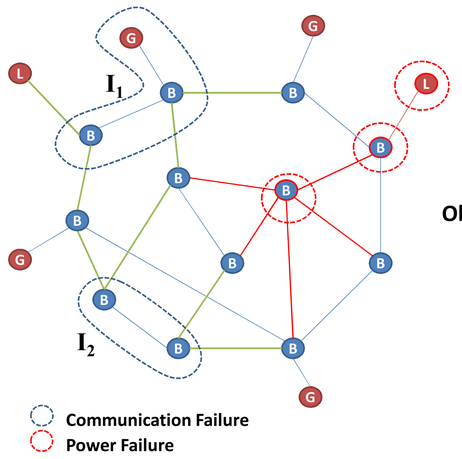


**Controllable Areas**: Full control
**Uncontrollable areas:**
1. Switch the Generators and Loads to a predefined strategy for CommLossMode;
2. Allow Trip border lines

**Objective: Stabilize Grid**
a) Minimize Load Shedding while keeping the nodes in the uncontrollable area at a predefined strategy
b) If keeping an uncontrollable area connected to the rest of grid is not feasible or costs a lot: Trip all border lines

## Simulation Results

- **Metric:** Yield (Percentage of served load)
- **Pre-defined Strategy:** The state of power nodes after disconnection from the communication network

**1) $P_{init}$:** Keep the generators and loads at their last state
**2) $P_{zero}$:** Trip the generators and shed the loads

**Observations:**

➢ Communication loss makes network more vulnerable (smaller yield)

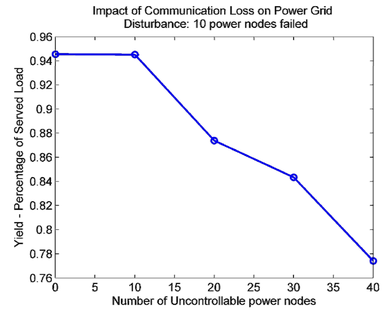


6% load shedding due to power disturbance
17% load shedding due to communication loss

➢ Impact is a function of several parameters such as:
1) size of uncontrollable area: yield decreases monotonically
2) size of uncontrollable clusters (topology of uncontrollable area)
3) Size of Power Failure: yield decreases monotonically

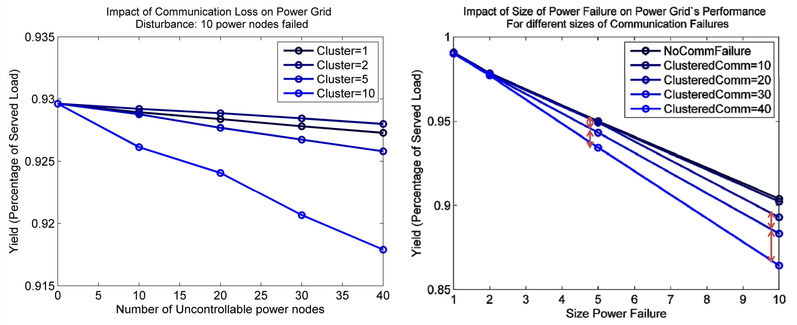


➢ Nodes both inside and outside the uncontrollable area could be affected

➢ $P_{init}$ is not always better than $P_{zero}$
1) For the same size of uncontrollable area, chance of Pzero>Pinit is higher in clustered areas
2) For the same size of clusters, chance of Pzero>Pinit is higher for smaller sizes of uncontrollable areas

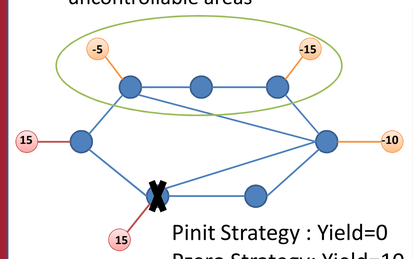


Pinit Strategy : Yield=0
Pzero Strategy: Yield=10

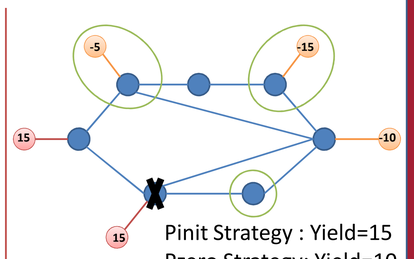


Pinit Strategy : Yield=15
Pzero Strategy: Yield=10

## References

1) Buldyrev, Sergey V., et al. "Catastrophic cascade of failures in interdependent networks." *Nature* 464.7291 (2010): 1025-1028.
2) Parandehgheibi, Marzieh, Eytan Modiano, and David Hay. "Mitigating cascading failures in interdependent power grids and communication networks."*Smart Grid Communications (SmartGridComm), 2014 IEEE International Conference on*. IEEE, 2014.

**Acknowledgement:** *This work has been funded by DTRA grant HDTRA1-13-1-0021*

# Short Term Solar Forecasting Using Sky Imagery and Its Applications in Control and Optimization for a Smart Grid

Andu Nguyen (andunguyen@ucsd.edu) and Jan Kleissl (jkleissl@ucsd.edu) at UC San Diego's SRAF Lab

## Short-term Solar Forecasting

**Goal**: Forecast solar generation in short time scale (0-30 minutes) with high temporal resolution to build smart controls for storage systems (charge/ discharge), power inverters, voltage regulators, smart switching devices, etc. This helps to save generation and maintenance cost while keeping power quality high.

Hardware

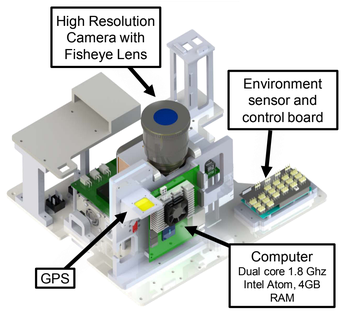


USI Deployed in Redlands, CA

Idea

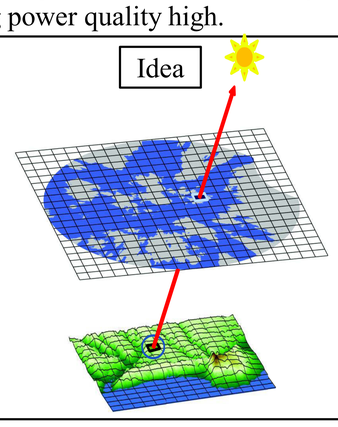

**Algorithm**: The fundamental idea is to detect cloud and predict its location in the future to determine whether and when it will cover the PV panels. The forecasting process includes several steps:

1. Cloud Detection: Using image processing to distinguish cloud from clear sky by RBR value.
2. Cloud projection into an earth coordinate system.
3. Cloud speed and direction calculation: Using image segment correlation.
4. Modeling cloud motion forward in time using the cloud detection and the motion vectors.
5. Projection of cloud shadows on the ground for irradiance forecasting of solar panels.

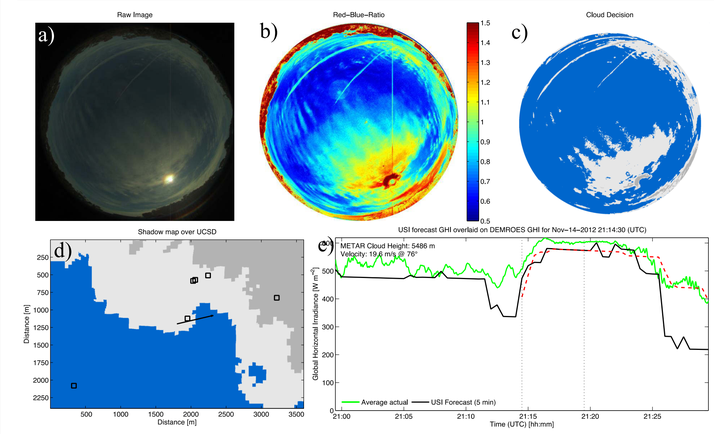


Sample of a forecast process done at UCSD. Green line is 5-minute forecast and black line is measured data.

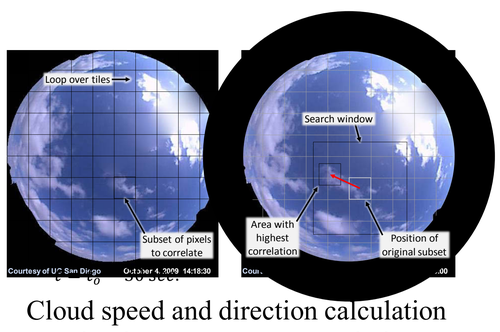


Cloud speed and direction calculation using image segment correlation

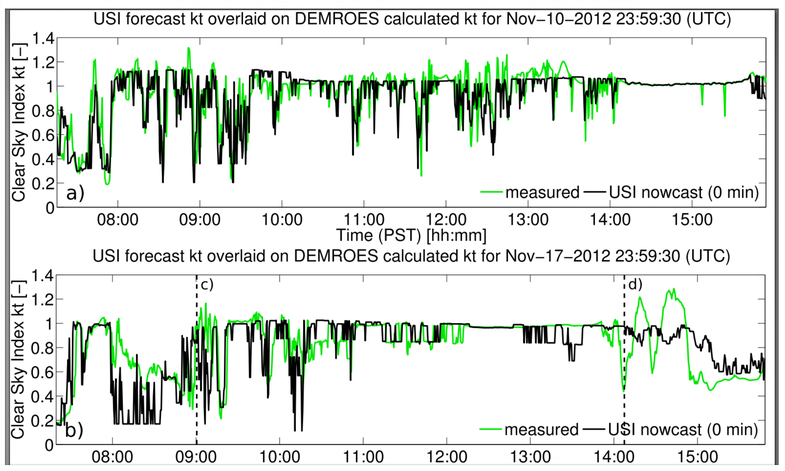


USI forecast and measured ***kt*** averaged across 6 pyranometers at UCSD for Nov 10 and Nov 17 with cumulus clouds.

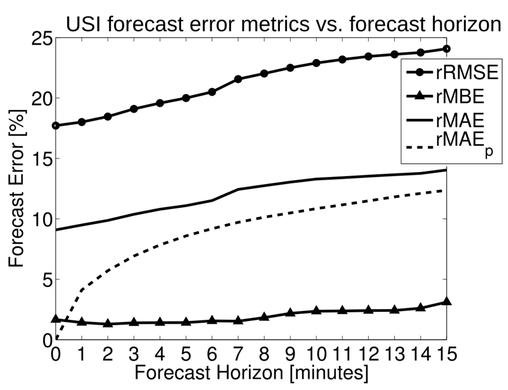


USI forecast's error metrics for all 31 days in Nov 2012. rMAE is 10% in average and increases as forecast horizon raises.

## Peak load shaving control with Short-term Solar Forecast for Storage System

Control with Sky Imager Solar Forecast was developed for a 31kW PV tied to a 31 kWh Li-ion at John Hopkins parking structure at UCSD, CA. The solar forecasts was used to optimize the charge/discharge cycling for peak load shaving and battery life longevity. The strategy for peak load shaving is "Time-of-use Energy Cost Management Plus Demand Charge Management."

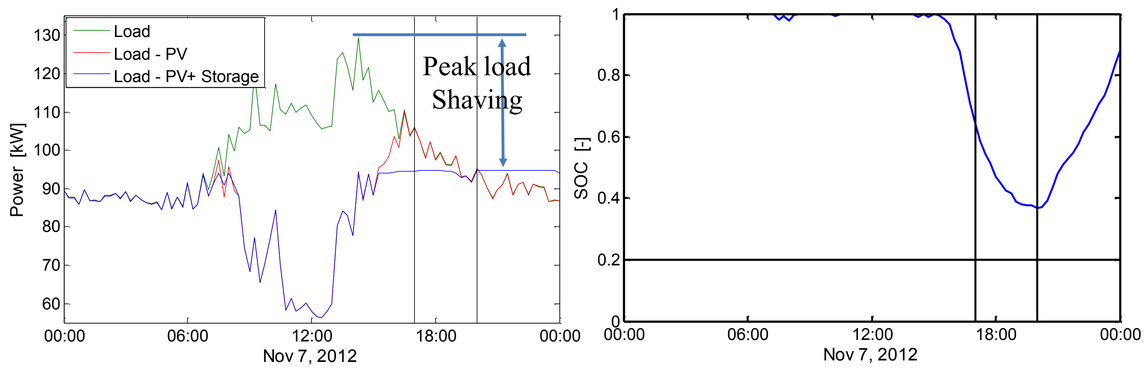


Control operation for Storage System at John Hopkins Building on Nov 7, 2012

| | Optimization with PV Power Output and Load Forecast | Off-Peak/On-Peak without PV Power Output and Load Forecast |
|---|---|---|
| Annual energy bill cost reduction [$] | 33,200 | 30,500 |
| Number of cycles at 80% DoD [cyc/yr] | 212 | 365 |
| Battery Lifetime [yrs] | 14.2 | 8.2 |
| Fixed cost simple payback time [yrs] | 5.7 | 6.2 |
| Total profit at end of battery lifetime (annual energy bill savings x battery lifetime - fixed costs) [$] | 281,000 | 60,000 |

Results in table below shows that the incorporation of forecast data was shown to dramatically increase system lifetime (6 years extra) and its lifetime profit (360% increase on a 31 kWh storage system).

## Local Vol-Var Control for PV Inverters

By combining USI-forecast and distribution system simulation using OpenDSS, we were able to design and demonstrate the impact of local volt-var control on the distribution network. With appropriate control design, the use of PV inverter reactive support will lessen the adverse impact of high PV penetration.

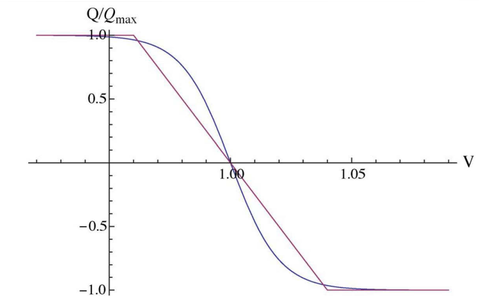


Local Vol-Var Control Scheme

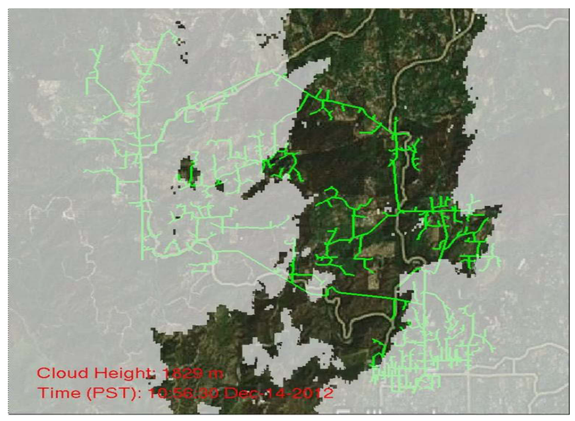


Cloud cover simulation on SDG&E feeder using sky imager forecast. The green lines are feeder distribution lines. Whitish area is covered by cloud.

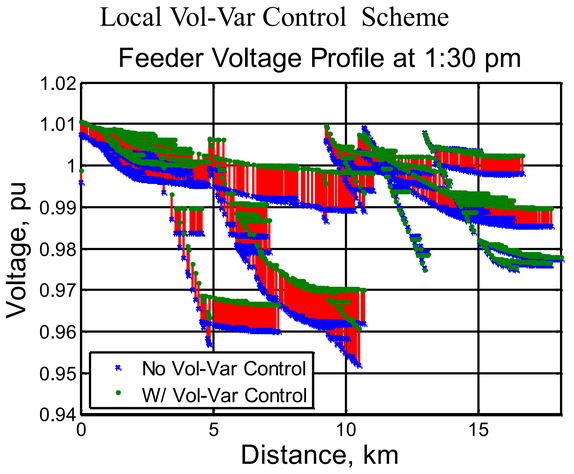


Local Volt-Var control helps to bring the voltage level of the whole feeder up. The red lines show the increase in voltage levels along the feeder.

## Issues with High PV Penetration

High PV penetration leads to various problems observed in both distribution and transmission systems:

- High frequency -> Impact frequency control and generators' synchronization -> power outage.
- Over-voltages -> damage electronic devices (light bulbs, computers, monitors, etc.)
- Voltage fluctuations -> shorten lifetime of voltage regulators, transformers, protection devices, etc.)

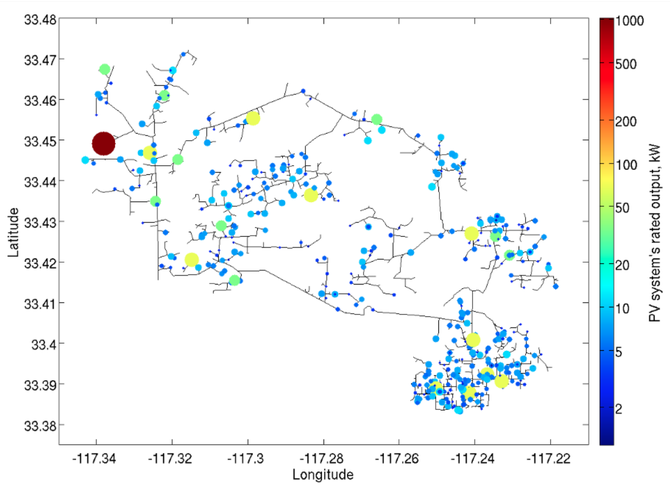


Real 12MW (1733 loads) SDGE distribution feeder with 2.3 MW PV. Simulated case with 5MW installed PV (42%) is shown.

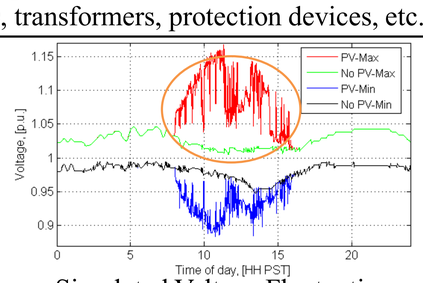


Simulated Voltage Fluctuation

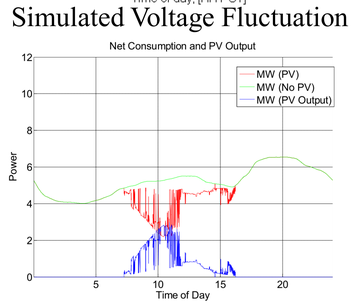


Simulated Power Fluctuation

## Centralized and Distributed Control for PV Inverters and ESSs

We are designing centralized and distributed control for multiple power inverters, storage systems, EV chargers, etc. for UCSD microgrid and SDG&E feeders. The distributed control will (1) mitigate the impact of high penetration PV and (2) optimize the communication and interaction between all devices in smart grid setup.

Cost: $J(u) = \sum_{t\in\tau}(J_{\text{loss}}(u(t)) + \delta J_{\text{power}}(u(t)))$

Optimization Problem:

$$\min_{q_G, v} J$$

$$\text{s.t.} \quad \forall t \in \tau \begin{cases} U_{\min} \le \|u_l(t)\|_C \le U_{\max}, & \forall l \in \mathcal{G}, \\ V_{\text{dis}}^l \le v_l(t) \le V_{\text{ch}}^l, & \forall l \in \mathcal{G} \cup \mathcal{S}, \\ 0 \le x_l(0) + \frac{1}{\beta_l}\sum_{s=1}^{T} v_l(s) \le 1, & \forall l \in \mathcal{G} \cup \mathcal{S}, \\ \text{Power flow equations hold} \end{cases}$$

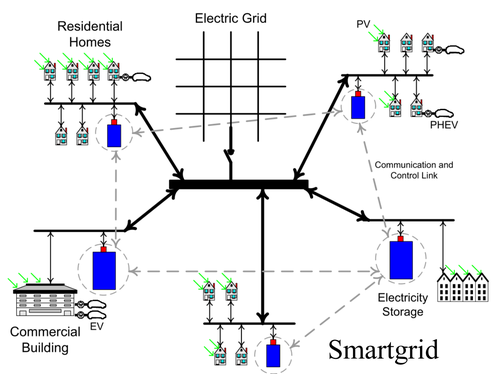


Smartgrid

# Power System Restoration With Transient Stability

**Terrence W.K. Mak**, Hassan Hijazi, and Pascal Van Hentenryck

NICTA — Australian National University

## Power System Restoration

- Why? Natural disasters, infrastructure ageing, operator errors …
- Outcome: A city could be in a total blackout

## Restoration Ordering Problem

- Goal: Compute the best restoration ordering $[x_1, x_2, x_3, \ldots, x_N]$ of damaged items such that loads could be brought up as quickly as possible [PSCC'11]

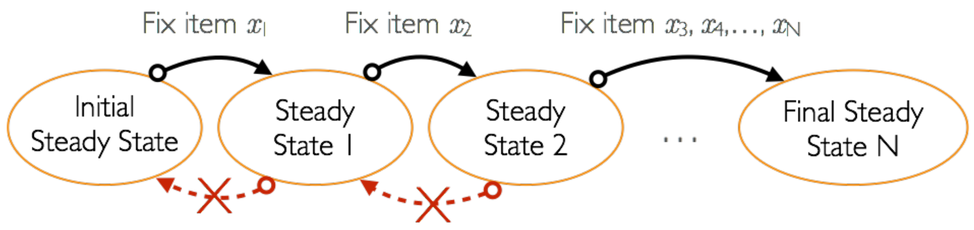


## Transient Stability Assumption

- Assumption: Traversing from one steady state to the other must always be feasible
- What we know: Different generator dispatches will have different rotor stability [PSCC'14]

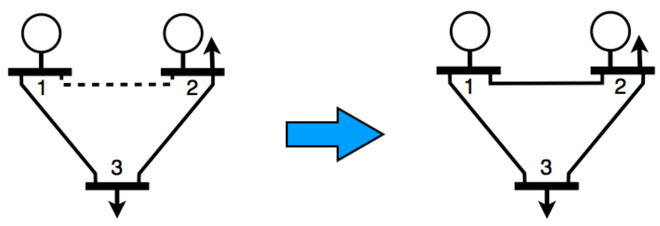


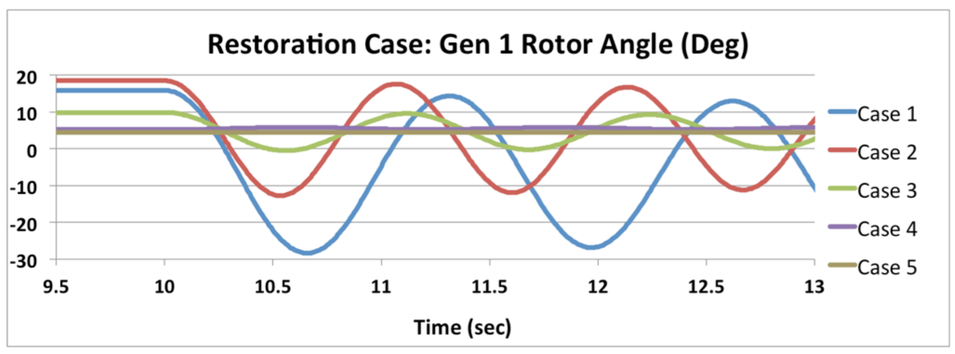


| Case | Bus 1 | Bus 2 | Bus 1 | Bus 2 | Gen 1 Pow. | Gen 2 Pow. | 1st Swing |
|---|---|---|---|---|---|---|---|
| | Volt. (kV) | Volt. (kV) | Ang. (deg) | Ang. (deg) | (MW/Mvar) | (MW/Mvar) | (deg) |
| 1 | 146.28 | 97.24 | 0.00 | -47.58 | 221.12/143.46 | 20.00/18.00 | 44.229 |
| 2 | 146.28 | 146.28 | 0.00 | -35.33 | 207.42/28.05 | 20.00/78.32 | 31.249 |
| 3 | 146.28 | 141.725 | 0 | -12.14 | 102.59/10.66 | 102.59/10.66 | 10.385 |
| 4 | 146.28 | 123.84 | 0.00 | 0.00 | 61.05/48.08 | 143.85/-30.00 | 0.619 |
| 5 | 146.28 | 146.28 | 0.00 | 0.00 | 45.37/6.10 | 157.31/3.16 | 0.002 |

## Stability Enhancement Routine

- Research goal: Given a restoration order, can we guarantee rotor stability?

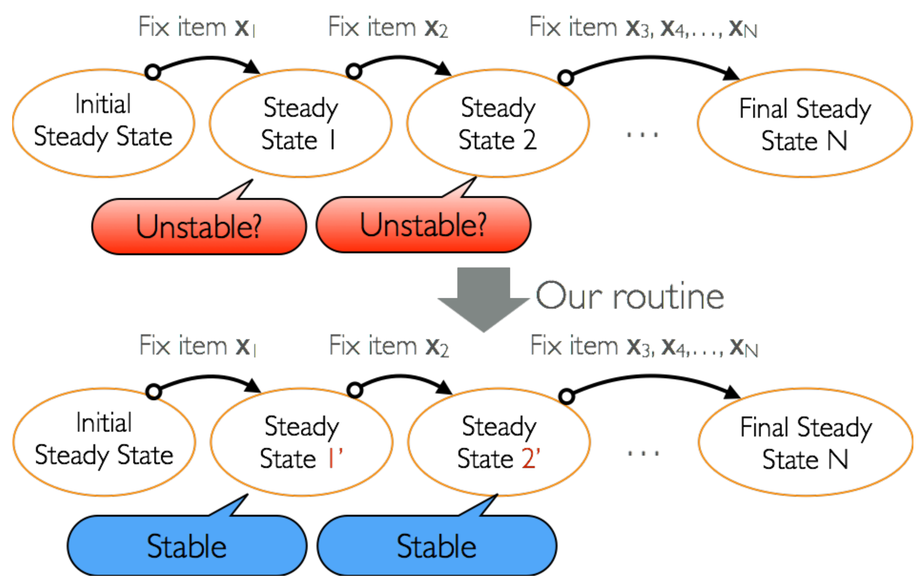


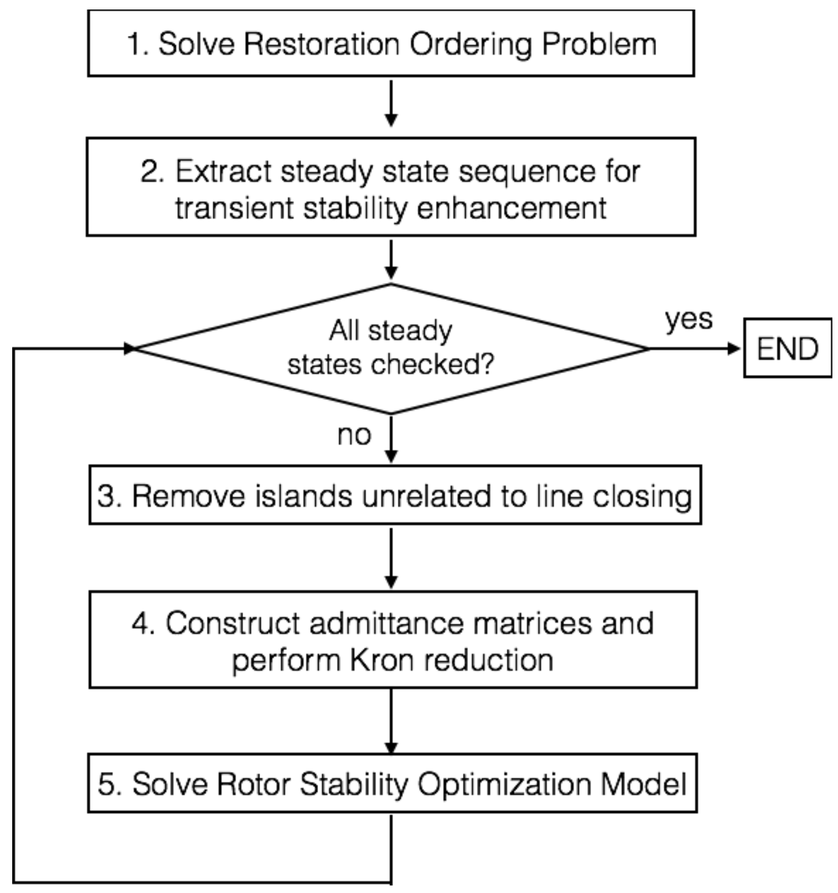


- Challenge: Rotor swings are governed by 1st order differential equations.
- We design a non-linear model including generator dispatches to minimize the rotor swings [AAAI'15]

## Experimental Results

- Study: whether the steady states returned by the ROP are transient-stable
- Measure: Minimum change in generator dispatches to ensure transient stability
- Benchmarks: 6, 14, 30, 39, 57 bus from MATPOWER
- Implementation: AMPL with IPOPT 3.11

| | 6 Bus | | | | 14 Bus | | | | 30 Bus | | | |
|---|---|---|---|---|---|---|---|---|---|---|---|---|
| | Maximum Rotor Swing | | | | Maximum Rotor Swing | | | | Maximum Rotor Swing | | | |
| Gen. Reactance | 90 | 40 | 10 | 1 | 90 | 40 | 10 | 1 | 90 | 40 | 10 | 1 |
| 0.02 | 0.00002 | 0.00002 | 0.00002 | 0.17967 | 0.00000 | 0.00000 | 0.00000 | 6.53902 | 0.00004 | 0.00003 | 0.00004 | 2.91547 |
| 0.06 | 0.00003 | 0.00003 | 0.00003 | 0.10593 | 0.00000 | 0.00000 | 0.00000 | 8.67193 | 0.00004 | 0.00003 | 0.00004 | 3.07084 |
| 0.10 | 0.00003 | 0.00002 | 0.00002 | 0.00843 | 0.00000 | 0.00000 | 0.00000 | 8.18311 | 0.00004 | 0.00004 | 0.00004 | 3.76922 |
| 0.14 | 0.00002 | 0.00003 | 0.00002 | 0.30335 | 0.00000 | 0.00000 | 0.00000 | 6.09923 (1) | 0.00004 | 0.00005 | 0.00004 | 4.17696 |
| 0.20 | 0.00003 | 0.00003 | 0.00003 | 1.01248 | 0.00000 | 0.00000 | 0.00000 | 3.66457 (3) | 0.00004 | 0.00004 | 0.00004 | 4.07680 |

| | 39 Bus | | | | 57 Bus | | | |
|---|---|---|---|---|---|---|---|---|
| | Maximum Rotor Swing | | | | Maximum Rotor Swing | | | |
| Gen. Reactance | 90 | 40 | 10 | 1 | 90 | 40 | 10 | 1 |
| 0.02 | 0.00001 | 0.00001 | 20.52951 | 7.95879 (6) | 0.00000 | 0.00000 | 0.66260 | 131.39311 |
| 0.06 | 0.00001 | 0.00001 | 81.80927 (1) | 0.00002 (7) | 0.00000 | 0.00000 | 1.36766 | 1.12417 (21) |
| 0.10 | 0.42052 | 0.28436 (1) | 78.24781 | 48.13747 (5) | 0.23766 | 0.23766 | 39.33088 | 1.14312 (21) |
| 0.14 | 0.49691 | 0.49698 | 60.35684 | 41.99449 (5) | 0.68299 | 0.67222 (1) | 73.84672 | 1.26118 (21) |
| 0.20 | 0.00002 | 0.00002 | 34.26957 | 69.35875 (3) | 0.83704 | 0.83744 | 120.01411 (1) | 1.41655 (21) |

# Optimal Charging of Vehicle-to-Grid Fleets via PDE Aggregation Techniques


Caroline Le Floch
Civil and Environmental Engineering
University of California, Berkeley
caroline.le-floch@berkeley.edu

*Caroline Le Floch, Florent di Meglio, Scott Moura*


eCAL energy, controls, & applications lab


## Abstract

Vehicle-to-grid (V2G) capable Plug-in Electric Vehicles (PEV) communicates with the grid, stores energy, and can return energy to the electric grid. We develop a novel modeling approach, which is based on a system of partial differential equations (PDEs), to aggregate and control large populations of PEVs. This framework is very well suited and computationally efficient to address tomorrow's challenge of designing the best strategies for PEV smart charging. First, we validate our model on the Vehicle-to-grid simulator (V2G-Sim). Then we demonstrate that this approach can be used to manage fleets of vehicles and permit a PEV aggregator to participate in the regulation market (provide energy to the grid), and supply PEV drivers with sufficient charge.


### Objective

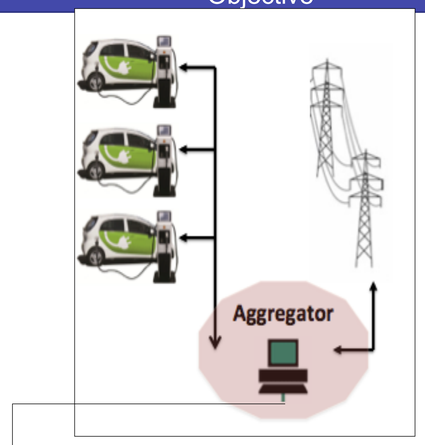


- Develop an aggregation model for large fleets of electric vehicles
- Design a smart control algorithm to participate in the regulation market
- Satisfy drivers' needs for mobility

**Design a combined smart-charging method for thousands / milions of Electric Vehicles**

**Prepare the country for the Transportation revolution**

**Facilitate emergence of V2G aggregators**

## Modeling aggregation of PEVs

### Transport Based model

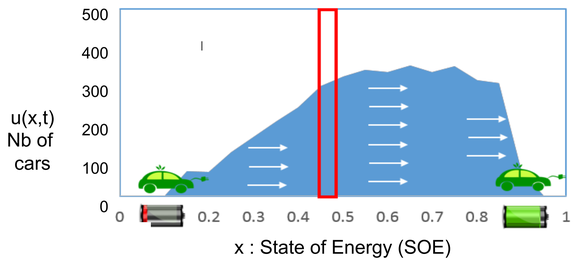


Vehicles charge at rate $q_c$ (x,t)
External flows of vehicles (from road) $\cdot\, \sigma_{i\to c}(x,t)dt.$

$$[u(x,t+dt)-u(x,t)]dx = \quad (6)$$
$$q_c(x,t)u(x,t)dt - q_c(x+dx,t)u(x+dx,t)dt + \sigma_{i\to c}(x,t)$$

### Vehicle-To-Grid Framework

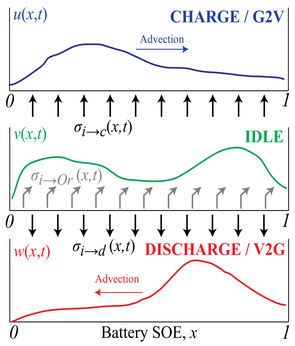


The aggregator controls the number of vehicles in each state:

- G2V: charging u(x,t)
- Idle v(x,t)
- V2G: discharging w(x,t) (sells energy)

Coupled system of PDEs:

$$\frac{\partial u}{\partial t}(x,t) = -\frac{\partial}{\partial x}[q_c(x,t)u(x,t)] + \sigma_{i\to c}(x,t).$$
$$\frac{\partial v}{\partial t}(x,t) = -\sigma_{i\to or}(x,t) - \sigma_{i\to c}(x,t) - \sigma_{i\to d}(x,t),$$
$$\frac{\partial w}{\partial t}(x,t) = \frac{\partial}{\partial x}[q_d(x,t)w(x,t)] + \sigma_{i\to d}(x,t).$$

### Validation

V2G-Sim is an agent-based simulator that models the driving and charging behavior of individual PEVs. It is developed by the Grid Integration Group at LBNL.

V2G-SIM

*Data*: 17805 vehicles in California during a week-day from National Household Travel Survey (NHTS) 2009. The fleet is composed of Nissan Leaf cars.

*2 control cases* : Open-Loop / Discharge during electricity peak hours
*2 charging rates* : L1 chargers (1.44kWh) / L2 chargers (6.6kWh)

$$e(t) = \frac{||(u+v+w)_{PDE}(\cdot,t) - (u+v+w)_{V2Gsim}(\cdot,t)||_2}{||(u+v+w)_{V2Gsim}(\cdot,t)||_2}$$

| Case | Mean error |
|---|---|
| Open Loop L1 charger | 1.1% |
| Open Loop L2 charger | 2.3% |
| V2G control L1 charger | 0.2% |
| V2G control L2 charger | 2.8% |

## Optimal control of vehicles

Choose the best flows between G2V, V2G and Idle (minimize aggregator cost) such that: every driver is satisfied and the aggregator supplies energy to the regulation market. Main assumptions:

- Electricity cost $C_{elec}$, departures $Dep$, regulation power $P^{des}$ are known one day in advance.
- Cars must depart with minimum SOE $X_{dep}$.

### Control Formulation

$$\min_{u,v,w,Dep} \Delta t\ \Delta x \sum_{n=0}^{N}\sum_{j=0}^{J} C_{elec}^n q_j^n w_j^n$$

subject to

$$[u+v+w]^{n+1} + \frac{Dep^{n+1}}{\Delta x} = M_c u^n + M_d w^n + \frac{Arr^{n+1}}{\Delta x}$$

$$u_0^n = 0, \quad v_j^n = 0,$$
$$u_j^0 = u_{0,j}(j\Delta x),\ v_j^0 = v_{0,j}(j\Delta x),\ w_j^0 = w_{0,j}(j\Delta x),\ \forall j,$$

$$u^n, v^n, w^n, Dep^n \geq 0,$$
$$u_j^n = 0\ \forall\ j \geq X_{max}\cdot J$$
$$v_j^n = 0\ \forall\ j \leq X_{min}\cdot J$$
$$w_j^n = 0\ \forall\ j \leq X_{min}\cdot J$$

$$\Delta x \sum_{j=0}^{J} q_{d,j}^n w_j^n \geq P^{des,n}$$
$$\sum_{j=X_{dep}\cdot J}^{J} Dep_j^n = Dem^n$$
$$\Delta x \sum_{j=X_{dep}\cdot J}^{J} u_j^N + v_j^N + w_j^N \geq N_{min}$$

After discretization of PDEs, we formulate the Linear Program above, and solve it using a LP solver.

- Time horizon: 24h
- Number of cars: 2300 (taken from NHTS)
- Charging rate: 1.9kWh

### Result and sensitivity analysis

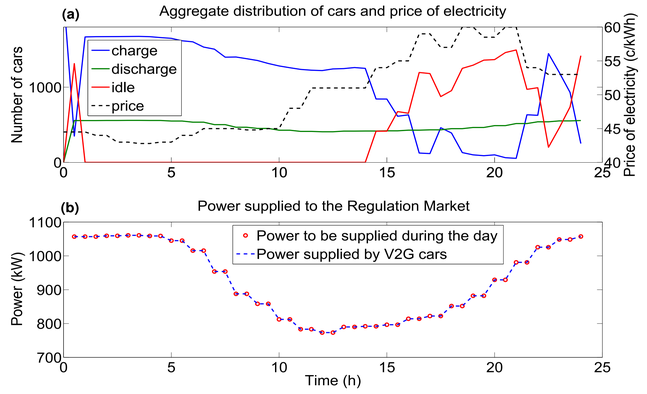


- The aggregator computes flows between idle and G2V: EVs charge when price of electricity is lower.
- V2G cars supply required energy to the grid.

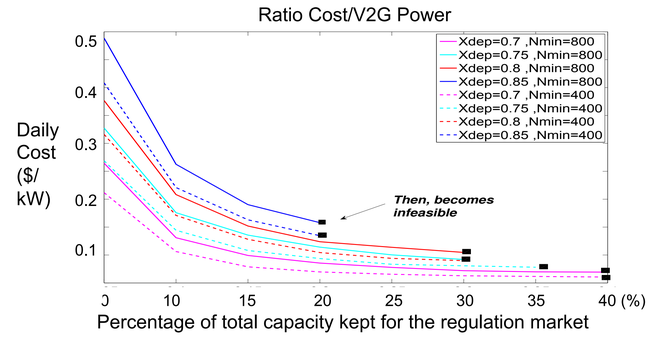


- The optimization allows economies of scale: cost per produced kW decreases as required energy increases.

## Conclusion

- The model is validated, PDE techniques are well suited for large populations of Evs.
- The optimization program allows EV aggregators to optimize their cost while participating to the regulation market and satisfy every driver.

- **How can we integrate grid constraints into this framework?**

## References


[1] S. Bashash and H. Fathy, "Transport-based load modeling and sliding mode control of plug-in electric vehicles for robust renewable power tracking," IEEE Transactions on Smart Grid, vol 3, no. 1, pp. 526–534, March 2012.
[2]W. Kempton and S. E. Letendre, "Electric vehicles as a new power source for electric utilities," Transportation Research Part D: Transport and Environment, vol. 2, no. 3, pp. 157–175, 1997.
[3] http://v2gsim.lbl.gov
[4] S. J. Moura, V. Ruiz, and J. Bendsten, "Observer design for boundary coupled pdes: Application to thermostatically controlled loads in smart grids," in 52nd IEEE Conference on Decision and Control, Florence, Italy, 2013

# Island Russkiy - test field for the research of emergency control in microgrids

Khmelik M.[1,2], Gorte O.[2], Arestova A.[3], Grobovoy A.[3]
Skolkovo Institute of Science and Technology[1], Novosibirsk State Technical University[2],
Novosibirsk State University[3]
E-mail: mikhail.khmelik@skoltech.ru

## Introduction

Russian power system doesn't have any test fields for study and development of scientific, technological and economic solutions in microgrids and virtual power plants (VPP). This fact stops the work on implementing modern technologies on electricity generation, distribution and consumption. However, this topic is one of the prioritized in Europe and US. Taking into account convenient geographical position of Island Russkiy and recently renewed energy infrastructure, as well as potential for solar and wind energy, one can find the island very perceptive, unique test field for experiments and research in microgrids.

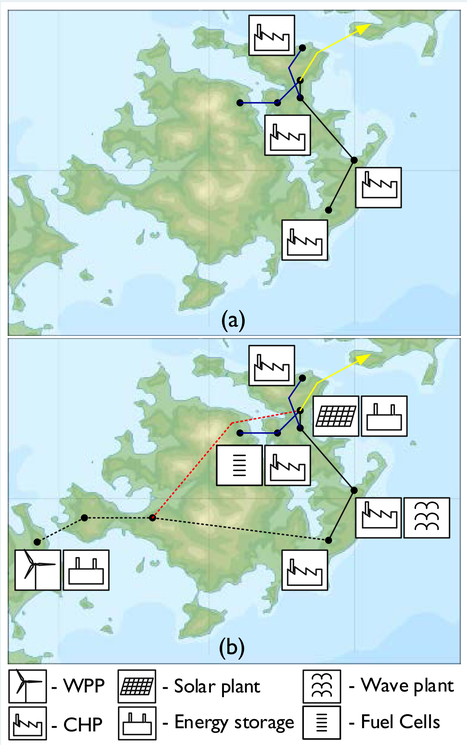


Figure 1 – Possible stages of power system development on the Island.
Solid lines – existing power lines, dashed lines – possible lines.
Voltage levels: yellow color – 220 kV, red – 100 kV, black – 35 kV, blue – 10 kV.

## Methods

The purpose of the work is to test possible smart grid components, such us energy storage devices, for emergency control in the microgrid power system. To do this an adequate mathematical model of Island Russkiy's power system is required.

Thus the first stage was focused on model creation and validation. The base regime is designed so there is a power flow from the main grid to the Island. Then, the following test was set:

Trip of the 220 kV overhead line that connects the Island to Primorskaya power system. The microgrid will operate in islanded mode.

The intent is to show the frequency control possibilities of an energy storage device as well as power oscillations damping during lack of generation.

## Model description

Island Russkiy's power system consists of four combined heat and power plants (CHPs) that have rated capacity from 2.8 to 28.4 MWe (see [1-3] for details) with total rated capacity on the island of 45 MWe.

Generation voltage level is 10 kV and all power plants are connected by 35kV radial cable lines. The microgrid has connection to the mainland by 220 kV marine cable and overhead line, through substation (SS) Russkaya.

Centralnaya CHP is the biggest one with 6 installed gas turbines (28.4 MWe). The highest consumption is Far East Federal University (35 MWe) and is located at the same node.

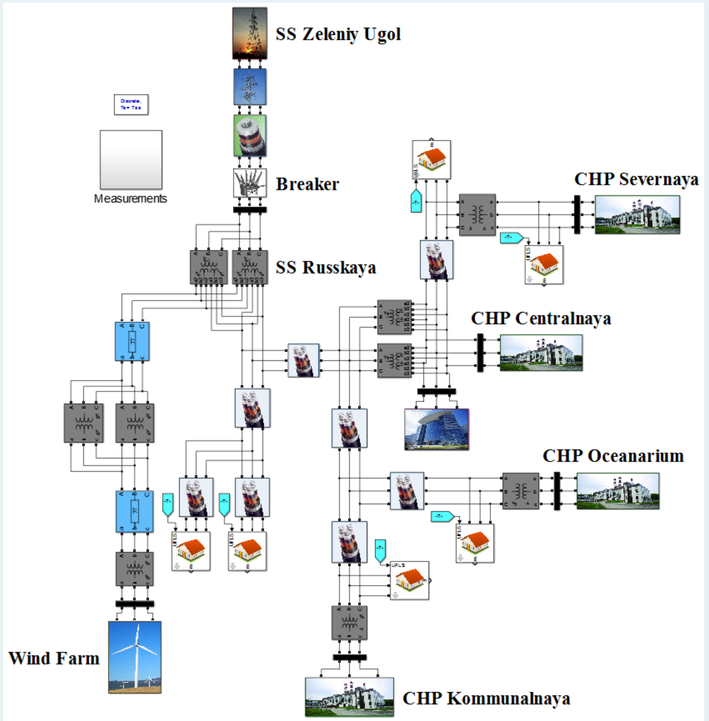


Figure 2 – MATLAB/Simulink model of the power system.

The model of the power system was created in EUROSTAG 5.1 as well as in MATLAB/Simulink. The first software was used for fast modelling of only electromechanical processes in the network. The second one was used for electromagnetic and electromechanical transients in more detailed model – it consists of full models of synchronous machines, Rowen's models for gas turbines [4] and energy storage device (ES) with on converter (figure 3). It was assumed that energy storage has rated capacity of 5 MWe and located on the Far East Federal University campus.

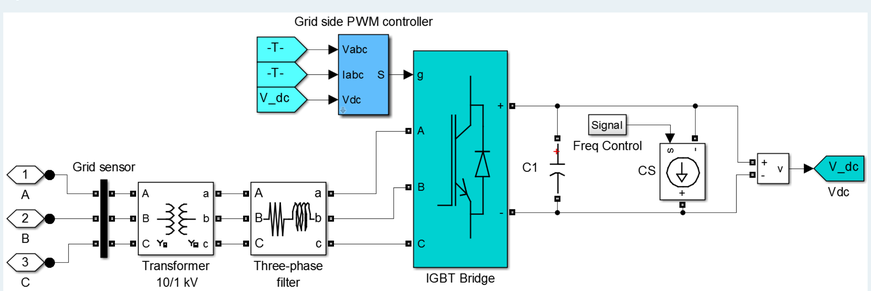


Figure 3 – MATLAB/Simulink model of the energy storage with AC/DC converter.

## Results

For both models disconnection from the grid was simulated. One can see the results for EUROSTAG on figure 4 and for MATLAB/Simulink on figure 5. in both cases under frequency load shedding (UFLS) was modelled as a standard tool for emergency control [5]. Then a joint operation of UFLS and ES was studied.

It is clear that energy storage device can significantly improve the quality of transients. For example, there were no load shedding during operation, after the disturbance. Also the resulting low-frequency oscillations of gas turbines' power due to speed controller characteristics were quickly dumped.

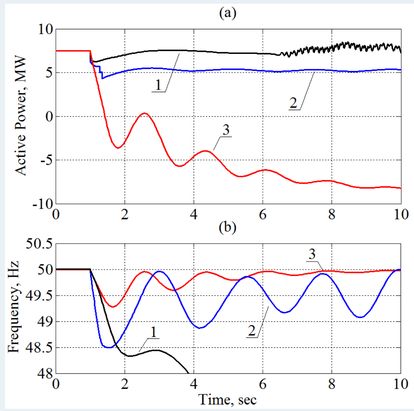


Figure 4 – Energy storage device active power (a) and frequency at the Centralnaya CHP node for EUROSTAG 5.1:
1) no control actions, 2) UFLS, 3) UFLS and ES

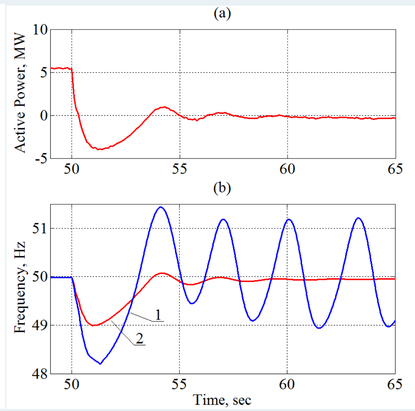


Figure 5 – Energy storage device active power (a) and frequency at the Centralnaya CHP node for MATLAB/Simulink:
1) UFLS, 2) UFLS and ES

## Conclusions

The Russkiy Island may become one of the most convenient places for testing new technologies in Russian power system. This work presents one of the most probable network topologies. Two models were designed based on this network configuration – simplified EUROSTAG 5.1 model and relatively detailed MATLAB/Simulink.

The study was focused on application of energy storage device for frequency control in the system. The results for both models showed that with proper control ES can be highly effective for microgrid stability.

Recently, detailed information on the current structure on Island Russkiy power system was obtained, so future work will be dedicated to model detalization and validation.

## References

[1] K. Skurikhina, A. Arestova, N. Latypova, A. Grobovoy, Island Russkiy Power Network Dynamics 5-th International Conference "Liberalization and Modernization of Power Systems: Smart Technologies for Joint Operation of Power Grids" August 6-10, 2012, Irkutsk, Russia.
[2] A. Grobovoy, A. Arestova, V. Shipilov and others., Application of Gramians method for Smart Grid investigations on the example of the Russky Island Power Network, IREP symposium, August 25-30, 2013, Rethymnon, Greece.
[3] Горте О.И., Кирьянова Н.Г., Остапенко А.И. и др. Остров Русский- экспериментальная база для исследования противоаварийной автоматики микроэнергосистем / XXII научно-практическая конференция «Релейная защита и автоматика энергосистем 2014» / Москва, 2014
[4] W. I. Rowen, "Simplified mathematical representations of heavy duty gas turbines", Transactions of the ASME. Journal of Engineering for Power, vol. 105, pp. 865-70, 1983.
[5] Автоматическое противоаварийное управление режимами энергосистем. Противоаварийная автоматика энергосистем. СТО59012820.29.240.001-2011., Москва, 2011г.

# Approximate-Current Instanton Analysis: Detecting Vulnerability in the Power Grid

*Jonas Kersulis[1], Dr. Michael Chertkov[2], Dr. Scott Backhaus[2], Dr. Ian Hiskens[1]*
1. University of Michigan Electrical Engineering: Systems., 2. Los Alamos National Lab Center for Nonlinear Studies

## Introduction

**Renewable fluctuations add vulnerability to the power grid.**
As renewable generation fluctuates about its forecast, power flows and voltage magnitudes throughout the grid undergo complicated shifts. Most variations are harmless, but even a seemingly benign perturbation can violate network constraints.

**The instanton is the most likely generation pattern that violates a constraint.**
Of all possible generation patterns, some violate network constraints. Of these, the most likely to occur is the instanton.

**The nonlinear AC instanton problem has no guaranteed solution.**
The accuracy of the AC instanton formulation has a price: the problem is non-convex and may not have a solution. This is unacceptable in a real-time environment.

**The linear DC instanton problem has questionable accuracy.**
When the DC power flow approximation is applied to the instanton problem, an analytic solution may be found by matrix inversion. Because the instanton lies on a network constraint, however, DC assumptions (like flat voltage profile) are suspect.

**Accommodating non-flat voltage profiles improves instanton accuracy.**
The new method maintains convexity while accommodating non-flat voltage profiles and reactive power injections.

## Objectives

1. To use approximate AC methods to develop an instanton-finding tool with
   a) greater accuracy than DC instanton method,
   b) guaranteed convergence,
   c) rapid solution time (sub-exponential in network size), and
   d) insightful output (ranked list of extreme events, reconfiguration assistance)
2. To characterize differences between DC and approximate AC instanton methods
3. To understand differences between DC and approximate AC power flow methods

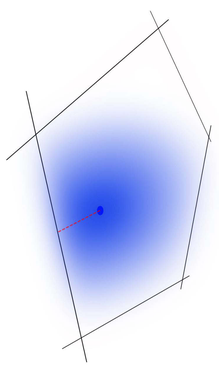

Two-dimensional depiction of instanton search. Starting from the forecast (dot), the dashed line shows the most likely shift in generation that would violate a constraint (solid line).

## New Method: Current Constraint

**Convexified network constraints form a tractable polytope.**
Network constraints form a high-order polytope. Because this object may be expressed in terms of renewable generation, our optimization scheme can minimize over each face separately to obtain a ranked list of extreme events.

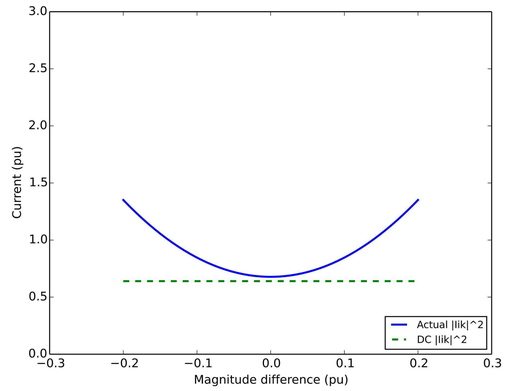


Comparison of improved current model with DC model

**Constrained optimization formalizes the instanton problem.**
By definition, the instanton is the most likely renewable generation pattern that violates one or more network constraints. To find the instanton candidate for a single constraint, we minimize deviation from forecast while saturating that constraint.

$$\min \frac{1}{2}(\boldsymbol{Q}_R - \boldsymbol{Q}_R^0)^\top \boldsymbol{\Lambda}(\boldsymbol{Q}_R - \boldsymbol{Q}_R^0)$$

subject to network constraints and saturated constraint

Previous analysis uses DC power flow assumptions: 1) no line resistance, 2) small angle differences, 3) flat voltage profile, 4) no reactive power flows. Retain first two assumptions, drop last two.

Approximate expressions for real and imaginary current:

$$Re(I_{ik}) \approx -B_{ik}[Im(E_i) - Im(E_k)]$$
$$Im(I_{ik}) \approx B_{ik}[Re(E_i) - Re(E_k)]$$

Square each term to obtain approximate current magnitude:

$$|I_{ik}|^2 \approx B_{ik}\left(V_i^2 + V_k^2 - 2V_iV_k\cos\theta_{ik}\right)$$

Solve for angle:

$$\theta_{ik} = \cos^{-1}\left(\frac{V_i^2 + V_k^2 - \left(\left|I_{ik}^{lim}\right|x_{ik}\right)^2}{2V_iV_k}\right)$$

Compare with DC constraint: $\theta_{ik} = x_{ik}P_{ik}^{\lim}$

Any line with significant voltage difference is more vulnerable than DC instanton analysis says.

PQ decoupling means we can pre-compute voltage magnitudes from reactive injections. (If voltages were not fixed, we would need to approximate cosine.)

## Acknowledgements

- Dr. Hiskens, my adviser
- Dr. Chertkov for hosting me at LANL this past summer
- Dr. Backhaus for discussions and decisions
- Dr. Bent for implementation discussions
- Miles Lubin for introducing me to Julia/JuMP
- Yury Dvorkin for stimulating discussions

*Funding from Department of Energy Grid Science Initiative*

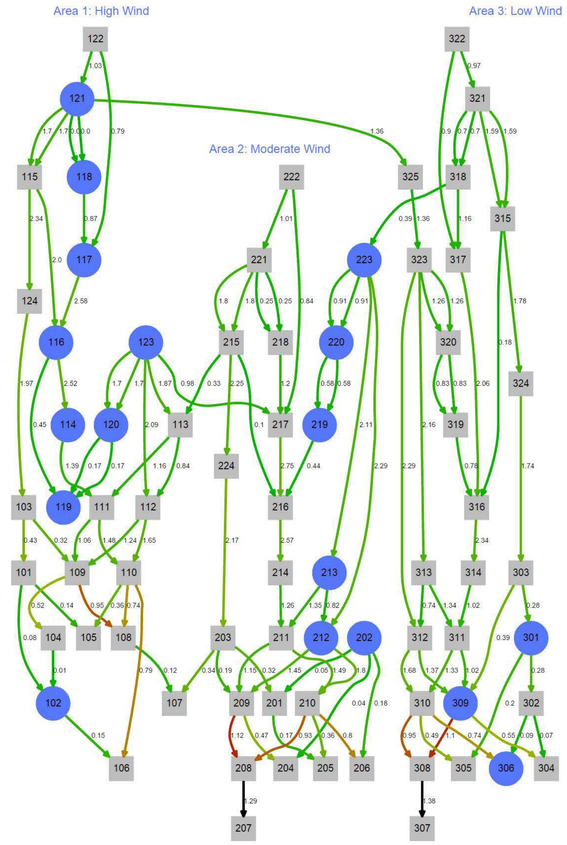


Implementation on IEEE RTS-96 Network

## References

[1] Baghsorkhi, S.S., and I.A. Hiskens. “Analysis Tools for Assessing the Impact of Wind Power on Weak Grids,” 1–8, 2012.

[2] Coffrin, Carleton, and Pascal Van Hentenryck. “A Linear-Programming Approximation of AC Power Flows,” unpublished.

[3] Coffrin, Carleton, P. Van Hentenryck, and R. Bent. “Approximating Line Losses and Apparent Power in AC Power Flow Linearizations.” In *2012 IEEE Power and Energy Society General Meeting*, 1–8, 2012.

# Stochastic Modeling and Simulations of Thermostatically Controlled Loads


**M. Goldshtein[a], V. Chernyak[b], M. Chertkov[c]**

[a] Moscow Institute of Physics and Technology (State University), Dolgoprudny, Moscow Region, Russia
[b] Department of Chemistry, Wayne State University, Detroit, MI, USA
[c] Theoretical Division, Los Alamos National Laboratory, Los Alamos, NM, USA


## Abstract


We study a stochastic model of an ensemble of Thermostatically Controlled Loads. The study includes direct Markov Chain simulations of the ensemble, validation of the results against the Fokker-Planck type of theory in the regimes amenable for analytics, and then numerical exploration of various non-equilibrium properties of the system in more challenging regimes, e.g. analyzing response to demand response perturbations of practical interest. This is an early report on the study aimed at designing new controls of the TCL ensembles.


## The simplest model without control

The simplest model describes a behavior of a large number N of identical customers under the effect of the ambient. The state of a customer is characterized by the temperature, denoted by T. Stochastic dynamics for the temperature relaxation process is given by the Langevin equation:

$\dot{T} = -\frac{1}{\tau}(T - T_{out}) + \xi(T,t)$, where the Gaussian noise $\xi(T,t)$ is assumed be $\begin{cases} <\xi(t)> = 0 \\ <\xi(t_1)\xi(t_2)> = D\cdot\delta(t_1 - t_2) \end{cases}$

The Fokker-Plank equation, established for such a system:

$$\begin{cases} \dot{\rho} = \frac{1}{\tau}\partial_T[(T - T_{out})\rho] + \frac{D}{2}\partial_{TT}^2\rho \\ \rho(T,0) = \delta(T - T_0) \end{cases}.$$

The solution:

$$\rho(T,t) = \frac{1}{\sqrt{\pi D\tau}}\cdot\frac{1}{\sqrt{1-e^{-2t/\tau}}}\cdot\exp\left(-\frac{\left((T-T_{out})+(T_{out}-T_0)e^{-t/\tau}\right)^2}{D\tau\left(1-e^{-2t/\tau}\right)}\right).$$

The simple iteration method in application to the Langevin equation:

$$T_{i+1} = T_i - \frac{dt}{\tau}(T_i - T_{out}) + \xi\sqrt{dt}.$$

## Two states control modelling

In the two states control modeling the state of a customer is described by the inside temperature, denoted by T and a discrete variable j that attains values j = 2 and j = 1 for the device (air conditioner) being off and on, respectively. Each regime is given by the Langevin equation aforementioned:

$$\dot{T} = -\frac{1}{\tau}(T - T_j) + \xi(T,t),$$

where $T_2$ and $T_1$ are the outside temperature and the inside temperature for permanently working air conditioner. We set dead-bands by initiating the bounds of the comfort zone $T_{down}$ and $T_{up}$. Achieving one of them we change over the conditioner program.
The system of Fokker-Plank equations, established for such a model:

$$\begin{cases} \frac{\partial\rho_1}{\partial t} = \frac{D}{2}\frac{\partial^2\rho_1}{\partial T^2} - \frac{\partial}{\partial T}(f_1(T)\rho_1) - r_{21}(T)\rho_2 + r_{12}(T)\rho_1 \\ \frac{\partial\rho_2}{\partial t} = \frac{D}{2}\frac{\partial^2\rho_2}{\partial T^2} - \frac{\partial}{\partial T}(f_2(T)\rho_2) - r_{12}(T)\rho_1 + r_{21}(T)\rho_2 \end{cases},$$

where $\begin{cases} f_j = -\frac{1}{\tau}(T - T_j) \\ r_{12}(T) = \mathrm{r}\cdot\theta(T - T_{up}) \\ r_{21}(T) = \mathrm{r}\cdot\theta(T - T_{down}) \end{cases}$

We use $r \to \infty$ limit, because it is a correct way to describe the situation of instantaneous switching, once out of range.

## Results of the simplest model simulations

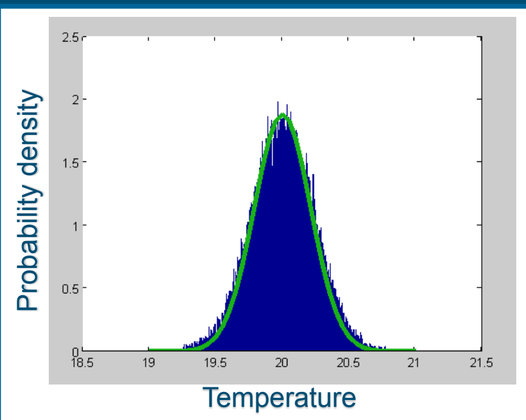


The stationary temperature distribution

Green line – solution to the Fokker-Plank equation

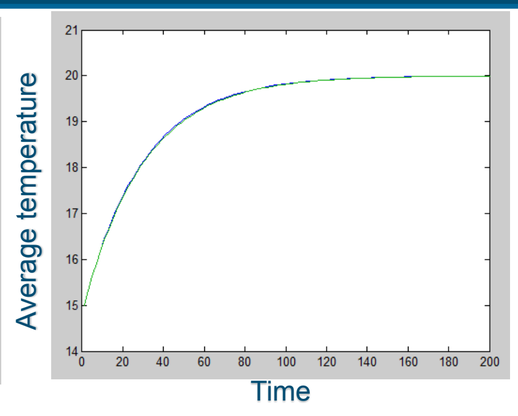


The average temperature dependence on time.

Blue line – simulation result
Green line – theoretically established function
$T_{average}(t) = T_{out} - (T_{out} - T_0)e^{-t/\tau}$

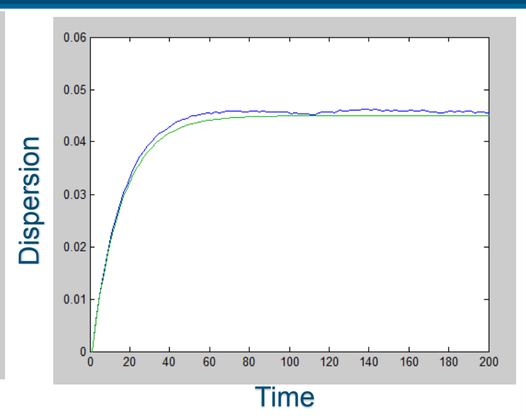


The dispersion dependence on time.

Blue line – simulation result
Green line – theoretically established function
$\sigma(t) = \frac{D\tau}{2}(1 - e^{-2t/\tau})$

**Simulation parameters** N = 50 000 Mtime = 1000 (dt = 0.01) D = 0.3 $\tau = 0.3$ $T_{out} = 20^0C$ $T_0 = 15^0C$

A range of parameters, such as D, $\tau$, $T_{out}$, N and Mtime, effect the temperature relaxation process. The more D or $\tau$ are, the wider the temperature distribution is and the more the stationary dispersion value is. The less dt is, the closer to reality we are, but the more time steps we have to do to achieve the stationarity so the more the time of calculations is. The diminution between $T_{out}$ and $T_0$ influences the relaxation time.

## Results of the two states control model simulations

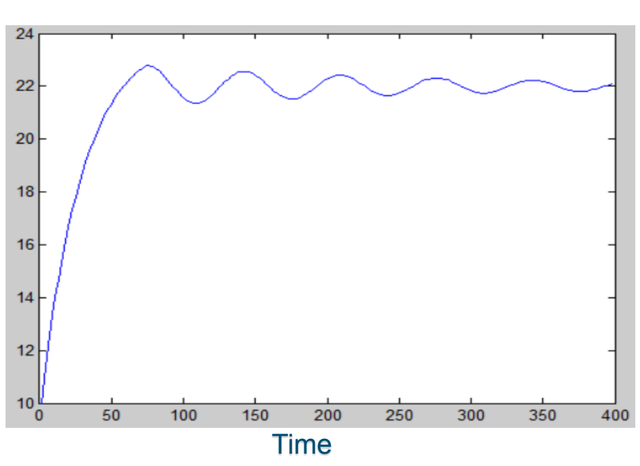


The average temperature dependence on time.

Perturbations are quite high at the beginning, but they are decreasing in time.

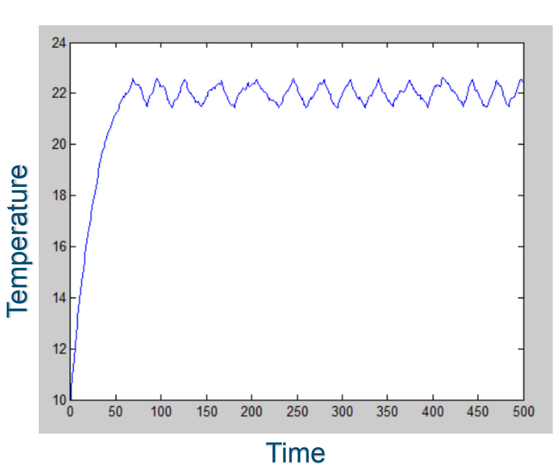


The temperature of a random customer on time.

Because of control the customers go back and forth between dead-bands passing round.

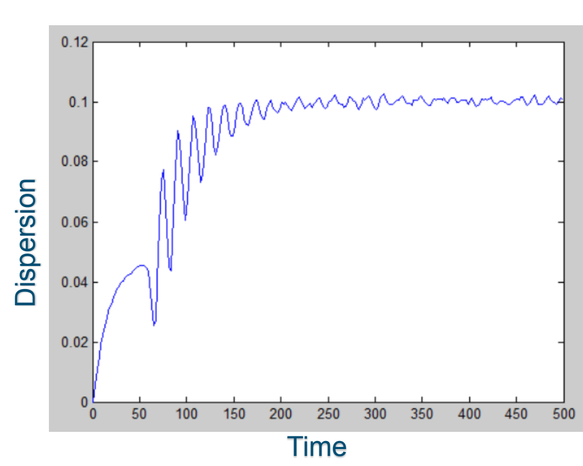


The dispersion dependence on time.

While all customers are switched off/on, the dispersion is as the same as in the simplest case without control. Perturbations of the dispersion are decreasing in time quite slowly.

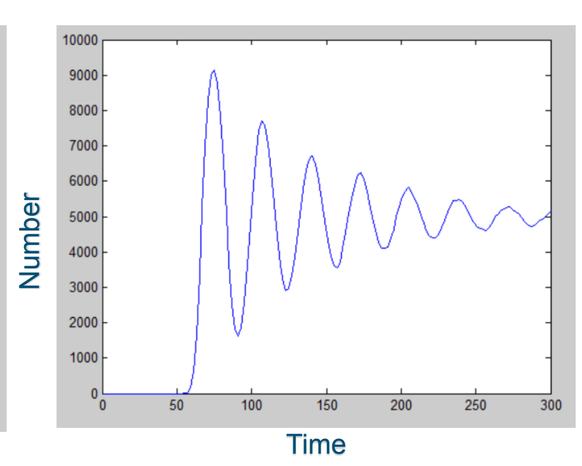


The number of ON-state customers on time.

Because of noise perturbations are decreasing in time and approaching to N/2. If we set, for example, heating force bigger than the freezing one, the stationary number will be bigger.

**Simulation parameters** N = 100 000 Mtime = 1000 dt = 0.01 D = 0.3 $\tau = 0.3$ $T_0 = 10^0C$ $T_1 = 20^0C$ $T_2 = 24^0C$ $T_{down} = 21^0C$ $T_{up} = 23^0C$

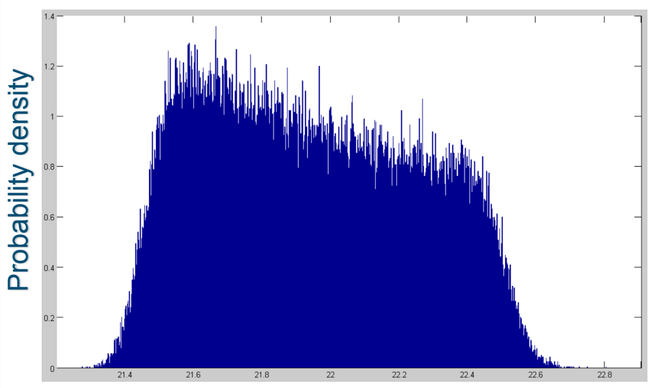


The stationary temperature distribution for ON-state customers

The peak is shifted to the left because the freezing force is getting less effective with the temperature decreasing.

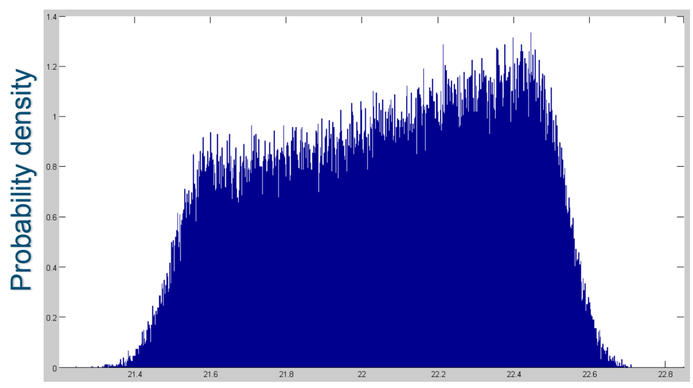


The stationary temperature distribution for OFF-state customers

The peak is shifted to the right because the heating force is getting less effective with the temperature increasing.




The stationary temperature distribution for all customers

**Simulation parameters**
N = 200 000 Mtime = 500 (dt = 0.01) D = 0.3 $\tau = 0.3$ $T_0 = 10^0C$ $T_1 = 20^0C$ $T_2 = 24^0C$ $T_{down} = 21^0C$ $T_{up} = 23^0C$

The probabilities of having any temperature from 21.6℃ to 22.4℃ are the same. The character of distribution tails is effected by noise.

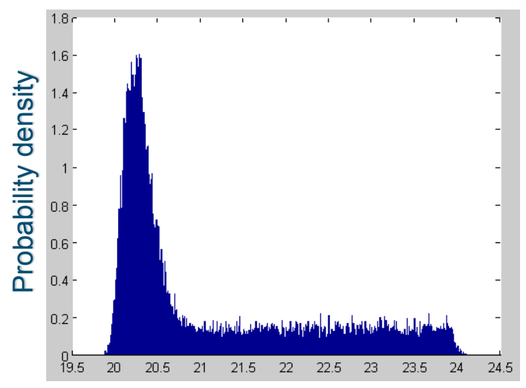


The stationary temperature distribution for ON-state customers

The freezing force is negligible close to $T_1$.

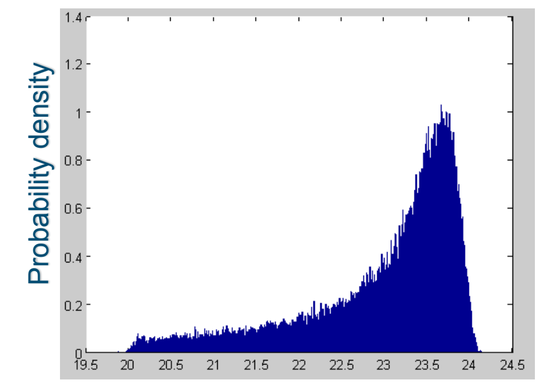


The stationary temperature distribution for OFF-state customers

The heating force is negligible close to $T_2$.

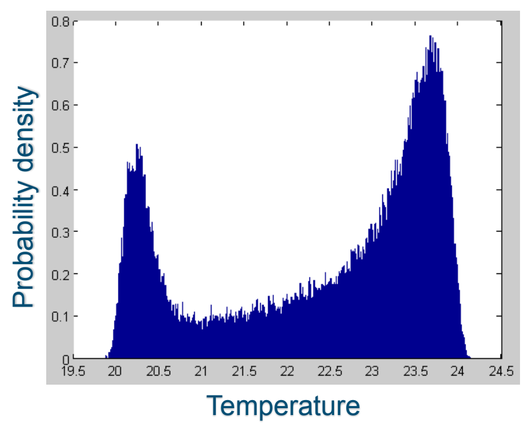


The stationary temperature distribution for all customers

**Simulation parameters**
N = 200 000 Mtime = 500 (dt = 0.01) D = 0.3 $\tau = 0.3$ $T_0 = 10^0C$ $T_1 = 20^0C$ $T_2 = 24^0C$ $T_{down} = 20^0C$ $T_{up} = 24^0C$

The closer to dead-band the temperature is, the more important the role of noise becomes.

## Conclusion and plans for future

We have researched some system properties concerning to stationary temperature distributions and some time-variable characteristics in different regimes. These results are preliminary. In the nearest future we are planning to validate our results theoretically. The system behavior researching brings us to creation of an algorithm of demand-response control.

# On Reactive Power Flow and Voltage Stability in Microgrids

**Basilio Gentile and Florian Dörfler**
Automatic Control Laboratory, ETH Zürich

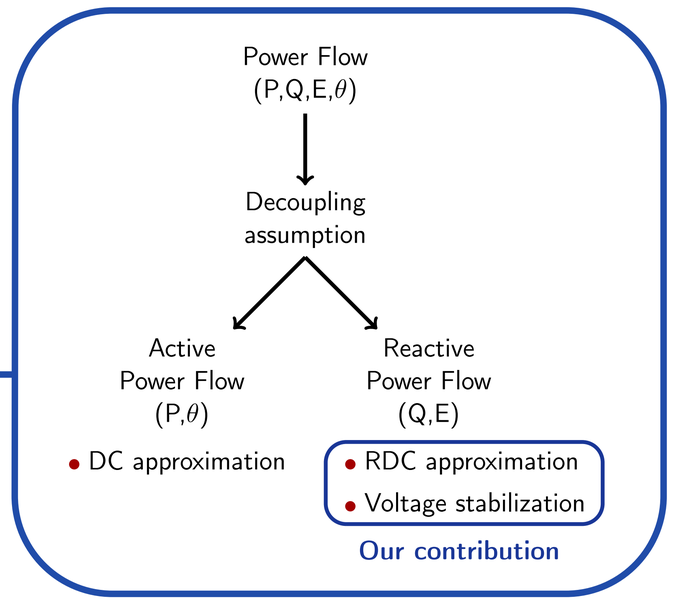


## ABSTRACT

As of today, solutions to the reactive power flow can be found only via numerical methods, yet an analytical understanding would be beneficial to the rigorous design of future electric grids. Firstly, for sufficiently high reference voltages, we guarantee the existence of a high-voltage solution for the reactive power flow and provide its approximate analytical expression (RDC approximation). We validate the accuracy of our approximation through numerical simulation of the IEEE 37 test case. Secondly, we consider a recently proposed droop control for voltage stabilization in a microgrid equipped with inverters. We prove the existence and the exponential stability of a high-voltage fixed point of the closed-loop dynamics. We provide an approximate expression for this fixed point.

## TWO-NODE GRID

Figure 1 shows a grid composed by a source (or PV bus) and a load (or PQ bus), connected by a power line. The reactive power flow at the load reads

$$Q_L = V_L^2 \ell - V_L V_S \cos(\theta_L - \theta_S)\ell - V_L V_S \sin(\theta_L - \theta_S) g \simeq V_L^2 \ell - V_L V_S \ell \,. \qquad (1)$$

The last approximation derives from the fact that during regular power system operation the angles difference is negligible.

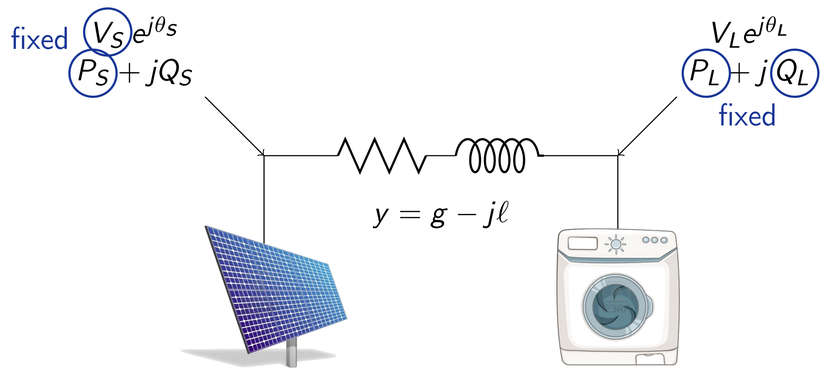


*Figure 1:* two-node grid

In the two-node case (1) becomes a second order equation with solution

$$V_{L,1,2} = V_S \left( \frac{1}{2} \pm \frac{1}{2} \sqrt{1 + \frac{4 Q_L}{\ell V_S^2}} \right) \qquad \text{if} \quad V_S \geq \sqrt{-\frac{4 Q_L}{\ell}} \,.$$

If $4Q_L/(\ell V_S^2) \ll 1$ the first-order Taylor expansion of the square root yields

$$V_{L,1} \simeq V_S + \frac{Q_L}{\ell V_S}, \qquad V_{L,2} \simeq -\frac{Q_L}{\ell V_S} \,.$$

The solution $V_{L,1}$ is the desired one, as it corresponds to a high-voltage low-current configuration for the network, resulting in low power losses. We can interpret the solution as being an odd-exponent power expansion in the source voltage $V_S$, with the first term neglected being of the order of $1/V_S^3$.

## RDC APPROXIMATION

In order to generalize the concepts introduced with the two-node grid, we model a power network in synchronous steady-state as a connected graph (see Figure 2). The nodes of the graph are partitioned into sources (or PV buses, red circles in Figure 2) and loads (or PQ buses, blue squares in Figure 2); the edges represent the power lines.
By applying the same decoupling assumption introduced for the two-node case, the reactive power flow reads

$$Q_L = \mathrm{diag}(V_L) \begin{bmatrix} L_{LL} & L_{LS} \end{bmatrix} \begin{bmatrix} V_L \\ V_S \end{bmatrix} \,. \qquad (2)$$

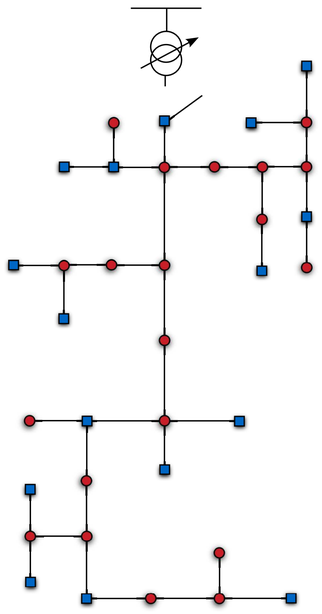

*Figure 2:* IEEE 37 grid

It is not possible to derive an explicit analytic solution for the system (2) of quadratic equations in the variables $V_L$, yet the practical importance of the reactive power flow motivates the interest in extending the results of the two-node case to the system (2). To this end the preliminary concepts of source baseline voltage $V_N$ and source voltage spread $\eta$ must be introduced:

$$V_N := \min_i \{V_i,\, i \in S\} \qquad \eta : \; V_S = (\mathbb{1} + \eta) V_N .$$

**Theorem (RDC approximation).**

If $E_N > \sqrt{\dfrac{4 ||L_{LL}^{-1}|| \cdot ||Q_L||}{\min_i \{|1 + (L_{LL}^{-1} L_{LS} \eta)_i|^2\}}}$ the reactive power flow admits the solution

$$V_L = V_L^{RDC} + \mathcal{O}\left(\frac{1}{V_N^3}\right)$$

$$\text{where} \quad V_L^{RDC} := V_N (\mathbb{1} - L_{LL}^{-1} L_{LS} \eta) + \frac{1}{V_N} \left( L_{LL}^{-1} \mathrm{diag}^{-1} (\mathbb{1} - L_{LL}^{-1} L_{LS} \eta) Q_L \right) .$$

It is worth noticing that the threshold above which the existence of a solution is guaranteed is a generalization of the threshold found for the two-node grid; in the same way, the RDC approximation $V_L^{RDC}$ generalizes the Taylor-expansion proposed in the two-node case.

## NUMERICAL ACCURACY

We studied the IEEE 37 test case (Figure 2) and compared the RDC approximation to the numerical solution of the system (2), for different values of the baseline voltage $V_N$. Figure 3 reports the relative approximation error: we can notice that at the network operating voltage of 4.8 kV the relative error is of the order of $10^{-6}$.
Moreover, one can measure from the plot that the approximation error tends to zero as $1/V_N^3$, as predicted by the above Theorem.

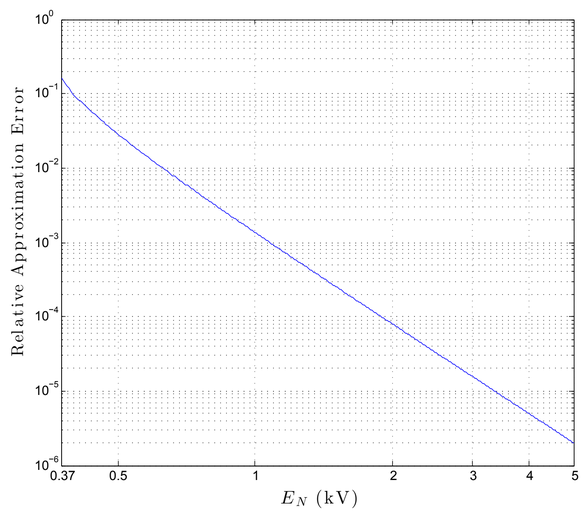


*Figure 3:* the relative approximation error

## APPLICATION TO DROOP CONTROL

The RDC approximation can be used to study the problem of voltage stabilization in an inverter-based microgrid. The sources of the grid represent inverters which are regulated by [2]:

$$\dot{V}_i = -C_i V_i (V_i - V_i^R) - Q_i \,, \qquad i \in S \,,$$

where $V_i^R$ is the reference voltage for inverter $i$ and $C_i$ is a fixed parameter. Coupling this control law with the reactive power flow (1) yields

$$\begin{bmatrix} \mathbf{0} \\ \dot{V}_S \end{bmatrix} = \begin{bmatrix} Q_L \\ C \mathrm{diag}(V_S)(V_R - V_S) \end{bmatrix} - \mathrm{diag}(V) L V \,.$$

By using the RDC approximation it is possible to show that such differential-algebraic system possesses a high-voltage locally exponentially stable fixed point and to provide an approximate expression of the fixed point.

## REFERENCES

[1] B. Gentile, J. W. Simpson-Porco, F. Dörfler, S. Zampieri, and F. Bullo, "On reactive power flow and voltage stability in microgrids," in *American Control Conference*, Portland, OR, USA, June 2014.

[2] J. W. Simpson-Porco, F. Dörfler, and F. Bullo, "Voltage stabilization in microgrids via quadratic droop control," in IEEE Conf. on Decision and Control, Florence, Italy, Dec. 2013, pp. 7582–7589.

# Structure Learning and Statistical Estimation in Radial Distribution Networks

DEEPJYOTI DEKA, MICHAEL CHERTKOV, AND SCOTT BACKHAUS
deepjyotideka@utexas.edu, chertkov@lanl.gov, and backhaus@lanl.gov

## MOTIVATION

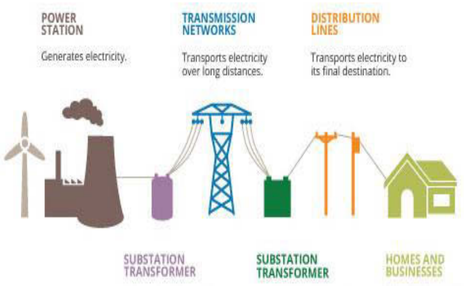


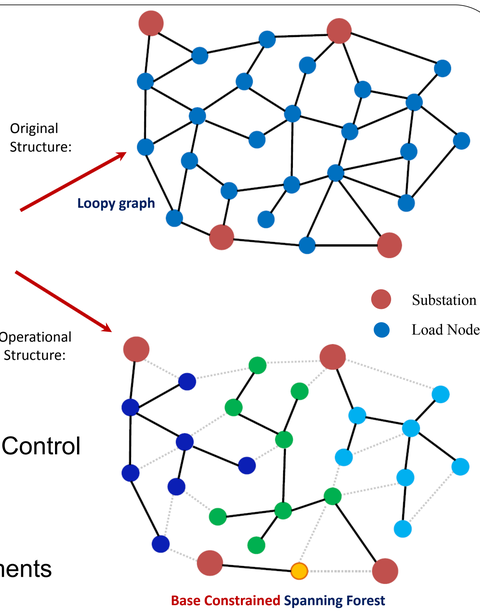


**Distribution Grid**

- ❑ Final tier in electricity transfer
- ❑ Influences: Demand Response/ Smart Control
- ❑ Insufficient measurements

**Data available:** *(No line data)*

- ❑ Node voltage and/or phasor measurements

## SYSTEM MODEL

**AC power flow:**

$$P_a + \hat{i}Q_a = \sum_{(a,b)\text{ is edge}} \frac{\varepsilon_a e^{\hat{i}\theta_a}\left(\varepsilon_a e^{-\hat{i}\theta_a} - \varepsilon_b e^{-\hat{i}\theta_b}\right)}{(R_{ab} - \hat{i}X_{ab})}$$

*** **LC lossless power flow** ***

$$V_a = \varepsilon_a - 1 \approx 0,\ \theta_a \approx 0$$

$$P = (M^T B M)\theta + (M^T G M)V = H_B\theta + H_G V$$
$$Q = -(M^T G M)\theta + (M^T B M)V = -H_G\theta + H_B V$$

$$\theta = H_{1/X}^{-1}P - H_{1/R}^{-1}Q$$
$$V = H_{1/R}^{-1}P + H_{1/X}^{-1}Q$$

Additive & Separable *(Good)*
Has weighted Laplacians *(Better)*

$\Sigma_V = \mathbb{E}[VV^T]$ ➢ *Second Moment*

$\Omega_V = \mathbb{E}[(V-\mu_V)(V-\mu_V)^T]$ ➢ *Covariance*

## TREES ARE GOOD!!

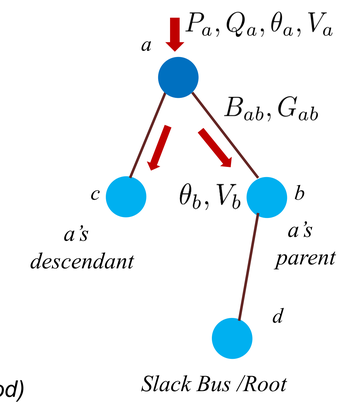


$$M = \begin{pmatrix} 1 & -1 & 0 & 0 \\ 1 & 0 & -1 & 0 \\ 0 & 1 & 0 & -1 \end{pmatrix} \qquad M^{-1} = \begin{pmatrix} 1 & 0 & 1 \\ 0 & 0 & 1 \\ 1 & -1 & 1 \end{pmatrix}$$

Reduced Incidence Matrix: *INVERSE IS 0 - 1*

$$H_B = \begin{pmatrix} B_{ab}+B_{ac} & -B_{ab} & -B_{ac} \\ -B_{ab} & B_{ab}+B_{bd} & -B_{bd} \\ -B_{ac} & 0 & B_{ac} \end{pmatrix}$$

Reduced Weighted Laplacian Matrix

$H_B^{-1}(a,b) = \sum_{(i,j)\in E_a \bigcap E_b} \frac{1}{B_{ij}}$ ***TRACTABLE*** INVERSE

*sum of inverse susceptance of lines common to paths from a & b to slack bus*

## SUMMARY OF RESULTS

**Considered Learning Problems:**

- ❑ ***Structure Learning***: current operational state
- ❑ Estimation of ***Load Statistics*** (mean/correlations)
- ❑ Learning with ***Missing Data*** (limited observations)

**Potential Uses**

- ➢ Failure detection
- ➢ Flow optimization
- ➢ Non-intrusive control
- ➢ Privacy quantification

## STATISTICAL TRENDS IN TREES

❑ If node ***b*** is parent of node ***a***,

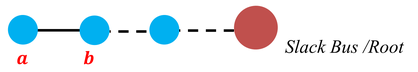


- $\Sigma_V(a,a) > \Sigma_V(b,b)$
- $\Omega_V(a,a) > \Omega_V(b,b)$
- *Highest second-moment at* ***leaf node***

- $\mathbb{E}[(V_a - V_b)^2] = \sum_{k_1,k_2 \in D_a^{\mathcal{T}_i}} R_{ab}^2 \Sigma_P(k_1,k_2) + 2R_{ab}X_{ab}\Sigma_{PQ}(k_1,k_2) + X_{ab}^2\Sigma_Q(k_1,k_2)$
- *Mean sq. difference contributed only by* ***descendant nodes***

- $b = \arg\min_{k \notin D_a^{\mathcal{T}_i}} \mathbb{E}[(V_a - \mu_{V_a}) - (V_k - \mu_{V_k})]^2$
- *Minimum mean sq. centered difference among non-descendants at* ***parent***

## STRUCTURE LEARNING ALGORITHMS

❑ **ASSUMPTIONS considered**

➢ $\Sigma_P(a,b) > 0, \Sigma_Q(a,b) > 0, \Sigma_{PQ}(a,b) > 0$

➢ $\Omega_{QP}(a,a) \geq 0$
$\Omega_P(a,b), \Omega_Q(a,b), \Omega_{QP}(a,b) \quad = 0 \forall a \neq b$

** *All load nodes are energy consumers*

** *Fluctuations at different nodes are uncorrelated, at same node are aligned*

❑ **ALGORITHM:**

- Pick undiscovered node ***b*** with largest $\Sigma_V$ OR $\Omega_V$
- For every discovered node ***a***, join ***b*** with ***a*** if

$$\mathbb{E}[(V_a - V_b)^2] = \sum_{k_1,k_2 \in D_a^{\mathcal{T}_i}} R_{ab}^2 \Sigma_P(k_1,k_2) + 2R_{ab}X_{ab}\Sigma_{PQ}(k_1,k_2) + X_{ab}^2\Sigma_Q(k_1,k_2)$$

If $\Sigma_P, \Sigma_Q, \Sigma_{PQ}$ are known

OR

$$b = \arg\min_{k \notin D_a^{\mathcal{T}_i}} \mathbb{E}[(V_a - \mu_{V_a}) - (V_k - \mu_{V_k})]^2$$

If $\Omega_P, \Omega_Q, \Omega_{PQ}$ are diagonal

- Estimate means, covariances of power injection using LC power flow equations.

## SIMULATION RESULTS

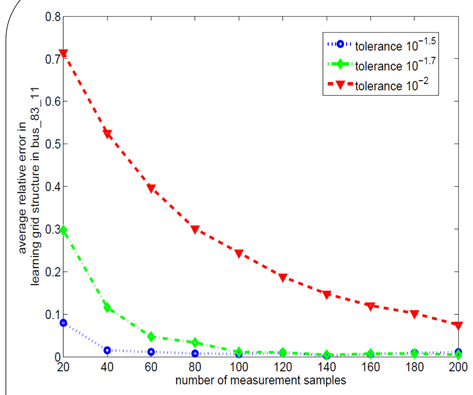


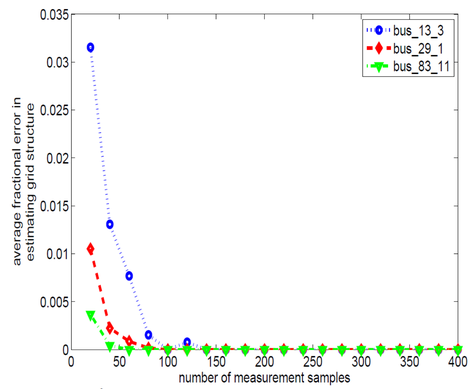


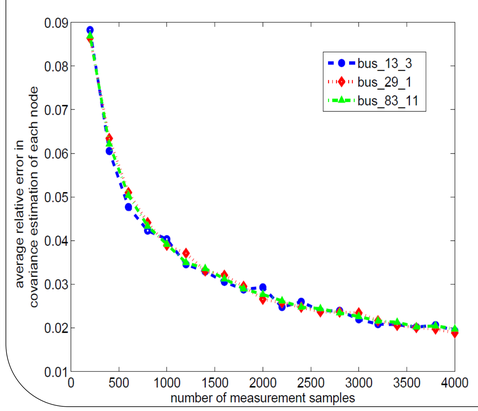


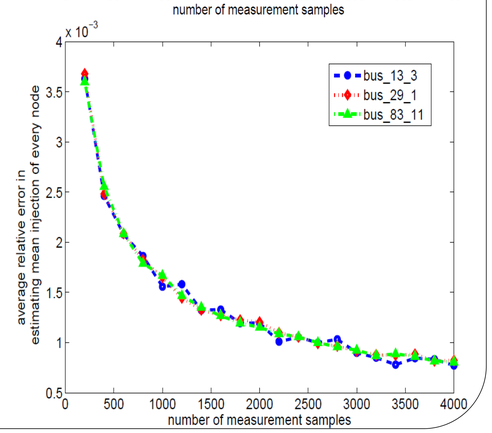


## MISSING DATA

- ❑ If separated by greater than two hops
- ❑ Polynomial time algorithm ($N^3$)
- ❑ Algorithm similar to general case
- ❑ Missing node ***c*** can exist in two cases:
  a) intermediate b) leaf

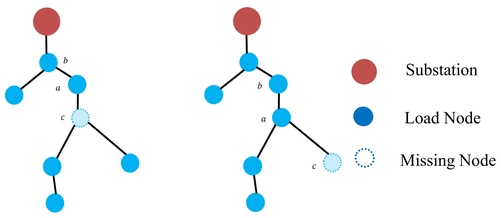


## REFERENCES

[1] M. Baran and F. Wu, "Optimal sizing of capacitors placed on a radial distribution system," Power Delivery, IEEE Transactions on, vol. 4, Jan 1989.

[2] J. Resh, "The inverse of a nonsingular submatrix of an incident matrix," IEEE Transactions on Circuit Theory, vol. 10.

[3] S. Civanlar, J. Grainger, H. Yin, and S. Lee, "Distribution feeder reconfiguration for loss reduction," Power Delivery, IEEE Transactions

# Power System Dynamic Estimation

Thomas Catanach[1 2], Earl Lawrence[3], Russell Bent[4], Scott Vander Wiel[3], Manuel Garcia[4]

[1]California Institute of Technology
[2]Center for Nonlinear Studies, Los Alamos National Laboratory
[3]Statistical Science, Los Alamos National Laboratory
[4]Energy and Infrastructure Analysis, Los Alamos National Laboratory

Contact: tcatanac@caltech.edu

## General Description

### Abstract

Developing methods for state estimation and system identification are essential for increasing the reliability of the power grid. Typically this problem has been solved on steady state time scales, however faster dynamics are becoming more important and with the deployment of phasor measurement units (PMUs) fast estimation is now possible. To do this fast estimation a layered architecture that integrates state estimation, change point detection, and disturbance classification is used. By thinking of these estimation algorithms along with controls as a layered system it improves our ability to design optimal architectures that are both fast and flexible. State Estimation can be achieved using Kalman filtering and particle based techniques which assume a system topology and dynamics model. These techniques are adapted to the differential algebraic equations that describe the power system and their robustness is explored. Using these estimates we can make predictions of the future outputs which then are compared to the PMU data to identify unexpected deviations. These change points then trigger a topology change classifier to identify the new topology of the system after a fault and also triggers a fault tracker to track the state through faults that are cleared. Finally, questions of general architecture design are raised such as how to optimally link these estimation modules and optimally place sensors to achieve all these objectives.

### Introduction

**Objective:**

Develop an architecture to track the dynamic state and topology of a power system over fast, sub-second, time scales that can then be used to make control decisions.

**Power System Model:**

Differential Algebraic Equations

ODEs:
- Machine Models
- Exciter Models
- Turbine Governor Models

$$\dot{x} = f(x, y, u)$$

Equality Constraints:
- Bus Power Injections
- Machine Constraints
- Control Constraints

$$0 = g(x, y, u)$$

Output:
- PMUs

$$z = h(x, y, u)$$

Variables

x : Dynamic State
- Generator Angles, Frequencies, Axis Voltages
- Control Internal States

y : Algebraic Variables
- Bus Voltages
- Generator Field Voltages, Powers, Torques
- Control Constraints

u : Inputs

z : Observations
- Bus Voltages

### Power System Estimation and Control Architecture

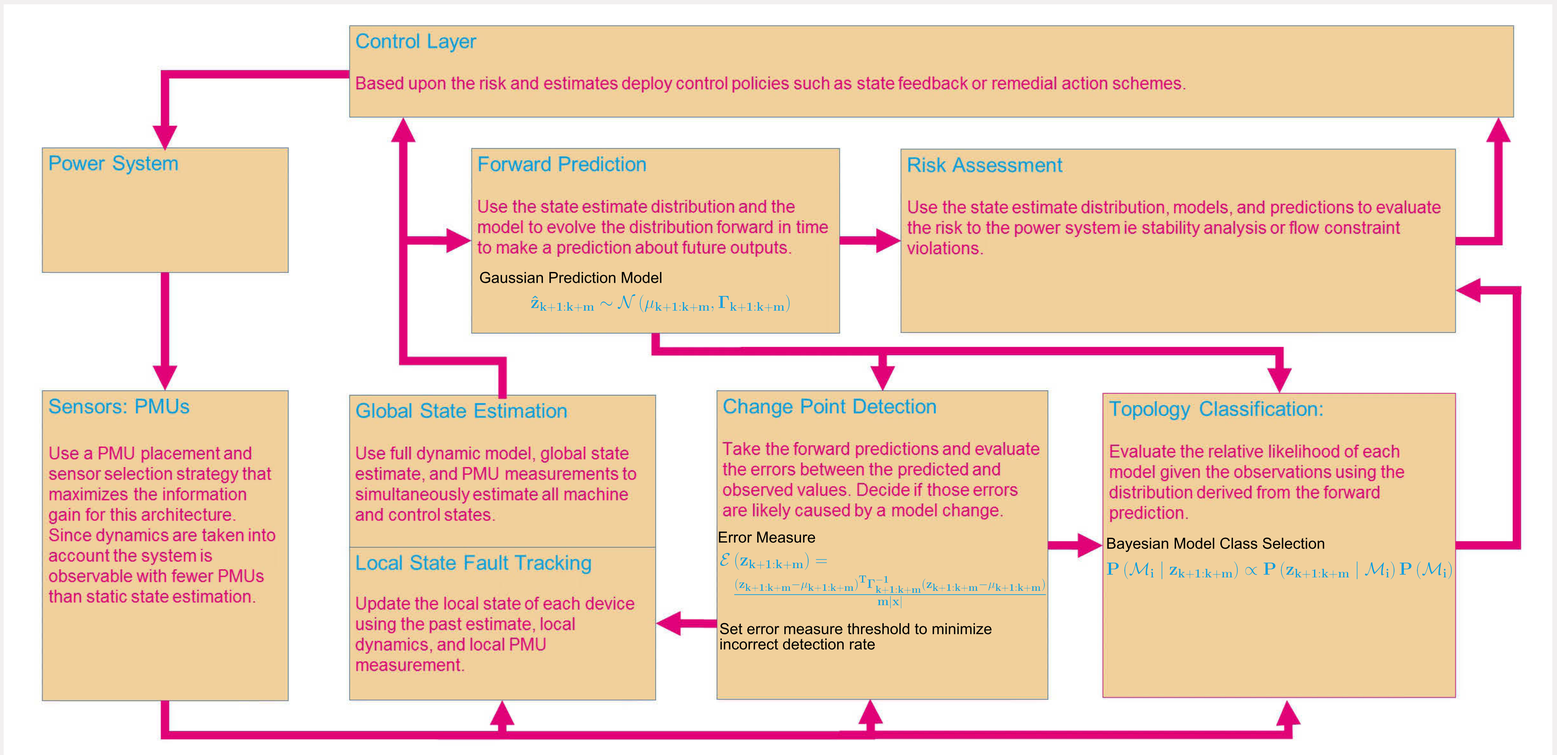


## Global and Local State Estimation Details

### State Estimation

Extended Kalman Filter

Nonlinear System

$$x_k = \mathfrak{F}(x_{k-1}) + w_k$$
$$z_k = \mathfrak{H}(x_k) + \nu_k$$

Prediction

$$\hat{x}_{k|k-1} = \mathfrak{F}(\hat{x}_{k-1|k-1})$$
$$P_{k|k-1} = F_{k-1} P_{k-1|k-1} F_{k-1}^T + Q_k$$
$$F_{k-1} = \frac{\partial \mathfrak{F}}{\partial x}\Big|_{\hat{x}_{k-1|k-1}}$$

State: $x \sim \mathcal{N}(\hat{x}, P)$

$$\hat{z}_{k|k-1} = \mathfrak{H}(\hat{x}_{k|k-1})$$
$$S_{k|k-1} = H_k P_{k|k-1} H_k^T + R_k$$
$$H_k = \frac{\partial \mathfrak{H}}{\partial x}\Big|_{\hat{x}_{k|k-1}}$$

Output: $z \sim \mathcal{N}(\hat{z}, S)$

Correction

$$K_{k|k-1} = P_{k|k-1} H_k^T S_{k|k-1}^{-1}$$
$$\hat{x}_{k|k} = \hat{x}_{k|k-1} + K_{k|k-1}(z_k - \hat{z}_{k|k-1})$$
$$P_{k|k} = (I - K_{k|k-1} H_k) P_{k|k-1}$$

Numerical Integration Methods

Euler:

$$x_k = x_{k-1} + f(x_{k-1}, y_{k-1})\Delta t$$
$$0 = g(x_{k-1}, y_{k-1})$$
$$0 = g(x_k, y_k)$$

Predictor Corrector:

$$x_k = x_{k-1} + \frac{\Delta t}{2}(f(x_{k-1}, y_{k-1}) + f(\tilde{x}_k, \tilde{y}_k))$$
$$\tilde{x}_k = x_{k-1} + \Delta t f(x_{k-1}, y_{k-1})$$
$$0 = g(x_{k-1}, y_{k-1})$$
$$0 = g(\tilde{x}_k, \tilde{y}_k)$$
$$0 = g(x_k, y_k)$$

Implicit Midpoint:

$$x_k = x_{k-1} + \frac{\Delta t}{2}(f(x_{k-1}, y_{k-1}) + f(x_k, y_k))$$
$$0 = g(x_{k-1}, y_{k-1})$$
$$0 = g(x_k, y_k)$$

Solve discrete DAE with Newton's Method

### Integration Robustness

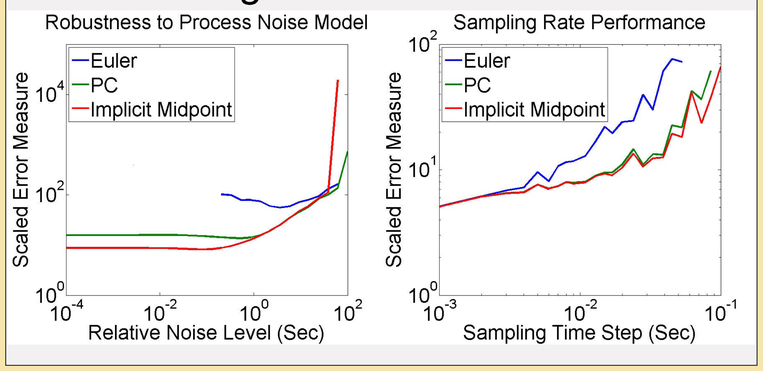


### Test System

Thirty Seven Bus System

PSAT implementation of a PowerWorld test system with thirty seven buses, nine machines and seven turbine governors. A three phase fault occurs at bus 54 and is cleared.

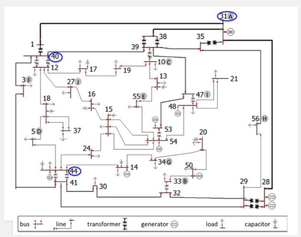


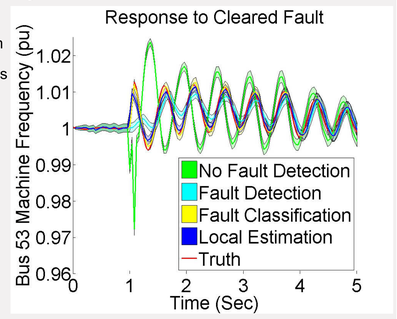


### Fault Handling

Local State Evolution

Local Variables

$$x = [\delta, \omega, e'_q, e'_d, \overrightarrow{x_c}]^T$$ Local Machine and Control States

$$u = [v, \theta]^T$$ Local Bus Voltage as Input

$$y = [i_q, i_d]^T$$ Local current as Algebraic Variable

Solve Local Dynamics

$$x_k = x_{k-1} + \frac{\Delta t}{2}(f(x_{k-1}, y_{k-1}, u_{k-1}) + f(x_k, y_k, u_k))$$
$$0 = g(x_{k-1}, y_{k-1}, u_{k-1})$$
$$0 = g(x_k, y_k, u_k)$$

Global Uncertainty Propagation

$$F_k = \begin{bmatrix} \frac{\partial x_k}{\partial x_{k-1}} & \frac{\partial x_k}{\partial v_{k-1}} & \frac{\partial x_k}{\partial v_k} \end{bmatrix}$$
$$\Sigma_{k-1|k-1} = \mathrm{cov}(x_{k-1}, u_{k-1}, u_k)$$
$$P_{k|k} = F_k \Sigma_{k-1|k-1} F_k^T + Q$$

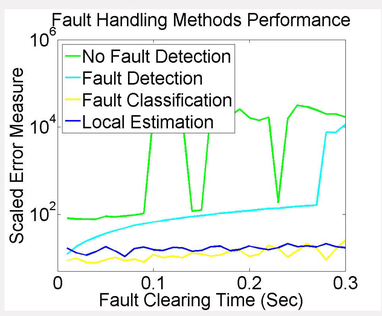


## Conclusion

### Discussion

Comments
- Robustness and performance can be improved by replacing the commonly used Euler's method with more advanced integration schemes
- Using a local estimation method drastically increases the ability of the estimator to track the system through a fault having almost as good performance as perfect classification

Accomplishments
- Demonstrated dynamic state estimation is possible for power systems and can track the state through faults
- Proposed a framework using these state estimates for change point detection and classification

Future Work
- Better characterize process and measurement noise distributions
- Developed better methods for uncertainty propagation particularly for prediction and local estimation

### References

Zhou, N. Meng, D. Huang, Z. Welch, G. Dynamic State Estimation of a Synchronous Machine Using PMU Data: A Comparative Study. Smart Grid, IEEE Transactions on, 2015

Esmaeil Ghahremani and Innocent Kamwa. Dynamic state estimation in power system by applying the extended kalman filter with unknown inputs to phasor measurements. Power Systems, IEEE Transactions on, 2011.

Zhenyu Huang, Pengwei Du, DN Kosterev, and Bo Yang. Application of extended kalman filter techniques for dynamic model parameter calibration. In Power & Energy Society General Meeting, 2009. PES'09. IEEE, 2009.

Zhenyu Huang and Jarek Nieplocha. Transforming power grid operations via high performance computing. In Power and Energy Society General Meeting-Conversion and Delivery of Electrical Energy in the 21st Century, 2008, 2008.

Zhenyu Huang, Kevin Schneider, and Jarek Nieplocha. Feasibility studies of applying kalman filter techniques to power system dynamic state estimation. In Power Engineering Conference, IEEE, 2007.

Milano, F.. An open source power system analysis toolbox. Power Systems, IEEE Transactions on, 2005.

# The Role of a Market Maker in Networked Cournot Competition

Subhonmesh Bose, Desmond Cai, Steven Low, Adam Wierman
California Institute of Technology

## Overview

We study different market clearing rules in a transmission constrained electricity market. We model the generators using a networked Cournot model and analyze three market clearing objectives – social welfare, residual social welfare, and consumer surplus. We find that:

1. Generalized Nash Equilibrium (GNE) may not exist under certain market maker clearing objectives.
2. In a 2-node network, when equilibria exist, the equilibrium flow could be completely different under the three objectives.

## Model

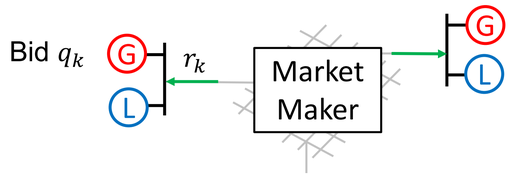


Linear demand $p_k(d_k) = a_k - b_k d_k$

Flow constraints:

$$S = \{r \mid q + r \geq 0, |Hr| \leq f, 1^T r = 0\}$$

Generator $k$ chooses bid $q_k \geq 0$ to maximize payoff:

$$\pi_k^G(q,r) = q_k p_k(q_k + r_k) - c_k q_k^2$$

Market maker chooses flows $r \in S$ to maximize one of:

$$W_{soc} = \sum_k \left( \int_0^{q_k + r_k} p_k(w_k) dw_k - c_k q_k^2 \right)$$

$$W_{res} = W_{soc} - \sum_k \pi_k^G(q,r)$$

$$W_{con} = \sum_k \left( \int_0^{q_k + r_k} p_k(w_k) dw_k - (q_k + r_k) p_k(q_k + r_k) \right)$$

## Main Results

Theorem 1: A GNE exists if the market maker maximizes $W_{soc}$ or $W_{res}$. However, a GNE may not exist if the market maker maximizes $W_{con}$.

Theorem 2: Consider a 2-node network with infinite line capacity and some system parameters such that a GNE always exists for all three market maker objectives.
(a) If market maker maximizes $W_{soc}$, then $r^* < 0$.
(b) If market maker maximizes $W_{res}$, then $r^* = 0$.
(c) If market maker maximizes $W_{con}$, then $r^* > 0$

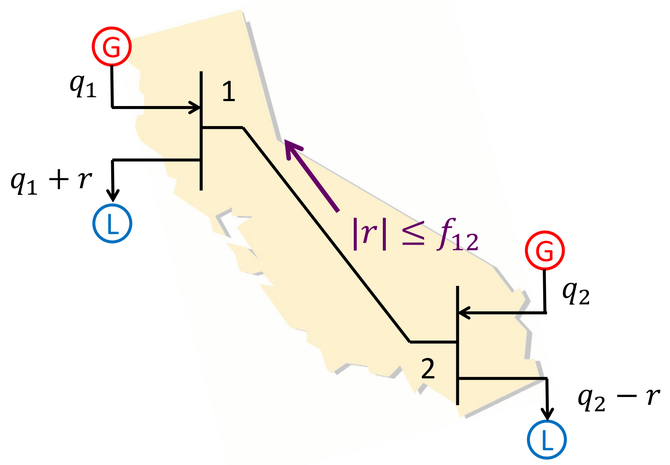


## Impact of Line Capacity

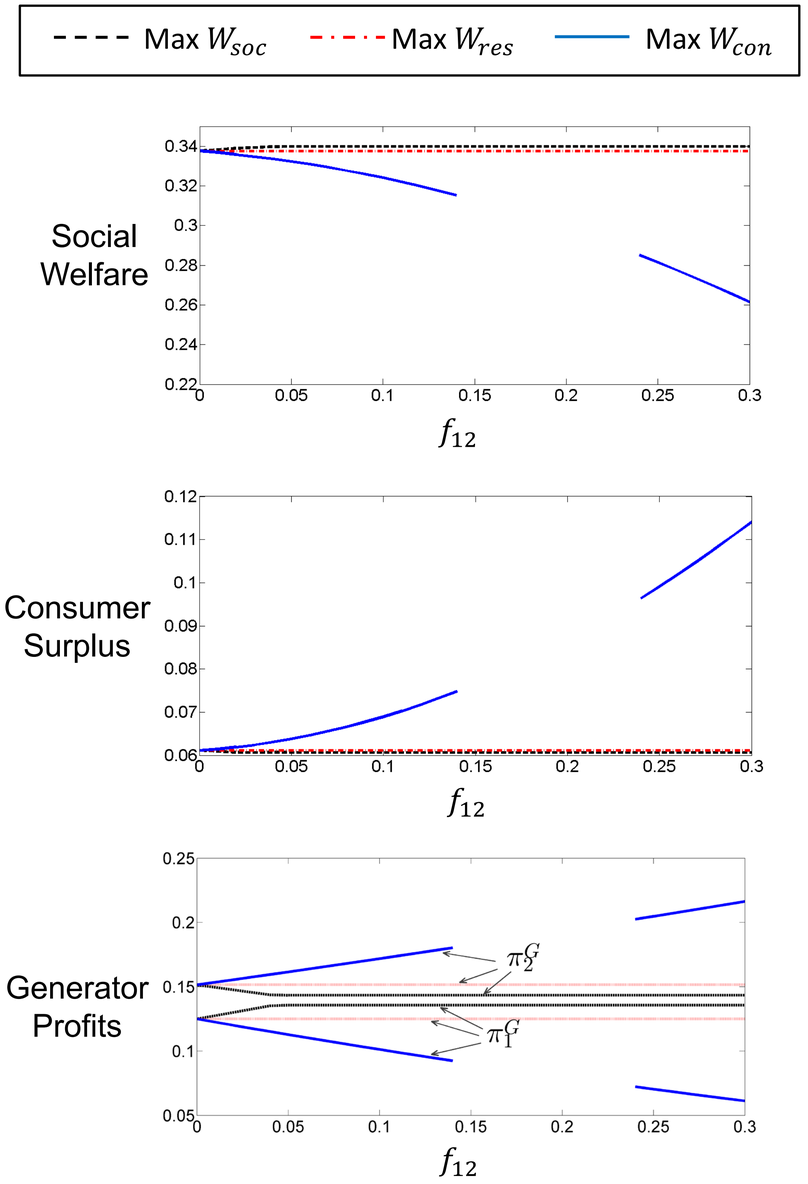


Supported by: NSF, ARPA-E, SCE, Resnick Institute, Okawa Foundation

ETH
Eidgenössische Technische Hochschule Zürich
Swiss Federal Institute of Technology Zurich

eeh power systems laboratory

# A Framework for the Coordination of Flexibility in Multi-Area Power Systems

*Matthias A. Bucher, Spyros Chatzivasileiadis, Göran Andersson*
*Power Systems Laboratory, ETH Zurich*

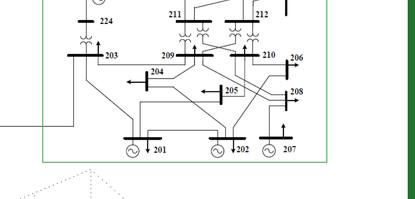

**Motivation**
- Decreasing reserve availability
- Increasing grid congestions
- Better coordination and sharing of operational flexibility between TSOs needed

**Goal**
Improve inter-TSO coordination of flexibility in a decentralized way incorporating *transmission constraints* by expressing possible deviations of *tie-line power flows* and related *costs*.

**Requirements**
- Data privacy
- Minimal information
- No centralized coordination entity
- Considering transmission constraints

## Modeling

Two area system split in two areas results in two MIMO-systems:

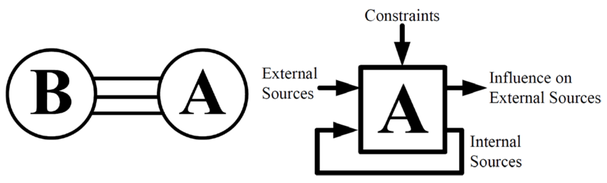


→ *internal* sources (index i): generators, loads
→ *external* sources (index e): tie-lines, HVDC,…

Shareable flexibility: feasible deviations of external sources, i.e. tie-line flow changes.

Power flow deviations due to deviations of internal/external sources ($\Delta_i$,$\Delta_e$) :

$$P_L^{actual} - P_L^{scheduled} = H_i\Delta_i + H_e\Delta_e$$

Constraints on $\Delta_{i/e}$:
- allowed redispatch of units
- ramping limitations («reaction time»)
- (linearized) grid constraints (H: PTDF)
- N-1 security constraints

## Method

### Operational Limits

Goal: Find allowed deviations of external sources $\Delta_e$.

Flexibility Set: All constraints are stacked to a linear matrix inequality.

$$F = \{(\Delta_i, \Delta_e) \in R^{ni\,x\,ne} | C_i\Delta_i + C_e\Delta_e \leq b\}$$

Explicit limits on $\Delta_e$: Projection of *F* (blue) on the axes of $\Delta_e$ (red).

$$F_d = \{\Delta_e \in R^{ne} | \exists\Delta_i, (\Delta_i, \Delta_e) \in F\} = \{\Delta_e | G\Delta_e \leq g\}$$

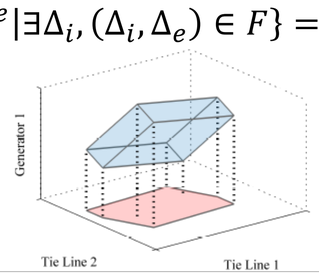


### Costs for shared flexibility

Goal: Construct lower bound for redispatch costs of generators for neighboring TSO using linear cuts.

Construction: Calculate redispatching costs $q_0^k$ for a number of selected $\Delta_e^k$. Using dual variables $\lambda$, improve bound by adding cuts:

$$q \geq q_o^k + \lambda^k \left(\Delta_e - \Delta_e^k\right)$$

## Application RTS-96 2-area system



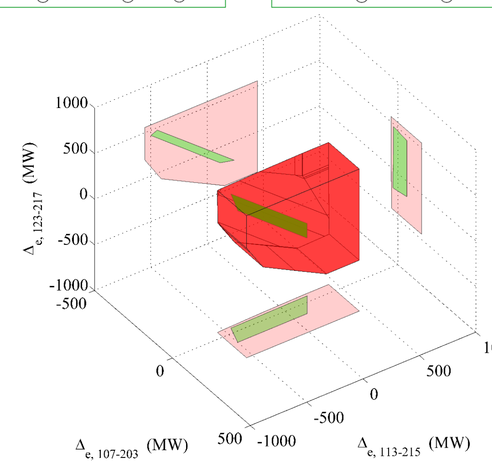


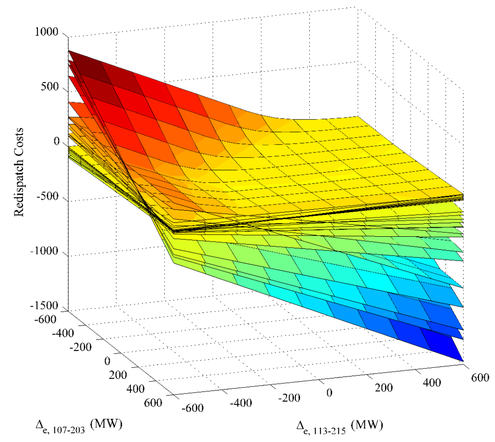


## Coordination

Every TSO prepares information on shareable flexibility and corresponding costs → Data exchange (interval-/event-based) → Incorporation of information, e.g. in redispatch optimization → Communication of remedial procedure to neighboring TSOs and initiation

## Comparison with ATC

Methods considering the ATC (available transfer capacity) for sharing flexibility result in a less flexible system (blue) compared to the method presented above (red), i.e. deviations need to be smaller.

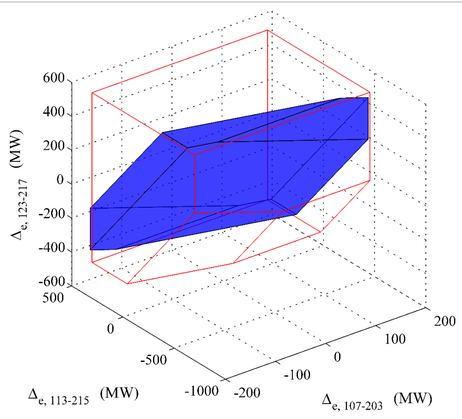


The figure shows the maximal possible deviations of bus injections in the neighboring area that can be balanced. In orange, a method considering the ATC is applied; blue: method above. The method can deal with larger deviations, e.g. from intermittent energy sources.

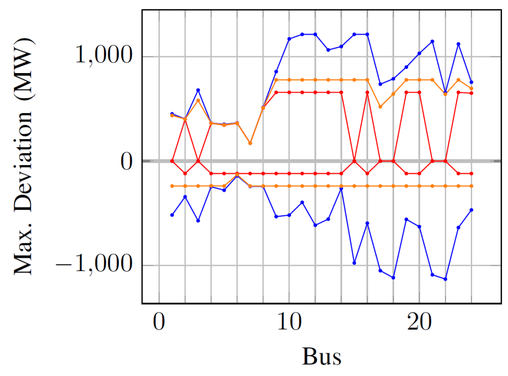


## Conclusion

→ Decentralized coordination of flexibility between different control areas
→ lower bound for costs can be determined using a cutting-plane approach
→ Allows to share more operational flexibility compared to methods respecting ATC

Contact: mb@eeh.ee.ethz.ch